Summer 8-2018

Macromolecule Loading on PLGA Particles through Surface Adsorption

Yiwei Wang

MACROMOLECULE LOADING ON PLGA PARTICLES THROUGH SURFACE ADSORPTION

A Thesis

Submitted to Duquesne University

Duquesne University

In partial fulfillment of the requirements for

the degree of Master of Science

By

Yiwei Wang

August 2018

MACROMOLECULE LOADING ON PLGA PARTICLES THROUGH SURFACE ADSORPTION

By

Yiwei Wang

Approved June 15, 2018

Wilson Meng, Ph.D. Associate Professor of Pharmaceutics Graduate School of Pharmaceutical Sciences Duquesne University, Pittsburgh, PA (Committee Chair)	Ellen Gawalt, Ph.D. Department Chair and Professor of Chemistry and Biochemistry Duquesne University, Pittsburgh, PA (Committee Member)
Devika Soundara Manickam, Ph.D. Assistant Professor of Pharmaceutics Graduate School of Pharmaceutical Sciences Duquesne University, Pittsburgh, PA (Committee Member)	Carl A. Anderson, Ph.D. Associate Professor of Pharmaceutics Graduate School of Pharmaceutical Sciences Duquesne University, Pittsburgh, PA
J. Douglas Bricker, PhD Dean, School of Pharmacy and Graduate School of Pharmaceutical Sciences Duquesne University, Pittsburgh, PA	

ABSTRACT

MACROMOLECULE LOADING ON PLGA PARTICLES THROUGH SURFACE ADSORPTION

By

Yiwei Wang

August 2018

Thesis supervised by Wilson Meng

The advent of biotherapeutics have impacted the ways in which diseases are treated. In many instances development of recombinant proteins and oligonucleotides into therapeutics are slowed by poor stability of the candidate drugs. Progress has been made in using polymeric particles as carriers of macromolecule drugs. Historically the method is to encapsulate biological drugs into spherical polymeric matrices. Owing to its biocompatible and biodegradable nature, poly (d,l-lactic-co-glycolic acid) (PLGA) has been used extensively in formulating biological drugs into nano- and micro-sized particles. The development of PLGA biologic formulations, however, has been hampered by matrix acidification; the hydrolysis of the polymer generates non-diffusive acid fragments by which the interior pH can be driven to as low as 2, a condition unfavorable for proteins and

oligonucleotides to remain intact. In addition, loading of proteins through encapsulation can lead to substantial loss of activity because of homogenization or sonication-induced denaturation. To circumvent these limitations yet still take advantage of the proven safety of PLGA in humans, I proposed to load macromolecules onto the surface of PLGA particles functionalized with biotin ("PLGA-biotin").

The specific binding between avidin and biotin (or desthiobiotin) was employed to enable surface adsorption. The pair has the strongest known non-covalent affinity, an interaction that is relatively insensitive to temperature and pH. PLGA-biotin particles were prepared by co-emulsifying the lipid DSPE-PEG-biotin with PLGA into a matrix. The tetravalent feature of avidin was used to bridge biotinylated proteins or oligonucleotides onto PLGA-biotin particles. The hypothesis of this project is that solvent-accessible biotin molecules are displayed on PLGA-biotin particles. The rationale for my hypothesis is that the co-emulsification of the biotinylated lipid DSPE-PEG-biotin and the polymer matrix PLGA has the potential to generate PLGA particles functionalized with biotin molecules embedded on the surface. As a result, the interaction between biotin and avidin can be utilized to load macromolecules onto the surface of these modified PLGA particles through adsorption, circumventing the challenges to the stability and bioactivity of the biological drugs caused by the encapsulation process and the acidic environment inside PLGA particles during the degradation of the polymer matrix. Two specific aims were carried out. In aim 1, the presence of biotin in PLGA-biotin particles was verified and the physical attributes of the particles, namely particle size and zeta potential, were characterized. Spectroscopic and biochemical studies indicated the presence of biotin on the particle

surface. In aim 2, the amount of biotin accessible on PLGA-biotin particles was quantified. Taken together, the data generated in this thesis support the notion that surface adsorption is a general method for loading macromolecules onto PLGA particles. The work presented is a step toward a new platform in formulating biotherapeutics.

ACKNOWLEDGEMENT

I would first like to express my deepest appreciation to my thesis advisor Dr. Wilson Meng for his inspiration, support, guidance, and advisory throughout my M.S. study at Duquesne University. His guidance helped me through difficulties and encouraged me to pursue advanced research in pharmaceutical science. Without Dr. Meng's patient help, this thesis project would not have been possible.

I would also like to thank my committee members, Dr. Ellen Gawalt and Dr. Devika Soundara Manickam, for their insightful comments, suggestions, and encouragement. They have provided me extensive personal and professional guidance and taught me a great deal about scientific research.

My next sincere thanks go to our current and previous group members and other students in the department of pharmaceutics at School of Pharmacy for their help and support during my study. I am also grateful to all of those with whom I have had the pleasure to work during this project.

Finally, I must express my very profound gratitude to my parents for providing me with unfailing support and continuous encouragement throughout the time of my research. This accomplishment would not have been possible without them.

TABLE OF CONTENTS

Page

LIST OF TABLES

Page

LIST OF FIGURES

Page

Chapter 1: Introduction

1.1. Biologics: Delivery Challenges

Biologics have revolutionized the treatment of diseases and attracted growing interests among drug development scientists during the past two decades (Morrow, T. and L. H. Felcone, et al. 2004). Whereas biologics used to be limited to peptides and natural proteins, the range of therapies has since expanded to include recombinant antibodies, antisense oligonucleotides, plasmid DNA, fusion proteins, and Crisper-Cas9 (Morrow, T. and L. H. Felcone, et al. 2004). An important consideration in formulating a biological drug is the need to protect and retain its structure and activity (Felcone, L. H. 2004), which can be negatively impacted by production processes and physiological factors.

Since the early 1980s there have been continuing interests in formulating recombinant proteins and nucleic acids for therapeutic purposes (Paulo, C. S., et al. 2011). The number of clinical trials studying proteins, peptides and antisense oligonucleotides has steadily increased for the past two decades. With their inherent high specificity and affinity, recombinant proteins are believed to be capable of treating chronic diseases, cancers and autoimmunity (Szlachcic, A., et al. 2011). As complex cellular pathways are being unveiled at a rapid pace, endogenous protein partners in checkpoint mechanisms are selected to become candidates for therapeutic agents.

One major problem of protein drugs is that they tend to be unstable both *in vitro* and *in vivo*. Thus, the applicability of proteins to work as effective therapeutics is restricted (Lin, S. 2015). In the absence of stabilizers, many proteins aggregate and/or undergo chemical degradation processes. The common causes of chemical instability are hydrolysis, deamidation, isomerization, racemization, oxidation, disulfide exchange, dimerization, β-elimination, and Maillard reaction (Jacob, S., et al. 2006). Their susceptibility to proteases also poses challenges in protein production and purification, resulting in inadequate concentration of protein drug *in vivo* to reach the targets (Jiskoot, W., et al. 2012). In addition, protein drugs can be the targets of translational modifications and immune responses under specific circumstances, which leads to reduced efficacy and possible hypersensitivity (Jiskoot, W., et al. 2012).

1.2. Application of Particles in Biotherapeutics Delivery

A number of encapsulation approaches have been used to formulate protein drugs (Pisal, D. S., et al. 2010). These include the use of micro-encapsulation to enable sustained release of protein drug and subsequently reduce the required frequency of administration (Gregoriadis, G., et al. 2005, Tan, M. L., et al. 2010). Among the materials and delivery vehicles that are currently under investigation for the delivery of nucleic acid therapeutics particle-mediated delivery, poly (lactic-co-glycolic acid) (PLGA) particles have advantages such as the ease and speed of preparation, the stability of the nucleic acids in preparation, the absence of viral antigens, and the ability to target different tissue depths and areas (Danhier, F., et al. 2012).

Poly (d,l-lactic-co-glycolic acid), or PLGA, one of the most successfully developed biodegradable polymers, has been intensively investigated for fabricating delivery vehicles for macromolecule drugs (Ye, M., et al. 2010, Pisal, D. S., et al. 2010). The PLGA particles developed for protein and oligonucleotides formulations typically have diameters ranging between 1 to 250 μm , in most cases designed as injectable (Pisal, D. S., et al. 2010). The rationale for using PLGA is partly due to its biodegradable nature, and that it is FDA-approved for use in humans for three decades. While many PLGA-based strategies have been characterized in preclinical studies, challenges remain in ensuring therapeutic concentration of the protein at the site of action without substantial adverse reaction. In many cases particles infused intravenously are trapped in the monocytic-phagocytic system, located primarily in the spleen and liver, but also in secondary lymphoid tissues (Furth, R. 1998, Trevaskis, N. L., et al. 2015). Nevertheless, PLGA remains an attractive polymer because of its long safety record in the general population.

Degradation of PLGA microparticles typically occurs on the scale of weeks or months, making such particles potentially viable carriers for sustained delivery of proteins and oligonucleotides (van de Weert, M., et al. 2000). According to a study (Makadia, H. K. and S. J. Siegel 2011) on the relationship between the degradation rate of PLGA and the percentage of PGA in PLGA matrices, the degradation rate of PLGA increases as the percentage of PGA increases from 25 to 50. Because of the chiral center in lactic acid, PLA has a higher crystallinity than PGA and a lower permeability. PLA has a slow degradation over several months, while PGA degrades over several weeks. Therefore, when the

percentage of PGA increases, PLGA becomes more amorphous and more rapidly biodegradable. Accordingly, PLGA with composition of PLA: PGA equals 50:50 has demonstrated the fastest biodegradation rate of the polymers with near complete degradation in 50–60 days (Figure 1-1). Because of this ideal degradation rate, $PLGA_{50:50}$ is currently the most widely used type of PLA-PGA copolymer in particle preparation and therefore is selected for preparing PLGA-Ni and PLGA-biotin particles in this project.

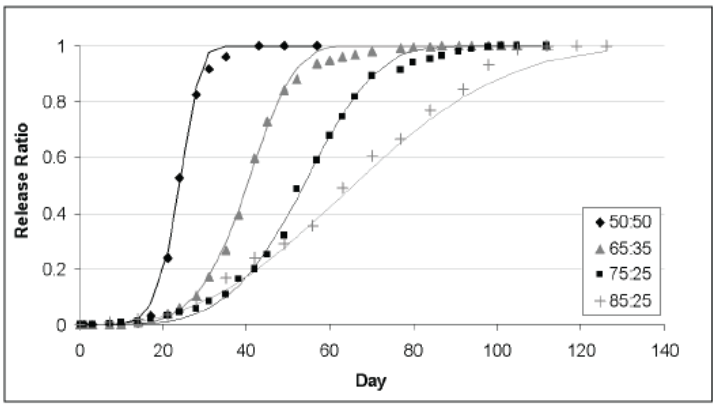

Figure 1-1. Degradation rate of PLGA with different ratios of PLA: PGA.

The biodegradation rate of PLGA is depending on not only the copolymer ratio but also the molecular weight. Thus, the molecular weight and composition of PLGA can be adjusted to change the chemical and physical properties of carriers and control the speed of degradation as well as the rate of drug-release. Molecular weight has a direct relation with the polymer chain size. Polymers having higher molecular weight have longer polymer chains, which require more time to degrade than small polymer chains. Increasing the molecular weight of PLGA polymers from 10 to 100 kDa, degradation rates ranging from several weeks to several months were reported (Gentile, P., et al. 2014). Generally,

the lower molecular weight PLGA nanocarriers/microcarriers degrade more quickly, resulting in a quick pH decline. Considering the influence of rapid decrease in pH inside PLGA particle on the macromolecules loaded, PLGA polymers with low molecular weights are not frequently used for the delivery of biological drugs, especially those requiring a sustained release.

In addition to formulation of proteins, the application of PLGA particles on gene therapy has also attracted a great deal of attention in recent years. Gene therapy, i.e., the expression in cells of genetic material with therapeutic activity, holds great promise for the treatment of human diseases (Resende, R. R., et al. 2007). A delivery vehicle (vector), of either viral or non-viral origin, must be used to carry the foreign gene into a cell. Viral vectors take advantage of the facile integration of the gene of interest into the host and the high probability of its long-term expression but are plagued by safety concerns (Auman, J. T. 2010). Non-viral vectors, although less efficient at introducing and maintaining foreign gene expression, have the profound advantage of being non-pathogenic and non-immunogenic (Thomas, M. and A. M. Klibanov 2003). PLGA particles are particularly attractive for non-viral gene therapy (e.g., Tahara, K., et al. 2008).

1.3. Challenges in Encapsulating Biologics into PLGA Particles

A particular challenge in using PLGA particles for biotherapeutic delivery is to ensure the payload retain the structure and biological activity (van de Weert, M., et al. 2000). It should be noticed that the hydrolysis of PLGA generates acidic fragments including glycolic acid

and lactic acid (Makadia, H. K. and S. J. Siegel 2011). Because PLGA is a bulk erosion polymer, its degradation rate is slower than the water penetration rate (von Burkersroda, F., et al. 2002). Therefore, the acidic fragments will be trapped inside the PLGA particle.

The accumulation of these acidic polymer fragments can decrease the pH in the matrix to as low as pH 3 to pH 2 (Figure 1-2), which would facilitate the degradation of the polymer, and also denature the encapsulated protein (Fu, K., et al. 2000, von Burkersroda, F., et al. 2002). Additionally, protein denaturation often occurs during microparticle preparation, such as the homogenization and/or sonication steps, and at the interface of organic phase and aqueous phase (Xiong Y.L. 1997). As a result, the loading efficiency of protein on PLGA particles varies and can be very poor. To circumvent these challenges, I propose to load proteins through surface adsorption onto a modified format of PLGA microparticles.

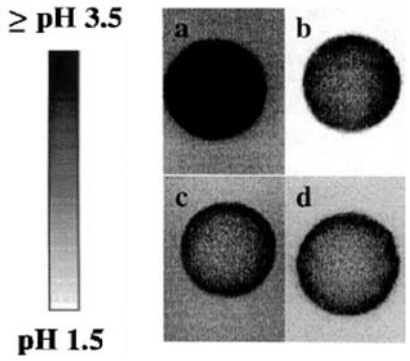

Figure 1-2. The pH change inside PLGA matrix caused by the accumulation of acidic degradants.

The phenomenon of adsorption is essentially an attraction of adsorbate molecules to an adsorbent surface. Adsorption processes can be classified as either physical adsorption (van

der Waals adsorption) or chemisorption (activated adsorption) depending on the type of forces between the adsorbate and the adsorbent.

The individuality of the adsorbate and the adsorbent are preserved in physical adsorption. In contrast, chemisorption involves a transfer or sharing of electron, or breakage of the adsorbate into atoms or radicals which are bound separately, forming chemical bonds between the adsorbate and adsorbent. In this project, noncovalent chemical bonds are utilized to enable chemisorption of biological drugs on the surface of PLGA-Ni or PLGA-biotin particles.

1.4. Ligands and Proteins Used for Surface Modification and Adsorption

1.4.1. Biotin

Biotin is a water-soluble B-vitamin, also called vitamin B_7 and vitamin H or coenzyme R (Ross, C., et al. 2014). As showed in Figure 1-3, it is composed of a ureido ring fused with a tetrahydrothiophene ring. A valeric acid substituent is attached to the tetrahydrothiophene ring, which can be derivatized in order to incorporate various reactive groups that facilitate the addition of a biotin tag to other molecules. Biotin is present in small amounts in all living cells, involved in the synthesis of fatty acids, isoleucine, and valine, and in gluconeogenesis (Zempleni, J., et al. 2007). Studies have shown that biotin binds tightly to the tetrameric protein avidin and its analogues (Table 1-1), including streptavidin and neutravidin (Laitinen, O. H., et al. 2006).

Table 1-1. Comparison of biotin-binding proteins.

	Avidin	Streptavidin (recombinant)	NeutrAvidin (from Avidin)
Molecular weight (kDa)	67	53	60
Biotin-binding sites	4	4	4
Affinity for biotin (K_d)	~1.3 x 10^{-15} M	~0.04 x 10^{-15} M	~1.3 x 10^{-15} M
Nonspecific binding	high	low	lowest

Because biotin is relatively small (244.3 Daltons), it can be conjugated to many proteins or other molecules without significantly altering their biological activity (Chapman-Smith, A. and J. E. Cronan, Jr. 1999). This process is called biotinylation. The highly specific interaction of biotin with biotin-binding proteins makes it a useful tool in assays designed to detect or target biological analytes.

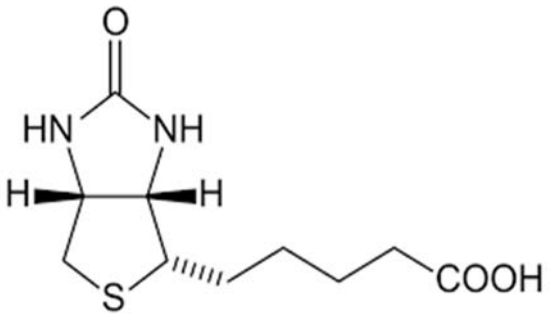

Figure 1-3. The chemical structure of biotin.

The normal biotin plasma level ranges from 400-1200 ng/L with daily fluctuations up to 100% (Trueb, R. M. 2016). If biotin is taken externally, excessive amounts are not absorbed and excreted with the feces. By contrast, absorbed amounts of biotin which exceed the storage capacity of the organism are eliminated in the urine. Shortly after an oral take up of biotin, the the biotin concentration in the plasma increases several times, but after 24 h the average value is reached again (Bonjour, J.P. 1984). Furthermore, most of the biotin in human plasma is not bound to protein. Approximately 81% of biotin in plasma is free and 7% is reversibly bound (Mock, D. M. and M. I. Malik 1992).

1.4.2. Avidin

Avidin is a protein derived from avians and amphibians, which shows considerable binding affinity for biotin (Korpela, J. 1984). The monomeric subunit of avidin consists of a highly similar topology comprising an eight-stranded antiparallel-barrel (Meir, A., et al. 2012, see Figure 1-4). Avidin and its analogues are homotetrameric proteins with four biotin-binding sites, and their high affinity characteristics are closely dependent on their quaternary assembly (Meir, A., et al. 2012). In its tetrameric form, avidin is estimated to be 66–69 kDa in size with 10% of is molecular weight contributed by carbohydrate (Green, N. M. 1975).

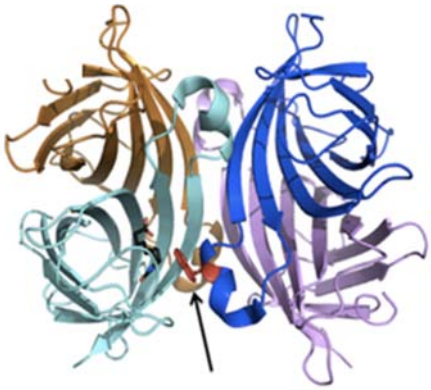

Figure 1-4. Structures of tetrameric egg white avidin. Monomers were shown in magenta, blue, cyan, and orange. The biotin ligand is shown in black in the binding site of the cyan monomer (for clarity). The Trp residue (shown in red) from an adjacent monomer (blue) contributes to the high affinity of biotin binding and is indicated by an arrow.

Through co-emulsification with biotinylated lipid, PLGA particles can be functionalized with biotin molecules on the surface to generate PLGA-biotin particles. In this project, avidin-biotin and avidin-desthiobion interactions provide the foundation for PLGA-biotin particles to load nucleic acid drugs such as antisense oligonucleotides. But it should be pointed out that the adsorption of biotherapeutics on PLGA-biotin particles, in this case, is not through direct interactions. Avidin works as an intermediate connecting PLGA-biotin particles and desthiobiotinylated biotherapeutics.

1.4.3. Desthiobiotin

Desthiobiotin is a derivative of biotin that lacks a sulfur atom. The lower affinity of desthiobiotin allows to break the desthiobiotin/avidin bound by displacement using biotin,

which makes desthiobiotin a label of choice to create reporter molecules dedicated to both detection and separation techniques (Hirsch, J. D., et al. 2002). Unlike biotinylated proteins, desthiobiotinylated proteins and their interacting partners can be readily and specifically eluted under mild conditions when captured on avidin by using a biotin elution buffer (Hirsch, J. D., et al. 2002). The soft release characteristic of desthiobiotin minimizes the isolation of naturally biotinylated molecules that can interfere with results and also eliminates the use of harsh elution conditions which can disassociate complexes and/or damage the target protein or cell (Levy, M. and A. D. Ellington 2008). This technique is ideal when using native or recombinant proteins that are not expressed with a fusion tag and when it is required to isolate captured proteins under native conditions such as targeting intact cells or cell surface proteins (Kimple, M. E., et al. 2013).

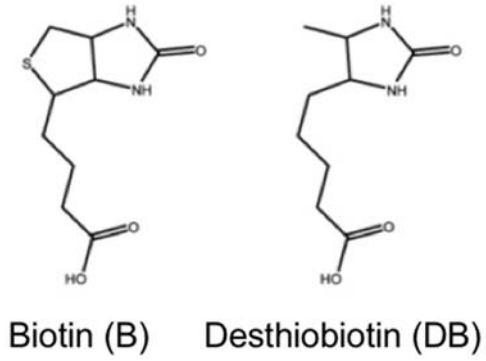

Figure 1-5. Chemical structures of biotin and desthiobiotin.

Chapter 2: Adsorption of Avidin on PLGA-biotin Particles for Biomacromolecules Delivery

2.1. Introduction

The avidin-biotin interaction is one of the strongest non-covalent interaction ($K_d = 10^{-15}$ M) interactions in the nature (Chivers, C. E., et al. 2011). The non-covalent interaction is characterized by a rapid on rate (K_{on}), and once formed, is unaffected by extremes of pH, temperature, organic solvents and other denaturing agents (Gitlin, G., et al. 1987). Therefore, the binding sites in avidin are stable and functional over a wide range of pH and temperature. Moreover, avidin is also amenable to many chemical modifications with little to no effect on function, making it useful for the detection and protein purification of biotinylated molecules (Meir, A., et al. 2012, Green, N. M. and E. J. Toms, 1973). Because of these useful features, there has been a growing interest in exploring the applications of avidin-biotin interaction in biochemical assays, affinity purification, and drug delivery. However, the carbohydrate content and basic pI (10-10.5) of avidin can result in a high amount of nonspecific binding (Green, N. M., 1975). Thus, careful optimization of blocking and proper design of biotinylated probes are required to obtain the best assay results.

Since the biotin label is stable and small, it rarely interferes with the labeled molecules and therefore enables the avidin-biotin interaction to be used in robust and highly sensitive assays. The following Figure 2-1 demonstrates how the amino acid residues from the

binding pocket in avidin surround and contact the biotin molecule during this interaction. Because desthiobiotin lacks a sulfur atom, the binding formed between the sulfur atom in biotin and the hydroxyl group in threonine (K. Stierand, M. Rarey 2010). Thus, desthiobiotin binds less tightly to avidin than biotin ($K_d=10^{-11}$ M) with avidin (Hirsch, J. D., et al. 2002).

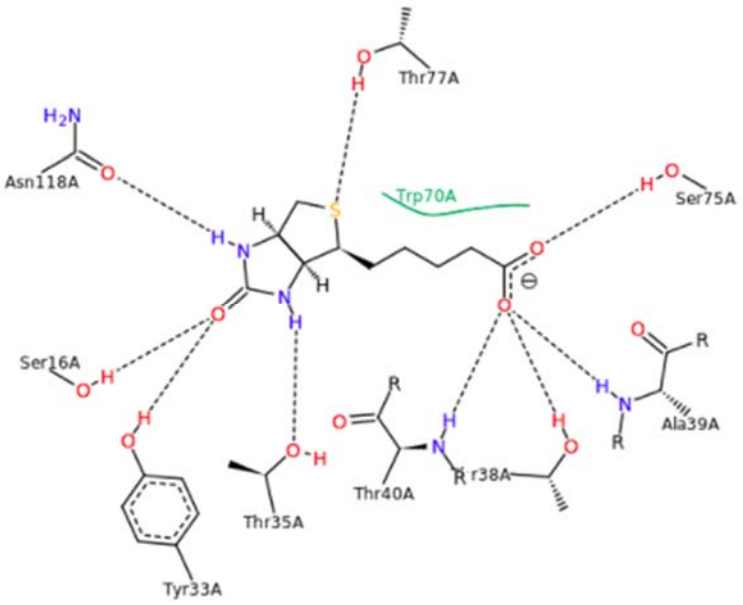

Figure 2-1. Amino acid residues surrounding and contacting biotin in the avidin binding pocket.

In this project, the non-covalent interaction between avidin and biotin was employed to deliver biological drugs (Figure 2-2). Particularly, the biotinylated lipid DSPE-PEG-biotin was used to co-emulsify with PLGA and PVA to generate particles functionalized with biotin molecules on the surface, i.e. PLGA-biotin particles. The ultimate goal for this project is to deliver biologics that are conjugated with desthiobiotin. Since desthiobiotin (DB) has a lower binding affinity, it can be displaced by biotin or other avidin-binding reagents such as 4-hydroxyazobenzene-2-carboxylic acid (Verdoliva, A., et al. 2010).

Consequently, the conjugated protein drug or other biologics will be released from PLGA-biotin particles and start to work *in vitro* or *in vivo*.

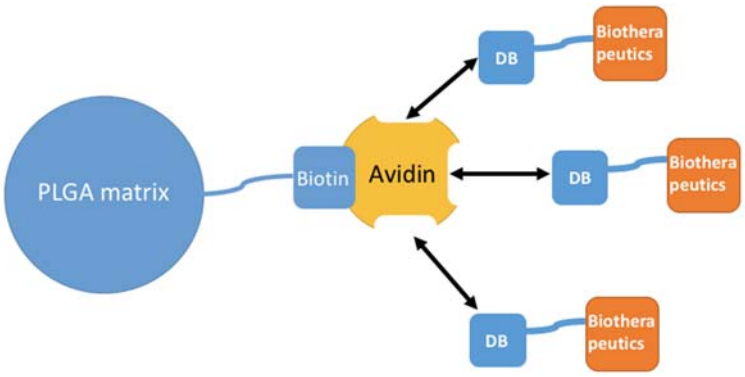

Figure 2-2. Deliver desthiobiotinylated macromolecules through PLGA-biotin particles (DB is the abbreviation of desthiobiotin).

2.2. Materials and Methods

2.2.1. Materials

DSPE-PEG (2000) biotin (3016.81 Da) was purchased from Avanti. Poly (D, L-lactide-co-glycolide) (PLGA, 50:50, IV 1.0 dl/g, 150000 g/mol, overall PDI 1.5-2.0) was purchased from Polysciences, Inc. Avidin (egg white protein content, 92%), polyvinyl alcohol (PVA, 86-89% hydrolyzed, low molecular weight), Invitrogen NativePAGE 4-16% Bis-Tris gel (1.0 mm x 10 well), Novex sharp protein standard, Pierce LAL chromogenic endotoxin quantitation kit, dichloromethane (DCM, 99.9%), Tris base, D-(+)-trehalose dihydrate, RPMI 1640 medium, ACK lysing buffer, endotoxin-free ultrapure water and HABA were purchased from Thermo Fisher Scientific. Protein G human recombinant, His tag (His-pG)

was purchased from ProSpec. Cy3-ASO-DB (1 μg/μl; 10740.9 Da) was purchased from Integrated DNA Technologies through custom synthesis. Anti-DEC205 Ab (160000 Da, 0.5 mg/ml, 25 μg 50 μl in total) and Allophycocyanin (APC)-labeled anti-CD86 Ab (0.2 mg/ml, 25 μg in total) were purchased from Biolegend. Purified Rat Anti-Mouse CD16/CD32 (Mouse BD Fc Block) (0.5 mg/ml, 0.1 mg 0.2 ml in total) was purchased from BD Biosciences. Paraformaldehyde was purchased from Sigma-Aldrich.

2.2.2. PLGA-biotin Particle Preparation

PLGA-biotin particles were prepared using the method of double-emulsion solvent evaporation. Specifically, DCM was used as the organic phase and 1% PVA aqueous solution was selected as the water phase. The aqueous solution of 8 ml 1% PVA was prepared by stirring with heating at 90 °C overnight. DSPE-PEG (2000) biotin (Figure 2-3) is the biotinylated lipid used to attach biotin molecules onto the surface of PLGA particles. Because biotin is hydrophilic, it will be oriented into the water phase, while the hydrophobic chain in DSPE-PEG (2000) biotin will be incorporated into the PLGA matrix. Prior to emulsification, 18 mg of $PLGA_{50:50}$ were dissolved in 1.2 ml of DCM and combined with 900 μl of 10 mg/ml DSPE-PEG (2000) biotin in DCM, followed by the addition of 1% PVA aqueous solution to the organic phase. Homogenization was performed at 25000 rpm for 5 min on ice. By magnetic stirring in hood for 3.5 h to evaporate DCM, the residual of the organic solvent was removed. Particles were collected through centrifugation and then washed twice with 5 ml of ultrapure water by centrifuging at 15k rcf, 4 °C for 20 min. To protect the freeze-dried material, 4 ml of 2% trehalose

aqueous solution was used as the lyoprotectants (Bissoyi, A., et al. 2016) and particles were re-suspended in this solution. Then, pre-freezing was performed by rotating the glassware containing particle suspension in dry ice-acetone bath (Phipps, A., et al. 1968). After overnight lyophilization, particles were collected and stored in a glass vial wrapped with parafilm and foil, and then saved inside a desiccator at 4 °C. The yield of this PLGA-biotin particle preparation is 86 mg of white powder.

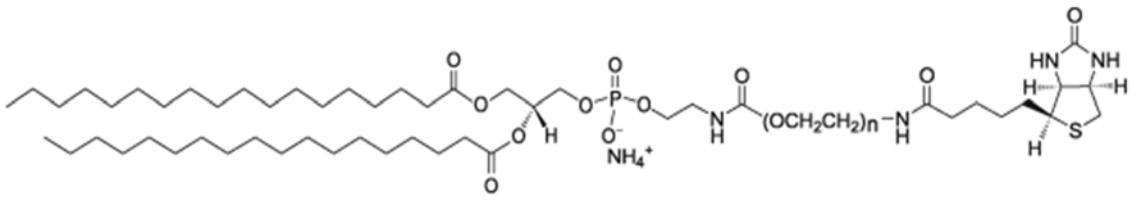

Figure 2-3. The chemical structure of DSPE-PEG-biotin.

2.2.3. PLGA-blank Particle Preparation

PLGA-blank particles were prepared to function as a proper control that can reveal the effect of surface modification on PLGA particles. The method employed is also double-emulsion solvent evaporation. Organic phase is composed of 45 mg $PLGA_{50:50}$ dissolved in 3 ml of DCM, while the water phase is 20 ml 1% PVA aqueous solution in ultrapure water prepared by stirring with heating around 90 ºC overnight. Water phase was added to organic phase prior to the homogenization at 25000 rpm for 5 min on ice. Residual DCM was evaporated by magnetic stirring in hood for 4 h. Particles were then washed twice with 10 ml ultrapure water by centrifuging at 15k rcf, 4 ºC for 20 min. Then, particles were re-suspended in 10 ml 2% trehalose aqueous solution. Particle suspension was pre-frozen in

dry ice-acetone bath, followed by overnight lyophilization. Finally, completely dried particles were collected and stored in a glass vial wrapped with parafilm and foil, and then saved inside a desiccator at 4 °C. After complete lyophilization, the yield of PLGA-blank particle preparation is 197 mg of white powder.

2.2.4. PLGA-biotin Particle Characterization

2.2.4.1. Characterize Particle Size and Zeta Potential of PLGA-biotin Particle

The size and Zeta potential of PLGA-biotin particles were measured by the Malvern Zetasizer Nano-S (Malvern Instruments, UK) using the method of DLS (Stetefeld, J., et al. 2016). Similar to the DLS measurement for PLGA-Ni particles, a series of PLGA-biotin particle suspensions were prepared to find the most suitable concentration for DLS measurements. First, 5 mg of PLGA-biotin particles were washed with 1ml of ultrapure water to get rid of trehalose, followed by re-suspending in 1 ml of ultrapure water. Next, this suspension was diluted 2X, 10X, 20X, 50X, and 100X to make particle suspensions with different concentrations. Then, particle size was measured on different dilutions using DLS. The concentration at which both the attenuation and number of runs are ideal is considered to be the best concentration for the measurement. Accordingly, both particle size and Zeta potential of PLGA-biotin particles were then measured at this concentration.

2.2.4.2. Determine the Endotoxin Level in PLGA-biotin Particles

To evaluate the level of endotoxin contained in PLGA-biotin particles, endotoxin-free water was used for all steps in the preparation of PLGA-biotin particles. The endotoxin concentration of prepared PLGA-biotin particles was quantified using Limulus Amebocyte Lysate (LAL) chromogenic endotoxin quantitation kit.

Determining endotoxin levels is important to assess the efficiency of endotoxin removal methods and prevent endotoxic shock, inflammation and/or sepsis in tissue culture cells and animals injected with formulations contaminated by endotoxin (Galanos, C. and M. A. Freudenberg, 1993). To evaluate the level of endotoxin contained in PLGA-Ni particles we prepared, endotoxin-free water was used for all steps in the preparation process of PLGA-Ni particles. The endotoxin concentration of PLGA-Ni particles was quantified using LAL chromogenic endotoxin quantitation kit via a chromogenic signal generated in the presence of endotoxins. Briefly, the LAL enzymatic cascade is activated by endotoxin at pH 6.0 to 7.5 and the amount of activated enzyme present is measured by its ability to cleave a chromogenic substrate at pH 8.0 to 9.0, where the color formation can be used to quantify endotoxin (Lindsay, G. K., et al. 1989, Roslansky, P. F. and T. J. Novitsky, 1991).

According to the user guide of Pierce LAL chromogenic endotoxin quantitation kit, a small volume of the sample (10 µl) is combined with LAL, and endotoxins in the sample activate the proteolytic activity of Factor C. When the chromogenic substrate is added, the activated protease catalyzes the cleavage of p-nitroalinine (pNA), resulting in yellow color that can be quantitated by measuring the absorbance at 405 nm (A405) and extrapolating against a standard curve. A standard curve was created using the E. coli endotoxin standard included

with each kit to calculate endotoxin levels as low as 0.1 EU/ml, where one endotoxin unit/ml (EU/ml) equals approximately 0.1 ng endotoxin/ml of solution.

By testing the endotoxin standard solutions, an endotoxin standard curve was established. Then, PLGA-biotin suspensions were measured on a microplate absorbance reader at 405 nm within about 30 minutes. Finally, the endotoxin concentrations of the samples, in this case PLGA-biotin suspensions, were calculated based on the linear regression equation from the standard curve.

2.2.4.3. FTIR Analysis for PLGA-biotin Particles

Fourier-transform infrared spectroscopy (FTIR) is a technique used extensively for the characterization of organic, polymeric, and in some cases, inorganic materials (Berthomieu, C. and R. Hienerwadel 2009). Because FTIR test uses infrared light to scan samples and produce different spectral fingerprints for different chemical structures, it is commonly used to observe chemical properties (Kocak, A., et al. 2009).

Before FTIR analysis begins, the first step is to collect a background spectrum that can be subtracted from the test spectra. This will ensure that the actual sample is all that is analyzed (Brault, J. W. 1996). Then the samples are analyzed by fully-computerized FTIR spectrometer. Three samples were tested in this experiment, namely, 5 mg of PLGA-biotin particles, 5 mg of PLGA-blank particles, and 5 mg of biotin. PLGA-blank particles were

included to eliminate the influence of PLGA and trehalose on the spectrum of PLGA-biotin, which facilitates effective comparison between PLGA-biotin and biotin.

A Nexus 470 Fourier Transform Infrared (FTIR) spectrometer was used to analyze the functional groups present at the surface of PLGA-biotin and PLGA-blank particles. Each sample was analyzed under inert conditions with 256 scans and a 4 cm^{-1} resolution. After each scanning, the FTIR spectrometer generates a profile in the form of an absorbance spectra, which shows the unique chemical bonds and the molecular structure of the sample material. To make the spectra in a form suitable for analysis, the absorbance peaks were converted to transmittance and the baseline was corrected for each sample.

2.2.5. Loading of Proteins on PLGA-biotin Particles

2.2.5.1. Loading of Avidin on PLGA-biotin Particles

It is expected that the PLGA-biotin particles prepared using the approach described above have the ability to bind avidin. To prove this, 5 mg of PLGA-biotin particles were washed and re-suspended in 0.5 ml PBS. Then, 5 µg of avidin was added to the particle suspension. To compare the function of biotin molecules and nickel atoms on the surface of PLGA particles, 5 mg of PLGA-Ni particles were included and treated using the same procedure. Three control groups were designed, namely, PLGA-biotin particle suspension without avidin, PLGA-Ni particle suspension without avidin, and 10 µg/ml avidin solution in PBS. All samples were incubated at room temperature for 1 h before the supernatants were

collected by centrifuging at 13600 rcf, 4 °C for 20 min. Pellets were re-suspended in 0.5 ml of PBS.

To identify the proteins contained in the supernatants and pellets, SDS-PAGE electrophoresis was conducted, followed by silver staining.

2.2.5.2. Loading of His-pG on PLGA-biotin Particles

It is expected that the PLGA-Ni particles prepared as described above have specific binding with His-pG. Conversely, PLGA-biotin particles should not show binding affinity for His-tagged proteins. To prove this, 5 mg of PLGA-Ni particles were washed and re-suspended in 0.5 ml pH 8 Tris buffer. Then, 3 μg of His-pG was added to the particle suspension. For the purpose of comparing the surface properties, 5 mg of PLGA-biotin particles were treated with the same procedure. There were also three control groups included, namely, PLGA-biotin particle suspension without His-pG, PLGA-Ni particle suspension without His-pG, and 10 mg/ml His-pG solution in PBS. All samples were incubated at room temperature for 1 h before the supernatants were collected by centrifuging at 13600 rcf, 4 °C for 20 min. Pellets were re-suspended in 0.5 ml of PBS solution.

The supernatants and pellets saved were then used to run SDS-PAGE electrophoresis to identify the proteins contained by silver staining.

2.2.6. Quantification of Biotin on the Surface of PLGA-biotin Particles Using HABA/Avidin Assay

HABA (4-hydroxyazobenzene-2-carboxylic acid) is an avidin-binding dye that binds to avidin to produce a yellow-orange colored complex which absorbs light at 500 nm (Green, N. M. 1965). The following Figure 2-4 and Figure 2-5 show the structure of HABA and the HABA molecule in the binding site of avidin, respectively (Livnah, O., et al. 1993). The H-bonds are shown in thin dashed lines. Biotin, Thr^{35} and Phe^{72} (displayed in dashed lines) from the avidin/biotin complex are superimposed to show the relative positions of the two ligands and the key differences in the positions of Thr^{35} and Phe^{72} in the binding sites of the complexes (Livnah, O., et al. 1993). It is demonstrated in Figure 2-5 that the confirmation of the aromatic amino acids in avidin, including tyrosine, tryptophan and phenylalanine, were changed. As a result, the complex of avidin and HABA absorbs light at 500 nm.

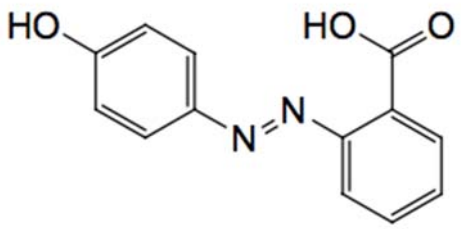

Figure 2-4. The chemical structure of HABA.

Because of the lower affinity of HABA for avidin (K_d = 5.8x10^{-6} M), biotin can stoichiometrically displace HABA from its interaction with avidin and subsequently

decrease the absorption of HABA-avidin complex at 500 nm (A500) proportionately (Verdoliva, A., et al. 2010). This change in A500 relates to the amount of biotin in the sample and provides a basis for spectrophotometric determination of biotin levels in biological samples (Green, N. M. 1965). HABA/avidin reagent, therefore, enables an estimation of the mole-to-mole ratio of biotin to avidin. By this method, an unknown amount of biotin present in a sample can be quickly evaluated by measuring the absorbance of the HABA-avidin solution before and after addition of the biotin-containing sample. It has been reported in many literatures that HABA can be used for detection, localization, isolation, and purification by taking advantage of its interaction with avidin that results in a red shift to 500 nm (Hofstetter, H., et al. 2000, Magnotti, R., et al. 1999, Moor, N., et al. 2007).

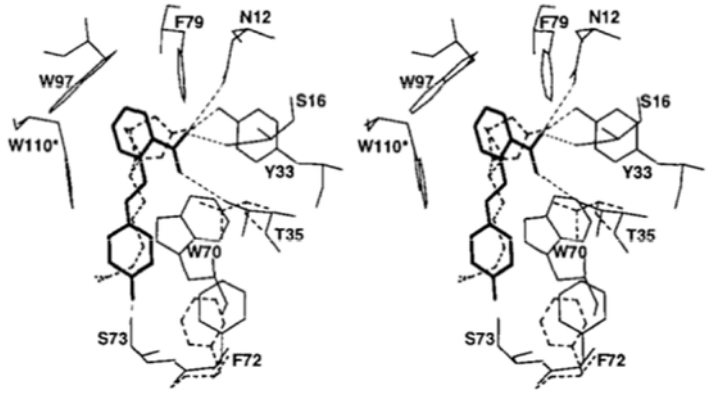

Figure 2-5. Stereoscopic view showing the amino acid residues involved in forming the avidin/HABA complex.

HABA/avidin reagent is specific for chromogenic applications that depend upon quantification of biotin (Green, N. M. 1965). To quantify the amount of biotin on the

surface of PLGA-biotin particles, a suspension of PLGA-biotin particles is added to the HABA/avidin solution, a mixture of HABA and avidin. The following assay is based on the binding of the dye HABA to avidin and the ability of biotin molecules on PLGA-biotin particles to displace the dye in proportions. By this method, the unknown amount of biotin present on PLGA-biotin particles can be evaluated by measuring the absorbance of the HABA-avidin solution before and after the addition of PLGA-biotin particle suspension.

Table 2-1. Compare biotin, desthiobiotin and HABA binding affinity for avidin.

	K_d
Biotin	10^{-15} M
Desthiobiotin	10^{-11} M
HABA	5.8x10-6 M

2.2.6.1. Standard curve for the interaction between biotin and HABA/avidin

Prior to analyzing particle samples, a standard curve was established according to the user guide of HABA from Thermo Scientific, in order to assess the dose-response relationship between the concentration of biotin standards and the corresponding decrease in A500. First, HABA solution was prepared by adding 24 mg HABA to 9.9 ml of ultrapure water with 0.1 ml of 1 mol/l NaOH. If HABA does not completely dissolve, add another 0.1 ml of 1N NaOH and filter solution before use. HABA solution was stored at 4 °C. Then, the HABA/avidin solution was prepared. Specifically, 67 µl of 10 mg/ml avidin aqueous solution was added to 40 µl of the HABA solution prepared, and was diluted by adding 1.93 ml PBS solution. The HABA/avidin solution can be stored at 4 °C for up to 2 weeks.

A series of biotin standard solutions were also prepared, including concentrations of 0.01 µg/µl, 0.02 µg/µl, 0.03 µg/µl, 0.04 µg/µl, 0.05 µg/µl, 0.06 µg/µl, 0.07 µg/µl, 0.08 µg/µl, 0.09 µg/µl, and 0.1 µg/µl. Biotin was dissolved in ultrapure water. Then, 150 µl of the HABA/avidin solution was added to each microplate well. The wells were marked with the concentration of biotin that was intended to add to the well after the first scan. Additionally, 150 µl of the HABA solution without avidin was also included to obtain the absorption of HABA itself, which is considered as the background signal in the test. Then, the plate was thoroughly mixed on an orbital shaker for 30 min. Plate reader was used to measure the absorbance of the HABA/avidin solution in each well at 500 nm and the value was recorded as "A500 of HABA/avidin solutions before biotin standards were added". Then, 20 µl of each biotin standard solution was added to a well containing the HABA/avidin solution. For the control, 20 µl of ultrapure water was added instead, to incorporate the biotin concentration of 0 µg/µl in the test. After mixing as described above for 2 h, the plate was scanned for the second time at 500 nm and the result was recorded as "A500 of HABA/avidin solutions after the incubation with biotin standards" once the value remains constant for at least 15 seconds. If the value tested is ≤ 0.15, dilute sample and repeat assay.

2.2.6.2. HABA/Avidin Assay for PLGA-biotin Particles

PLGA-biotin particles were used in this experiment to replace HABA in the HABA/avidin binding assay, for the purpose of quantifying the amount of biotin on PLGA-biotin particles that is solvent-accessible. Similar to the procedure used in establishing the standard curve,

HABA solution and the HABA/avidin solution were prepared first as described above. Then, 10 mg of PLGA-biotin particles were wash 3 times with PBS solution and re-suspended in 20 µl of PBS solution to prepare the PLGA-bioitin suspension. In order to exclude the influence of other functional groups on the surface of PLGA-biotin particles, PLGA-blank particles were included to demonstrate the differences between PLGA-blank and PLGA-biotin. The suspension of PLGA-blank particles was prepared using the same method. The control was also used in this test, where ultrapure water instead of particle suspension was added after the first scan. Moreover, the HABA solution was added as the blank, providing the background signal in the measurements.

For the first scan, 150 µl of the HABA/avidin solution was added to each microplate well. The plate was thoroughly mixed on orbital shaker for 30 min. Plate reader was then used to measure the absorbance of the HABA/avidin solution at 500 nm and the value was recorded as "A500 of HABA/avidin solutions before particles were added". Next, the HABA/Avidin solution was pipetted from each well to an eppendorf tube and added with 20 µl of the PLGA-biotin/PLGA-blank particle suspension. For the control, 20 µl of ultrapure water was added instead to compare the effect of particle suspension against water, which contains 0 µg/µl of biotin. The eppendorf tubes were mixed on a shaker at room temperature overnight, followed by centrifuging at 15k rcf, 4 ºC for 20 min. Then, 100 µl of each supernatant was pipetted to a microplate well. Finally, the plate was scanned for the second time at 500 nm and the results were recorded as "A500 of HABA/avidin solutions before after the incubation with particles" once the values remained constant for at least 15 seconds.

2.2.7. Loading of Antisense Oligonucleotides on PLGA-biotin Particles

Antisense oligonucleotides (ASO) are synthetic single stranded strings of nucleic acids that can bind to RNA and thereby reduce or alter the expression of the target RNA (Goyal, N. and P. Narayanaswami, 2018). They can not only reduce expression of mutant proteins by breakdown of the targeted transcript, but also restore protein expression or modify proteins through interference with pre-mRNA splicing. There has been a recent revival of interest in the use of antisense oligonucleotides to treat diseases such as neurodegenerative disorders using different approaches to prevent disease onset or halt disease progression (Xue, X. Y., et al. 2018, Evers, M. M., et al. 2015). Table 2-2 shows the applications of antisense oligonucleotide drugs in recent studies (Goyal, N. and P. Narayanaswami, 2018).

Table 2-2. Antisense oligonucleotide chemistry and properties.

ASO generation	Chemical modification	Major representative	Nuclease resistance	Target-binding affinity
First generation	Phosphate Backbone	Phosphorothioate oligonucleotides	Yes	Poor
Second generation	Sugar Modification	2'-O-methyl and 2'-O-methoxyethyl ASOs,	Yes	Strong

		Locked nucleic acids (LNA)		
Third generation	Phosphate, ribose and nucleoside modifications	Peptide nucleic acids, Phosphorodiamidate morpholino oligomers	Yes	Strong

Recent studies have shown that ASO is capable of down-regulating the expression of CD86 protein expression on pulmonary dendritic cells and macrophages (Liao, W., et al. 2017). CD86 is a B7-family molecule that is expressed on the surface of pulmonary and thoracic lymph node antigen-presenting cells and is able to deliver essential costimulatory signals to prime naive T-cells upon allergen (Larche, M., et al. 1998). Thus, it is believed that CD86 expression on pulmonary antigen-presenting cells plays a vital role in regulating immune responses and the treatment with ASO may have utility in asthma and other inflammatory lung conditions (Crosby, J. R., et al. 2007).

By combining with mRNA and subsequently disturbing protein translation, ASO is able to reduce the expression of CD86 on the surface of target cells. In this project, ASO is conjugated with Cy3, a dye that can be detected by fluorescence measurement (Mujumdar, R. B., et al. 1993). With attachment of desthiobiotin, Cy3-ASO can be loaded onto avidin through the interaction between desthiobiotin and avidin. Desthiobiotin is a biotin analogue that binds less tightly ($K_d = 10^{-11}$ M) to biotin-binding proteins and is easily displaced by

biotin (Hirsch, J. D., et al. 2002). Although biotin has extremely high binding affinity towards avidin ($K_d = 10^{-15}$ M), desthiobiotin instead of biotin is utilized to bind avidin in this experiment because the biotin/avidin interaction is essentially irreversible under physiological conditions, which is disadvantage to its application (Chivers, C. E., et al. 2010). On the contrary, desthiobiotinylated molecules are easily eluted from the complex in the presence of excess biotin.

On the other hand, avidin can also bind the biotin molecules on PLGA-biotin particles in the mean time since there are four binding sites available on avidin. With proper molar ratio in reaction, Cy3-ASO-desthiobiotin-avidin can be delivered by PLGA-biotin particles. Therefore, PLGA-biotin particle is a promising carrier for ASO delivery. It should be pointed out that desthiobiotinylated ASO is investigated in this project as an application example of biological drugs that can be delivered via PLGA-biotin particles.

2.2.7.1. Standard Curve for the Fluorescence Intensity of Cy3-ASO-DB

To determine the loading efficiency of Cy3-ASO-desthiobiotin on PLGA-biotin particles, the standard curve for fluorescence intensity from Cy3 versus the concentration of ASO was established first. To begin with, a series of Cy3-ASO-desthiobiotin solutions with different concentrations were prepared, including 0.025 μM, 0.05 μM, 0.1 μM, 0.2 μM, 0.4 μM, 0.8 μM, 1.6 μM, 3.2 μM, 6.35 μM, 12.7 μM. Considering the possible influence of PLGA on fluorescence signals, the suspension of 5 mg PLGA-blank particles was then added to each standard solution prior to the two-hour incubation at room temperature. Next,

micro-plate reader was used to scan the fluorescence intensity from Cy3 (excitation: 550 nm/emission: 570 nm) in the Cy3-ASO-desthiobiotin standard solutions. Finally, the standard curve was depicted using the readout from the fluorescence scan.

2.2.7.2. Loading Efficiency of Cy3-ASO-DB on PLGA-biotin Particles

In this experiment, PLGA-biotin particles were incubated with avidin-Cy3-ASO-desthiobiotin complex, followed by scanning the fluorescent from Cy3 in the pellets to determine the loading efficiency of Cy3-ASO-desthiobiotin. First, 5 µl of 10 mg/ml avidin aqueous solution was used to incubate with 15 µl of 1 µg/µl Cy3-ASO-desthiobiotin aqueous solution for 30 min at room temperature. During this incubation, the avidin-Cy3-ASO-desthiobiotin complex was formed. Next, the suspension of 5 mg PLGA-biotin particles was added and incubated with the avidin-Cy3-ASO-desthiobiotin complex at room temperature for 2 h with gentle shaking. Particles were centrifuged down and washed with PBS solution to remove unspecific bindings. By re-suspending the pellets in 100 µl of PBS solution, the sample for fluorescent scan was prepared. In the final step, micro-plate reader was used to scan the fluorescence intensity from Cy3 (excitation: 550 nm/emission: 570 nm) in each sample.

2.2.7.3. Sustained Release of Cy3-ASO-DB on PLGA-biotin Particles

Following the experiment of loading Cy3-ASO-DB to PLGA-biotin particles, pellets were centrifuged down and re-suspended in 1 ml PBS. To monitor the release kinetics of Cy3-

ASO-DB from PLGA-biotin, particle suspension was incubated at 37 ºC. At each predetermined time point (1h, 2h, 3h, 4h, 5h on Day 1, and then once a day from Day 2 to Day 16), centrifuge the pellets at 13500 rcf, 4 °C for 20 min and collect the supernatant (950 µl) for fluorescence scan. Then, the eppendorf tube was replenished with another 950 µl PBS before resuming incubation at 37 ºC. By scanning the fluorescence intensity in the supernatant saved at each time point from the dye Cy3, which has an excitation wavelength at 550 nm and an emission wavelength at 570 nm, the amount of Cy3-ASO-DB released into the supernatant sample was determined. Finally, the cumulative release of Cy3-ASO-DB in PBS was depicted based on the fluorescence scan for each sample.

2.2.8. Targeting Effect of Anti-DEC205 Ab Adsorbed and Delivered by PLGA-biotin Particles

DEC205 is a type I cell surface protein expressed primarily by dendritic cells (DC). As a phagocytosis receptor associated with CD8 T-cell responses, DEC205 plays an essential role in mediating antigen uptake (Birkholz, K., et al. 2010). DEC205+ DCs mediate cross-presentation of antigen, resulting in modulation of CD8+ T-cell responses (Katakowski, J. A., et al. 2016). Thus, DEC205 targeting represents a feasible method to deliver biological drugs to DCs and regulate CD8+ T-cell activation. For instance, when ASO drug is delivered by targeting DEC205+ DCs, the expression of CD86 on the surface of DEC205+ DCs will be decreased after the uptake of ASO and subsequently less CD8+ T-cells will be activated and the inflammatory conditions will be relieved.

To determine the targeting effect of anti-DEC205 antibody as well as the impact of anti-DEC205 antibody on the accumulation of ASO in MHC class-II bone marrow cells *in vitro*, Cy3-ASO-desthiobiotin adsorbed PLGA-biotin particles were loaded with desthiobiotinylated anti-DEC205 antibody, followed by incubation with bone marrow cells. Flow cytometry was utilized to analyze the uptake of the ASO drug in bone marrow cells with and without the treatment of anti-DEC205 antibody, by detecting the fluorescence intensity from Cy3 conjugated on the ASO drug.

First, bone marrow cells were harvested using the following procedure: 1). Euthanize mice and spray the animal surface with 70 % ethanol. 2). Make an incision of the skin in the mid-abdomen and remove the skin from the distal part including the skin covering the lower extremities. 3). Cut off the muscles from the lower extremities using scissors and carefully dislocate the acetabulum from the hip joint, while avoiding breaking the femur head. 4). Remove the remaining muscles from the femur and tibia using a scalpel and scissors and separate the femur from the tibia at the knee joint exercising care to not break the bone ends. Place the bones in a Petri dish containing RPMI on ice. 5). Proceed to the following steps in a hood. Take extra precaution to maintain strict sterile techniques to avoid neutrophil activation. 6). Rinse each bone with 70% ethanol in a Petri dish, followed by washing in sterile PBS within a Petri dish. 7). Inside a clean sterile Petri dish, cut off the epiphyses of the bones and keep them aside. 8). Use a 25-gauge needle and a 10 ml syringe filled with about 5 ml of RPMI (warm up to 37 ºC before using) to flush the bone marrow cells from both ends of the bone shafts onto a 50 ml tube with a 70 μm cell strainer attached. 9). Spin down the suspension at 400 x g for 5 min. Add 5 ml ACK lysing buffer

on ice for 5 min. Then add 5 ml RPMI. Centrifuge at 400 x g for 5 min and remove the supernatant. Wash remaining ACK with 5 ml of RPMI through centrifugation at 400xg for 5 min and remove the supernatant. 10). Wash cells twice with 5 ml sterile PBS, re-suspend in 8 ml of RPMI and count. Keep the cells at 4 ºC. 11). Dispense 1 ml of cell suspension into each well in a 24-well plate. Incubate the cells for 0.5 h at 37 ºC, 5% CO_2.

Next, 3.8 µl of 1 µg/µl Cy3-ASO-dethiobiotin stock solution was incubated with 2.5 µl of 10 mg/ml avidin aqueous solution in an eppendorf tube for 30 min at room temperature. Then, 11 µl of 0.5 mg/ml anti-DEC205 Ab stock solution was added to the avidin Cy3-ASO-dethiobiotin complex and incubated for 30 min at room temperature. The mixture was transferred to another eppendorf tube containing the suspension of 2.5 mg of washed PLGA-biotin particles. Particles were incubated with ASO and anti-DEC205 Ab at room temperature for 2 h to form Cy3-ASO-DB-avidin adsorbed PLGA-biotin particles, which is referred to as "Cy3-ASO-DB-avidin-PB" in the following. The particle suspension was then incubated with 1 ml of bone marrow cells harvested as described above (single cell suspension, $1x10^6$ cells/ml) in serum free media RPMI for 1 h at 37 °C, 5% CO_2. The molar ratio of anti-DEC205 Ab: Cy3-ASO-dethiobiotin: avidin: biotin on PLGA-biotin is 0.1: 1: 1: 10. To stimulate the expression of CD86, each well containing the bone marrow cell suspension was added with 500 ng of lipopolysaccharides (LPS) in 1 ml of serum medium, followed by overnight incubation at 37 ºC, 5% CO_2.

On the next day, cells were pipetted out from each well and washed with 0.5 ml of FACS buffer twice. Then, cells were re-suspend in 200 µl of FACS wash buffer (5% fetal bovine

serum in PBS with 0.1% NaN_3) and dispensed into eppendorf centrifuge tubes. The following procedure was used to stain the bone marrow cells: 1). Split the 200 µl of cell suspension in each tube to two tubes, resulting in $5x10^5$ cells per tube. 2). For half of the tubes, add 4.7 µl of 0.5 mg/ml Mouse BD Fc Block (Purified Rat Anti-Mouse CD16/CD32) to block Fc receptors in flow cytometric analysis. Incubate on ice for 30 min. The following steps are only conducted for these tubes. 3). Quantum satis each tube to 1 ml with FACS wash buffer. Spin at 4 ºC, 10000 rcf for 5 min. Remove the supernatant after each wash carefully. Finally, re-suspend each pellet with 100 µl FACS wash buffer. 4). Based on the amount of cells in each well, add 3 µl Allophycocyanin (APC)-labeled anti-CD86 Ab to each required sample (see Table 2-3 below). Incubate for 30 min on ice, wrapped with aluminium foil. Allophycocyanin (APC) is a fluorescent dye. APC-labeled anti-mouse CD86 antibody is used for cell staining. 5). Wash cells twice with 1 ml FACS wash buffer. Spin at 4 ºC, 10000 rcf for 5 min. 6). Re-suspend cells in 200 µl FACS fixing buffer (2% paraformaldehyde in PBS) and incubate for 10-15 min at room temperature. 7). Wash cells 2-3 times with FACS wash buffer and re-suspend the pellets in 100 µl FACS wash buffer. Ready for flow cytometric analysis. 8). Use the BD Accuri flow cytometer to analyze each sample.

Table 2-3. Sample order of bone marrow targeting experiment.

Name	Bone marrow cells	Cy3-ASO-DB-avidin-PB	avidin-PB	anti-DEC205 Ab	APC-labeled anti-CD86 Ab	Comment
Control 1	+	-	-	-	-	cells only
Control 2	+	-	+	-	-	cells + particles without ASO
Control 3	+	-	+	-	+	stained cells +particles without ASO
Control 4	+	-	-	-	+	single color control for APC
Control 5	+	+	-	-	-	single color control for Cy3
Control 6	+	+	-	-	+	not treated by anti-DEC205 Ab
Exp 1	+	+	-	+	-	not stained by APC
Exp 2	+	+	-	+	+	treated by anti-DEC205 Ab

Flow cytometry was used to measure the differences between bone marrow cells treated and not treated with anti-DEC205 adsorbed PLGA-biotin particles. Fluorescence signal from APC was detected in channel FL4-A; fluorescence from Cy3, the dye conjugated on ASO, was in channel FL2-A. Thus, the fluorescence intensity in FL4-A indicates the amount of cells expressed CD86 on the surface and subsequently interacted with APC-labeled anti-mouse CD86 antibody. On the other hand, the fluorescence in FL2-A channel suggests the accumulation of ASO in the bone marrow cells.

2.3. Results

2.3.1. PLGA-biotin Particle Characterization

2.3.1.1. Characterize Particle Size and Zeta Potential of PLGA-biotin Particle

Dynamic light scattering (DLS) is commonly used to analyze microparticles and nanoparticles. Because small particles in suspension undergo random thermal motion known as Brownian motion, the light scattered by particles can imprint information about their motion and size distribution profile. The best concentration of PLGA-biotin particle suspension for DLS measurement was tested to be 2.5 mg/ml, at which both the attenuation and number of runs showed an ideal value. Hence, the PLGA-biotin particle suspension with 2 times dilution in PBS was selected as the appropriate particle suspension for following DLS measurements including particle size and Zeta potential. The ideal

Figure 2-6. PLGA-biotin particles.

The average particle size detected is 717.83 nm (PDI 0.23) as showed in Figure 2-7, indicating that the size of the PLGA-biotin particles prepared using the method described above are microparticles with a moderately size distribution. Ideally, PLGA-biotin

particles should show a polydispersity index (PDI) lower than 0.1. The PDI measured for this batch of PLGA-biotin particles is slightly higher, but it is still in the acceptable range (0.1-0.4). On the other hand, zeta potential values more electronegative than -30 mV generally represent sufficient mutual repulsion to result in good stability. The average zeta potential of PLGA-biotin particles is measured to be -21.4±0.153 mV (Figure 2-8), which is lower than the ideal values but in the range of the threshold for delicate dispersions where either coagulation or dispersion exists. To improve particle size distribution and zeta potential, the process of preparation needs to be optimized in terms of the homogenization time and rate, the amount of surfactant, and control of temperature throughout the process.

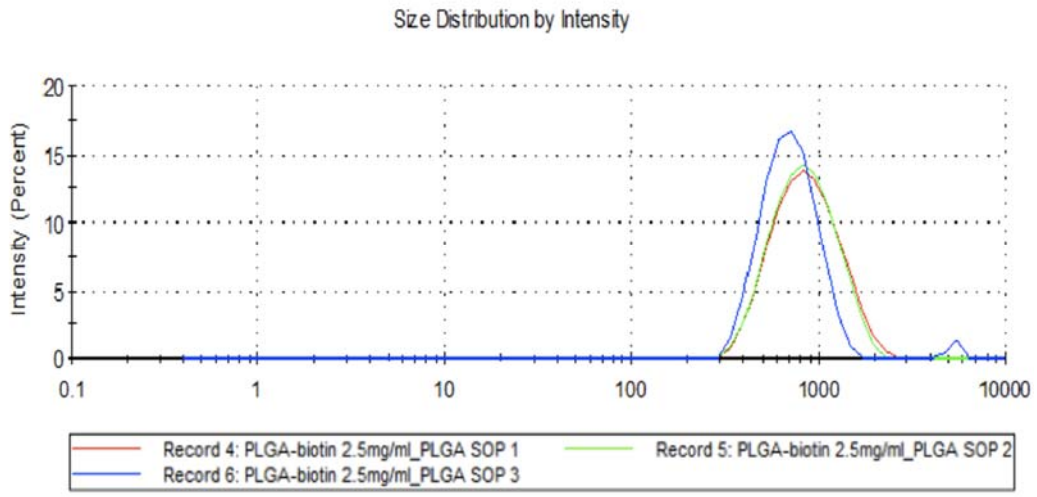

Figure 2-7. Particle size distribution of PLGA-biotin particles using DLS (the concentration of PLGA-biotin is 2.5 mg/ml in pH 7 PBS solution with ionic strength of 162.7 mM).

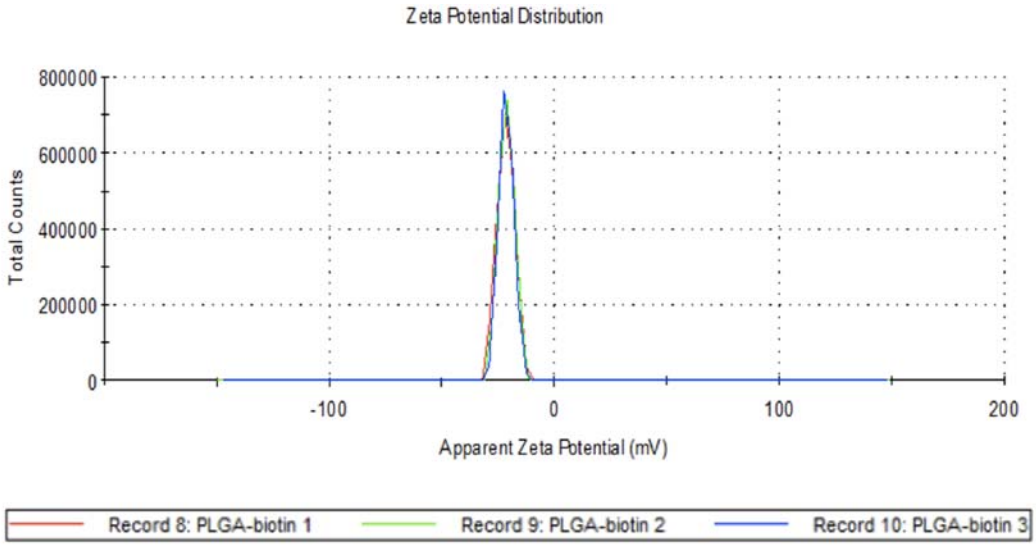

Figure 2-8. Zeta potential of PLGA-biotin particles using DLS (the concentration of PLGA-biotin is 2.5 mg/ml in de-ionized water).

According to our previous study (Reger, N., et al. 2017), the average size of unmodified PLGA particles was 426.8±11.7 nm with a PDI of 0.210±0.008, while the average zeta potential of unmodified PLGA particles was −20.9±0.3 mV. Thus, the measurements of PLGA-biotin showed that the attachment of biotin on PLGA particle has increased the particle size and slightly decreased zeta potential, suggesting the difference between PLGA-biotin and unmodified PLGA particles.

Table 2-4. The results of particle size and zeta potential measurements for PLGA-blank and PLGA-biotin particles using DLS.

	Particle Size (nm)	PDI	Zeta Potential (mV)
PLGA-blank	426.8	0.21	-20.9
PLGA-biotin	717.8	0.23	-21.4

2.3.1.2. Determine the Endotoxin Level in PLGA-biotin Particles

Endotoxin standard curve was established (Figure 2-9) and the linear regression equation was y = 3.2435x - 0.2669, R^2=0.9724. The measurement showed that endotoxin concentration of PLGA-biotin particles was 0.226 EU/mg or 1.01 EU/ml. According to the manual of Pierce LAL Chromogenic Endotoxin Quantitation Kit, the correlation between absorbance and endotoxin concentration is linear in the 0.1-1 EU/ml range. Therefore, the endotoxin level of PLGA-biotin particles dosed *in vivo* could be acceptable as long as the amount of PLGA-biotin particles is determined accordingly to ensure the endotoxin level in dosage is below 5 EU/kg.

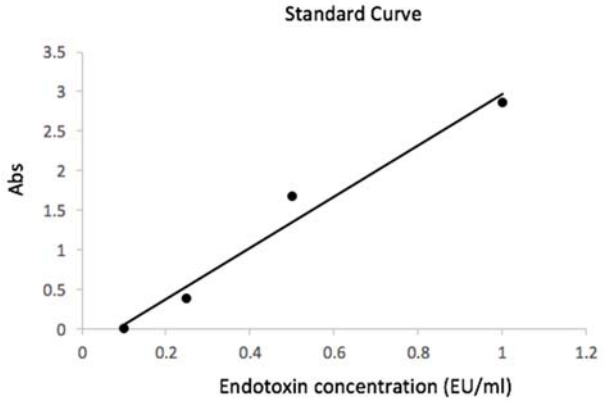

Figure 2-9. Standard curve for the determination of the endotoxin level in PLGA-biotin particles.

2.3.1.3. FTIR Analysis for PLGA-biotin Particles

In this project, FTIR was used to characterize the structure features of PLGA-biotin and to verify the existence of biotin molecules on the surface of PLGA-biotin particles. Because different types of bonds absorb infrared radiation of different wavelengths, the absorbance peaks play an important role in determining whether the functional groups from biotin appeared on PLGA-biotin. The FTIR spectra was then overlapped to provide more detailed information about the functional groups in each sample.

Identification of the chemical features of PLGA and biotin were based on the structures in Figure 2-10 and Figure 2-11. From the FTIR spectrum of PLGA-blank particles, peaks indicating the functional groups found in PLGA were identified (Figure 2-12). The strongest peak at 1761 cm^{-1} can be assigned to the stretching vibration of the carbonyl group (C=O) in PLGA. The band at 802 cm^{-1} is assigned to the C-O-C deformation vibration in the ester bond (R_1-COO-R_2) in PLGA. The band at 916 cm^{-1} most likely arises from the C-H out-of-plane deformation vibration in the aliphatic polyester of PLGA.

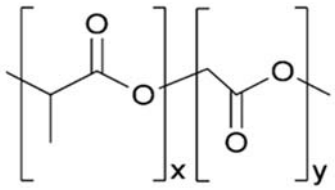

Figure 2-10. The chemical structure of PLGA.

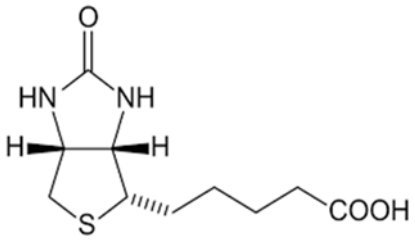

Figure 2-11. The chemical structure of biotin.

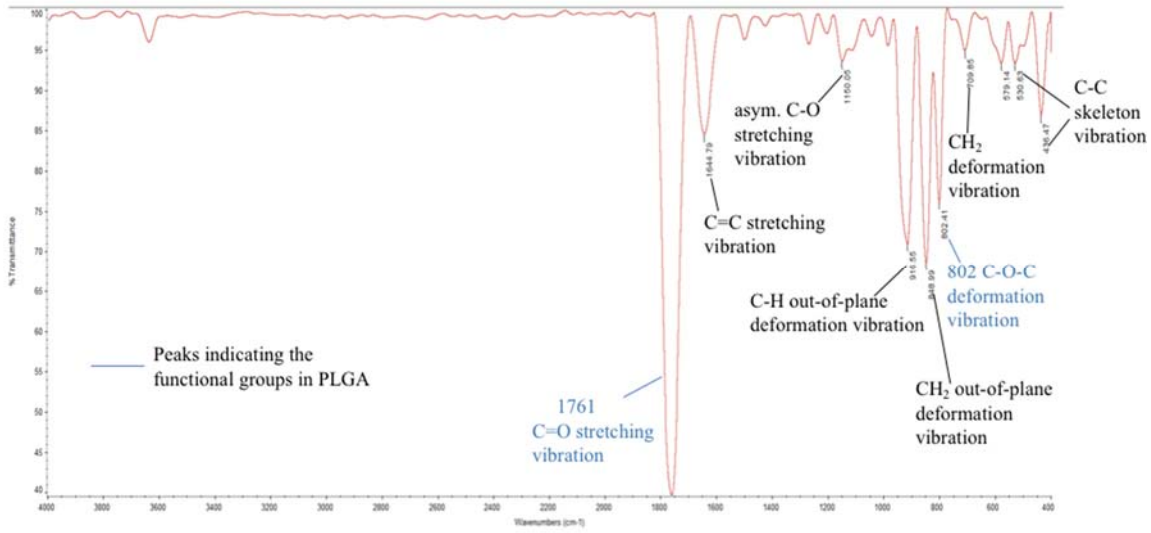

Figure 2-12. FTIR spectrum of PLGA-blank and the peaks indicating the functional groups in PLGA.

The FTIR spectrum of biotin is shown in Figure 2-13. The focus here is biotin-specific spectra features. The strong peak at 3362 cm^{-1} can be attributed to N-H stretching vibration in biotin, specifically the -OC-NH- structure. In addition, the bands at 754 cm^{-1} and 640 cm^{-1} are likely originated from N-H deformation vibration and N-H out-of-plane deformation vibration respectively, supporting the presence of biotin. Additionally, there are two peaks indicating the existence of C-N bond. One is at 1147 cm^{-1}, corresponding to the C-N stretching vibration in -C-NH-C- group; the other is at 1014 cm^{-1}, which

corresponds to stretching vibration of N-C-N. Evidence for the S-C bond in biotin can be found in the PLGA-biotin spectrum: the band at 842 cm^{-1} is attributed to the stretching vibration of S-C, which is one of the structural features of biotin.

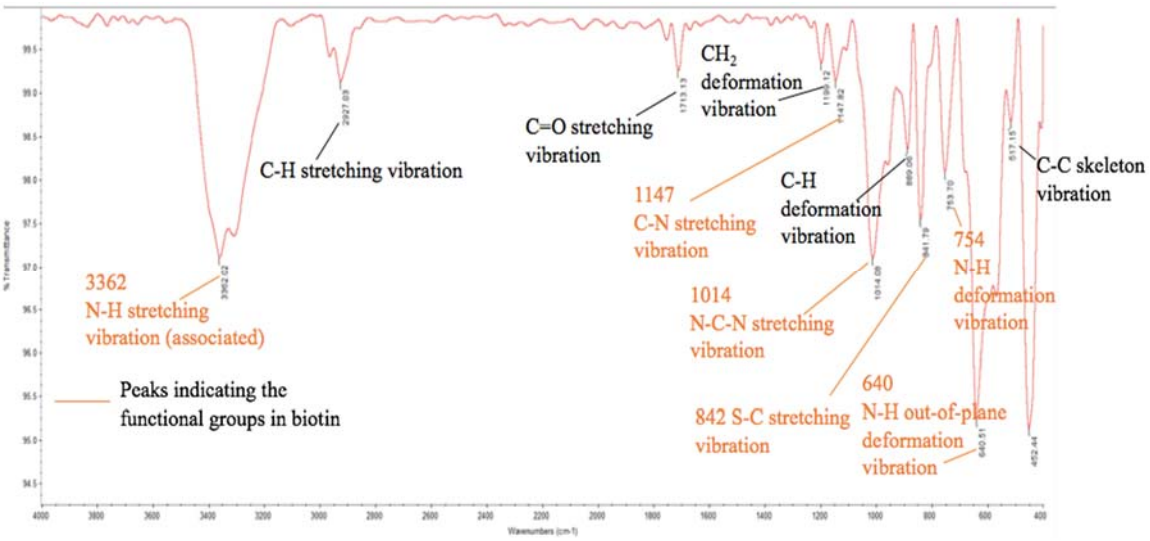

Figure 2-13. FTIR spectrum of biotin and the peaks indicating the functional groups in biotin.

The peaks in the FTIR spectrum of PLGA-biotin particles indicate structural features of both PLGA and biotin (Figure 2-14). First, the strongest peak at 1759 cm^{-1} coincides with the 1761 cm^{-1} peak in the FTIR spectrum of PLGA-blank particles. Thus, it is reasonable to assign this peak to the stretching vibration of the carbonyl group (C=O) in PLGA. Furthermore, the peak at 800 cm^{-1} is similar to the 802 cm^{-1} peak in the FTIR spectrum of PLGA-blank particles. Both can be assigned to deformation vibration of C-O-C, originating from the ester bond (R_1-COO-R_2) in PLGA. This comparison supports the supposition that PLGA-biotin particles share common structural features with PLGA-blank particles as expected.

In addition, peaks indicating the presence of biotin can be found in the spectrum of PLGA-biotin particles. The strong peak at 990 cm^{-1} can be assigned to the stretching vibration of C-N bond and the 690 cm^{-1} peak is due to the out-of-plane deformation vibration of N-H bond in the biotin structure. The peak at 845 cm^{-1} resembles the peak at 842 cm^{-1} peak in biotin spectrum of biotin, as both can be attributed to the stretching vibration of S-C bond. These similar peaks validate the attachment of biotin on PLGA-biotin particles. In addition, the 940 cm^{-1} band is likely due to the stretching vibration of the P-O bond, which is presented in the structure linking the long alkane chain and PEG in DSPE-PEG-biotin (Figure 2-3). The presence of this peak suggests the presence of the biotinylated lipid in the PLGA-biotin sample.

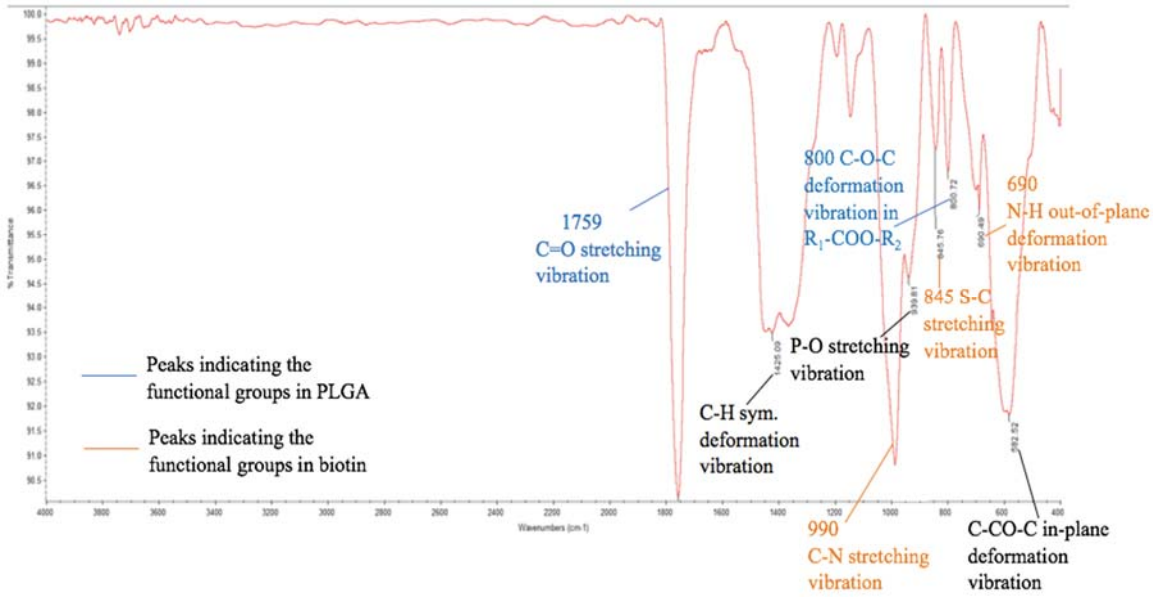

Figure 2-14. FTIR spectrum of PLGA-biotin and the peaks indicating the functional groups in PLGA and biotin.

To highlight the differences in their chemical features, the FTIR spectra of PLGA-biotin, PLGA-blank and biotin were overlapped. When overlapping the spectrum of PLGA-biotin with that of biotin, several pairs of peaks appeared at similar wavelengths (Figure 2-15, Figure 2-16). For example, the 990 cm^{-1} peak in PLGA-biotin and the 1014 cm^{-1} peak in biotin are both related to the stretching vibration of C-N bond. The peak at 845 cm^{-1} in PLGA-biotin and the peak at 842 cm^{-1} in biotin are assigned to the same chemical structure, S-C bond, which features the chemical structure of biotin.

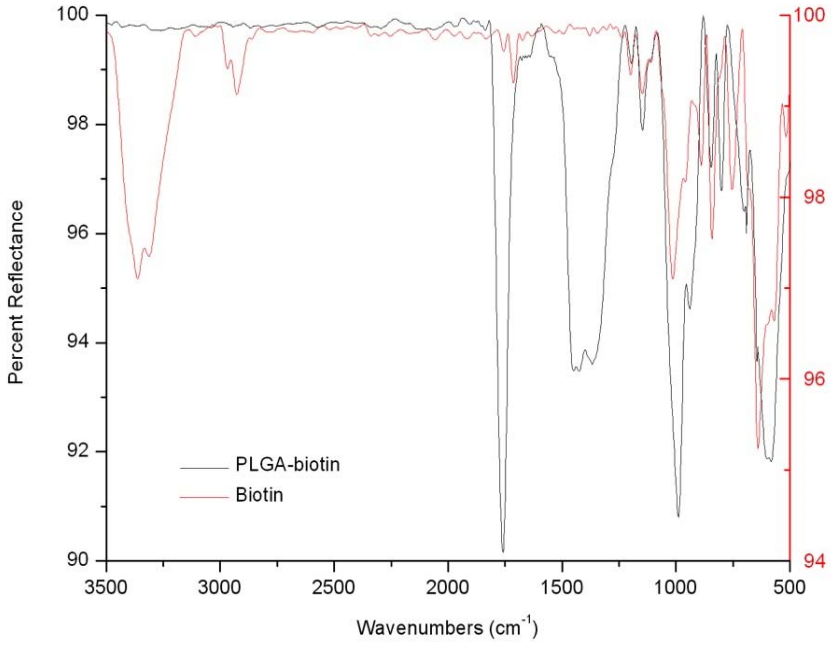

Figure 2-15. Overlap the FTIR spectra of PLGA-biotin and biotin using Origin.

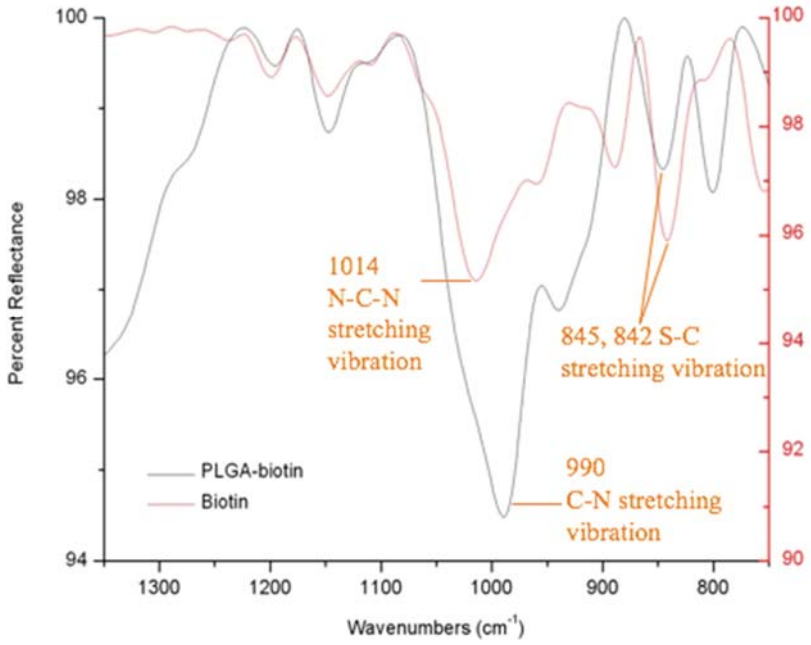

Figure 2-16. Zoomed in overlapped region of PLGA-biotin and biotin.

Such identical peaks are not found in the overlapped spectra of PLGA-blank particles and biotin. In Figure 2-18, the two peaks mentioned above, 842 cm^{-1} and 1014 cm^{-1} in the spectra of biotin were zoomed in. The former is formed by the stretching vibration of S-C bond, and the latter is from the stretching vibration of C-N bond. In contrast to PLGA-biotin particles, the spectrum of PLGA-blank particles does not contain these peaks, which indicate the structural features of biotin were not presented in PLGA-blank sample.

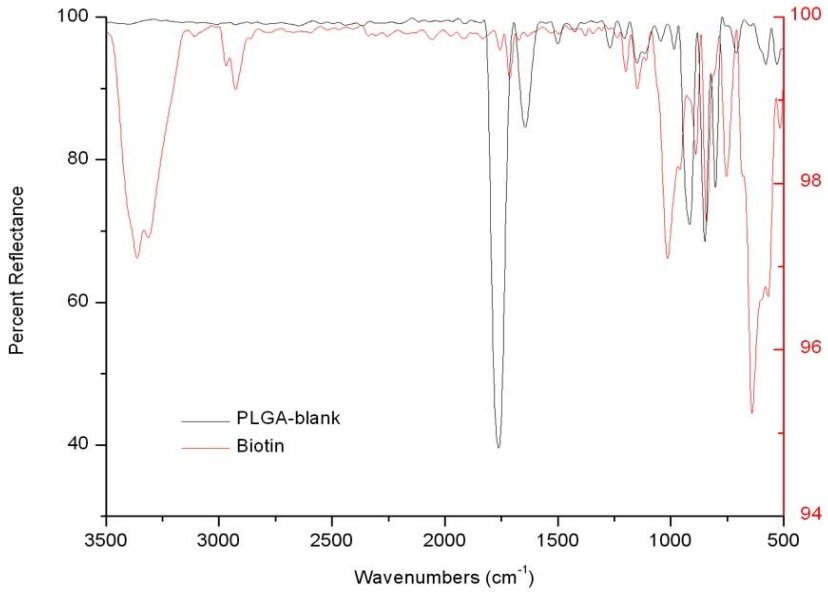

Figure 2-17. Overlap the FTIR spectra of PLGA-blank and biotin using Origin.

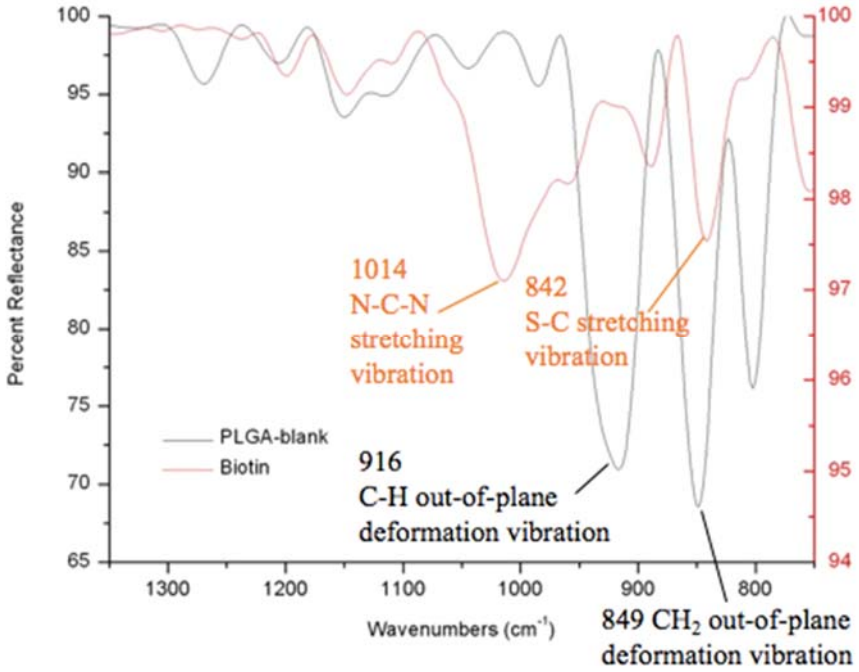

Figure 2-18. Zoomed in overlapped region of PLGA-blank and biotin.

The FTIR spectra of PLGA-biotin and PLGA-blank were also compared by overlapping with each other. As showed in Figure 2-19 and Figure 2-20, similar bands appeared at the wavelengths indicating the chemical structure of PLGA. More specifically, the peak at 800 cm^{-1} in PLGA-biotin and the peak at 802 cm^{-1} in PLGA-blank are both attributed to the C-O-C deformation vibration in PLGA. In consistent with the previous analysis, peaks such as the one from C-N stretching vibration at 990 cm^{-1} showed up again in the FTIR spectrum of PLGA-biotin, suggesting that PLGA-biotin shares peaks with biotin in the mean time.

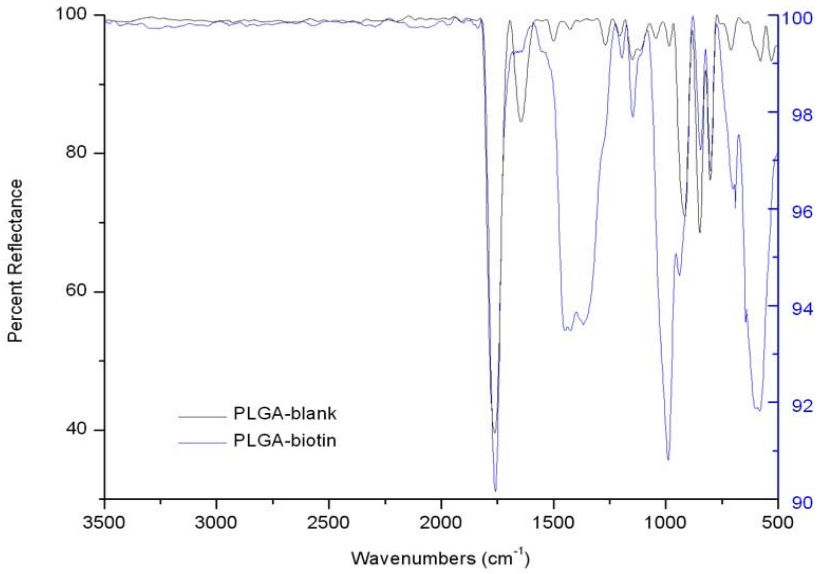

Figure 2-19. Overlap the FTIR spectra of PLGA-blank and PLGA-biotin using Origin.

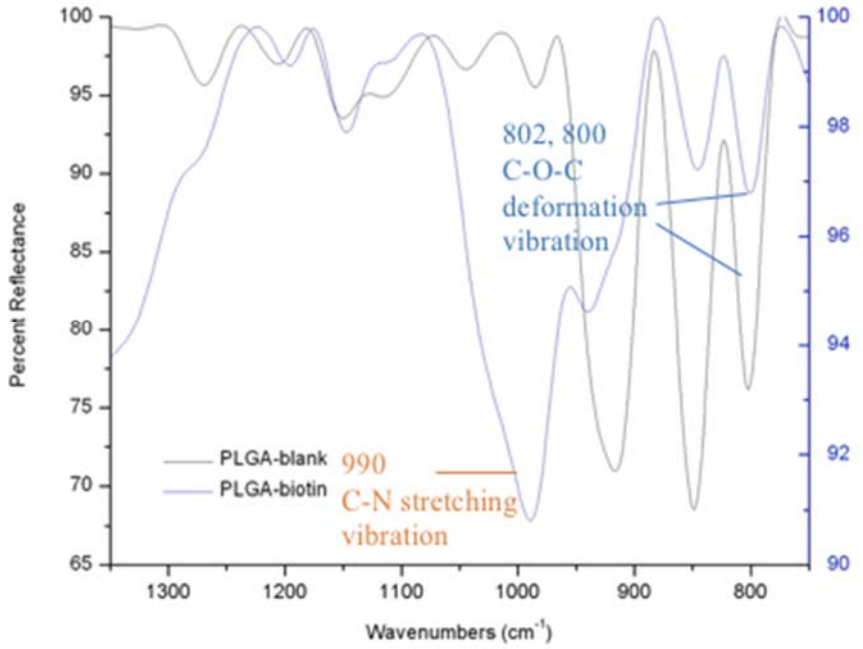

Figure 2-20. Zoomed in overlapped region of PLGA-blank and PLGA-biotin.

From the analysis above, it is observed that PLGA-biotin shares similar FTIR peaks with both PLGA-blank and biotin (Table 2-4). But the common peaks of PLGA-biotin and biotin did not appear in the spectrum of PLGA-blank. It should be noticed that the peak from the deformation vibration of N-H bond was shifted from 640 cm^{-1} in biotin to 690 cm^{-1} in PLGA-biotin. One possible reason for this change is because the biotin molecules were immobilized on the surface of PLGA-biotin particles and thereby absorb at a higher frequency. In addition, the non-specific hydrogen binding between biotin molecules and PVA, which has hydroxyl groups in the structure, on PLGA-biotin is another potential cause for this energy shift. Thus, these results suggest that biotin was detected on PLGA-biotin particles but not on PLGA-blank particles.

Table 2-5. Common peaks between PLGA-biotin and biotin/PLGA-blank.

PLGA-biotin	biotin	Functional Group	Comment
990 cm-1	1014 cm-1	C-N, N-C-N	C-N stretching vibration
845 cm-1	842 cm-1	S-C	S-C stretching vibration
690 cm-1	640 cm-1	-NH-	N-H out-of-plane deformation vibration
PLGA-biotin	**PLGA-blank**	**Functional Group**	**Comment**
1759 cm-1	1761 cm-1	C=O	C=O stretching vibration
800 cm-1	802 cm-1	R_1-COO-R_2	C-O-C deformation vibration

2.3.2. Loading of Proteins on PLGA-biotin Particles

2.3.2.1. Loading of Avidin on PLGA-biotin Particles

The capacity of PLGA-biotin to capture proteins were examined using gel electrophoresis. According to the SDS-PAGE gel image (Figure 2-21), the sample of 3 μg/μl avidin aqueous solution in lane 9 showed the strongest band intensity at 17 kDa, which should be the molecular weight of each subunit in denatured avidin. Because the molecular weight of avidin used is 68 kDa and there are 4 subunits, every subunit should be 17 kDa, which is the same as the protein band identified in the result of SDS-PAGE electrophoresis. Moreover, it has been reported in previous studies that under denaturing conditions, a

spectrum of avidin subunit molecular weight could be ranging between 15-19 kDa (Bayer, E. A., et al. 1986).

The 17 kDa band also appeared in lane 3 and lane 5, supernatants recovered after incubation with avidin. This band did not appear in the pellets of PLGA-Ni after incubating with avidin (lane 4). In contrast, the pellets of PLGA-biotin after incubating with avidin (lane 6) showed this band at 17 kDa. This result demonstrated that avidin was adsorbed on PLGA-biotin particles but did not show specific binding to PLGA-Ni particles, suggesting that biotin molecules were successfully attached onto the surface of PLGA-biotin particles.

Apart from the avidin solutions in lane 7 and lane 9, avidin (68 kDa) only appeared in the supernatants of lanes 3 and 5), in which excess avidin remained undenatured. The reason why this band was not found in the pellets of PLGA-biotin could due to the denaturation of avidin adsorbed on PLGA-biotin particles during sample processing for electrophoresis. The intensity of each protein band was quantified (Figure 2-21). It can be seen that lane 4 showed no significant band intensity at 17 kDa, while the pellets from incubating PLGA-biotin with avidin (lane 6) displayed a band intensity of 502 at 17 kDa. Additionally, by comparing the band intensities in lane 6 and lane 7, Image J analysis suggested that roughly 1/3 of the protein added were captured by PLGA-biotin particles. These results indicate that avidin only has specific binding with PLGA-biotin particles instead of PLGA-Ni particles.

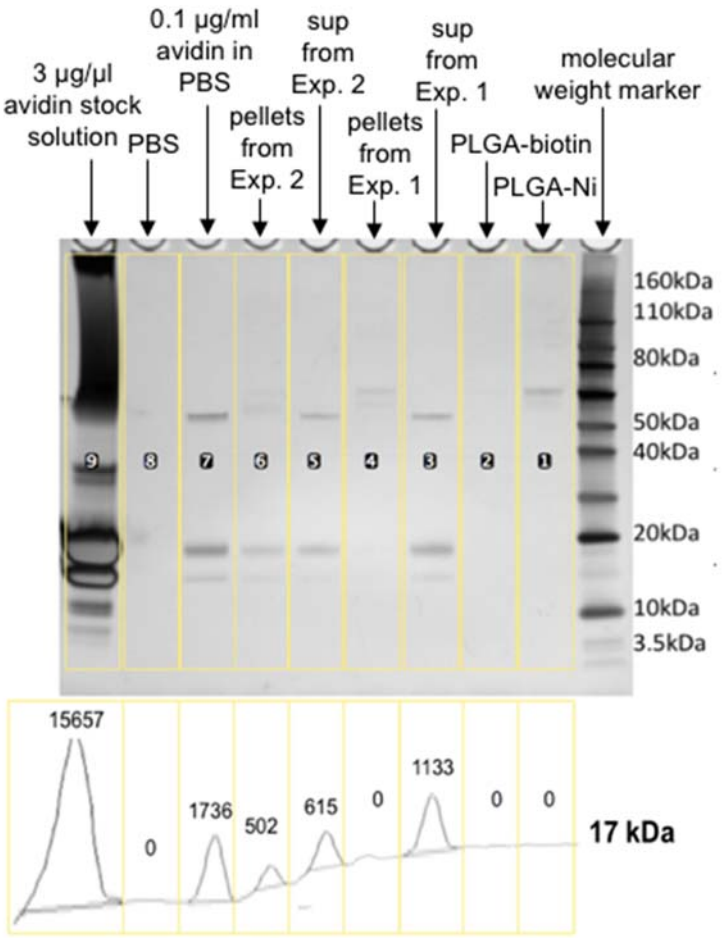

Figure 2-21. Image J analysis for the SDS-PAGE result verifying the loading of avidin on PLGA-biotin and PLGA-Ni particles. Sample order: lane 1-Control 1: PLGA-Ni suspension, lane 2-Control 2: PLGA-biotin suspension, lane 3-supernatant from Exp 1: PLGA-Ni suspension with avidin added, lane 4-pellets from Exp 1, lane 5- supernatant from Exp 2: PLGA-biotin suspension with avidin added, lane 6-pellets from Exp 2, lane 7-Control 3: 5 µg avidin in 0.5 ml PBS, lane 8-Blank: PBS, lane 9-3 µg/µl avidin stock solution, lane mw: molecular weight marker.

The avidin stock solution was added in lane 9, which showed many proteins bands with a higher molecular weight than avidin. One reason for this is that the avidin stock solution is

92% pure with other egg white proteins included. Moreover, under the denaturing condition in SDS-PAGE electrophoresis, avidin is likely to be denatured and the degradants may have aggregations that leads to the upper proteins bands in the gel. However, the strongest band at 17 kDa should come from avidin, since avidin is the main component in this stock solution.

2.3.2.2. Loading of His-pG on PLGA-biotin Particles

The capacity of PLGA-Ni to capture proteins were also examined using gel electrophoresis. In the SDS-PAGE gel image (Figure 2-22), the control His-pG (10 mg/ml PBS) in lane 7 showed the strongest band at 32 kDa, which is the close to the predicted molecular weight of protein G. Because the amount of His-pG added was in excess, both the supernatants collected after particles were incubated with His-pG in lanes 3 and 5 showed an identical band around 32 kDa. However, the pellets collected upon centrifugation demonstrated significant differences in proteins recovered. Following incubation with His-pG, the pellets of PLGA-Ni were loaded in lane 4 and the pellets of PLGA-biotin were added to lane 6. It can be observed that the band of His-pG at 32 kDa showed up in lane 4, but lane 6 did not show this band or any protein bands. This result supports the claim that His-pG binds specifically to PLGA-Ni particles but not PLGA-biotin particles.

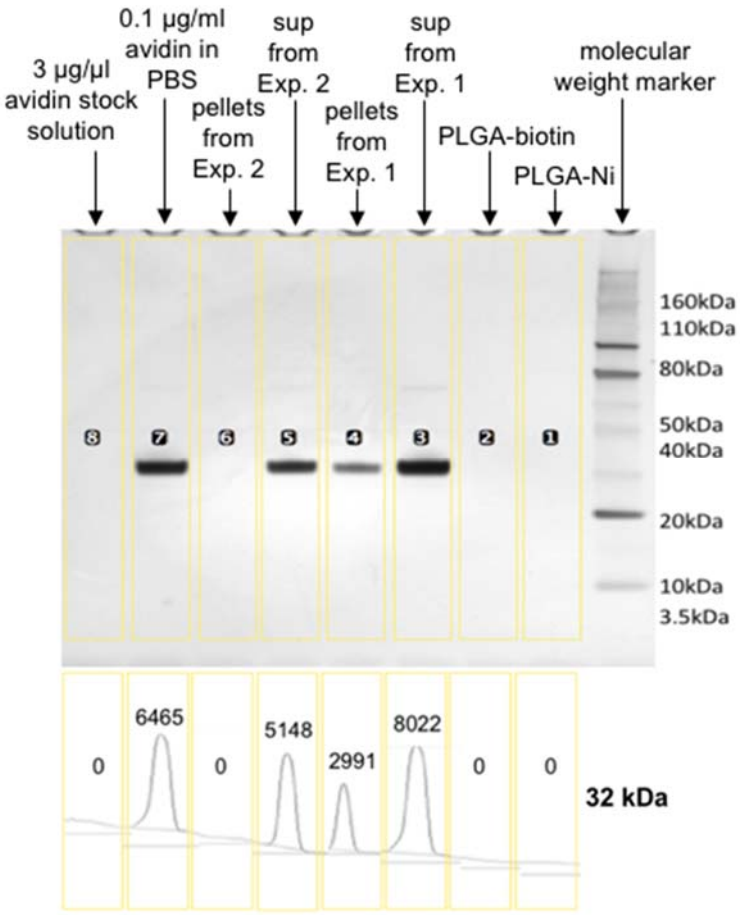

Figure 2-22. Image J analysis for the SDS-PAGE result verifying the loading of His-pG on PLGA-biotin and PLGA-Ni particles. Sample order: lane 1-Control 1: PLGA-Ni suspension, lane 2-Control 2: PLGA-biotin suspension, lane 3-supernatant from Exp 1: PLGA-Ni suspension with His-pG added, lane 4- pellets from Exp 1, lane 5- supernatant from Exp 2: PLGA-biotin suspension with His-pG added, lane 6-pellets from Exp 2, lane 7-Control: 10 mg/ml His-pG in PBS, lane 8-Blank: pH 8 Tris buffer.

2.3.3. Quantification of Biotin on the Surface of PLGA-biotin Particles Using HABA/Avidin Assay

2.3.3.1. Standard Curve for the Interaction between Biotin and HABA/Avidin

By scanning the absorbance of HABA solutions and the HABA/avidin complex, it was observed that the absorbance of HABA, which was higher than 2 at 348 nm, was decreased to around 1.6 after avidin was added (Figure 2-23). In contrast, the absorption at 500 nm was increased from 0.09 in HABA solution to 0.3 in the HABA/avidin complex. Therefore, these results suggest that the HABA/avidin complex has different absorbance properties than HABA solutions due to the binding between HABA and avidin. This shift in absorbance also provides the basis for relating the reduction in A500 to the displacement of HABA from the HABA/avidin complex in HABA/avidin binding assay. Because biotin can displace HABA and consequently decrease the absorption at 500 nm of the HABA/avidin complex, HABA/avidin reagent was used in the binding assay to quantify the amount of solvent-accessible biotin on the surface of PLGA-biotin particles.

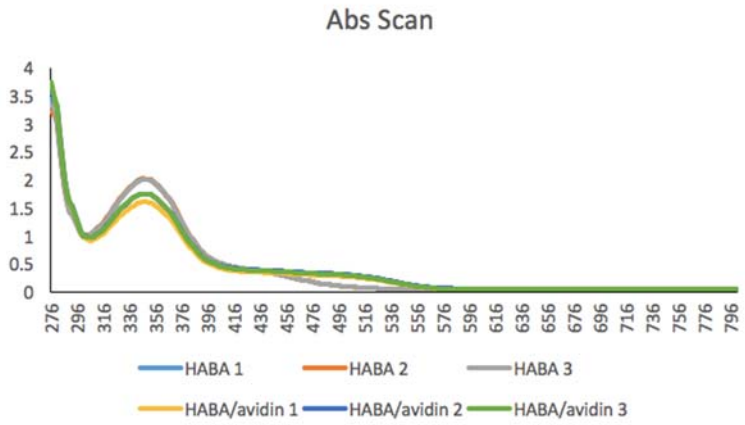

Figure 2-23. Absorbance scan for HABA solutions and HABA/avidin complex.

Specifically, a standard curve was depicted first by incubating biotin standards with the HABA/avidin complex prior to the quantification of biotin using the samples of PLGA-biotin particle suspensions. All the wells showed similar absorption at 500 nm when biotin standards were not added to the mixture of HABA solution and avidin solution. However, distinct changes in A500 were observed in the scan result after incubating the HABA/avidin complex with biotin standards.

Based on these results before and after biotin standards were added, the displacement of HABA was almost completed when the concentration of biotin is higher than 0.08 μg/μl, resulting in an absorption close to the background signal. Therefore, biotin concentrations in the range from 0 to 0.08 μg/μl were selected to depict a standard curve, as showed in Figure 2-24. According to this standard curve, the reaction between biotin and the HABA/avidin complex is very sensitive. The absorption of the HABA/avidin complex at 500 nm starts to decrease significantly when the concentration of biotin solution exceeds 0.03 μg/μl.

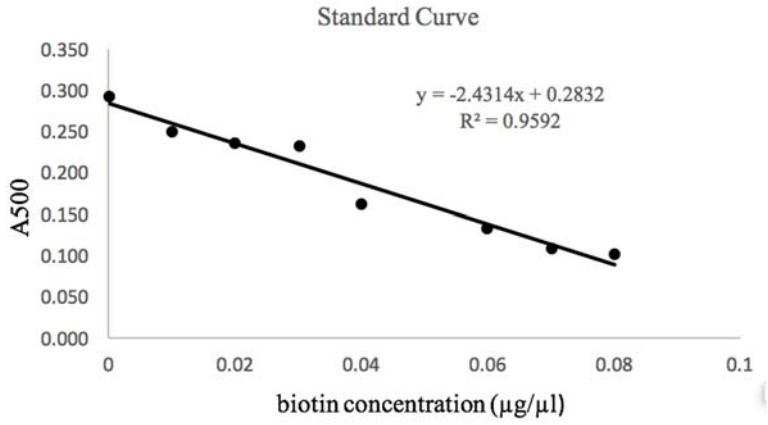

Figure 2-24. Standard curve for HABA/avidin assay.

Using this standard curve, the concentration of biotin in the sample of PLGA-biotin suspension were calculated as the basis for quantifying the amounts of solvent-accessible biotin on PLGA-biotin and the loading efficiency of the biotinylated lipid DSPE-PEG-biotin on PLGA-biotin.

2.3.3.2. HABA/Avidin Assay for PLGA-biotin Particles

HABA/avidin assay was then used to quantify solvent-accessible biotin on PLGA-biotin particles. It should be pointed out that the initial absorbance values were obtained prior to adding the particulate samples. These wells showed similar absorptions at 500 nm before particles were added, which should be the A500 of the HABA/avidin solution (Figure 2-25). The wells marked with "HABA" contained only the HABA solution and showed a weak absorption, which is considered as the background signal.

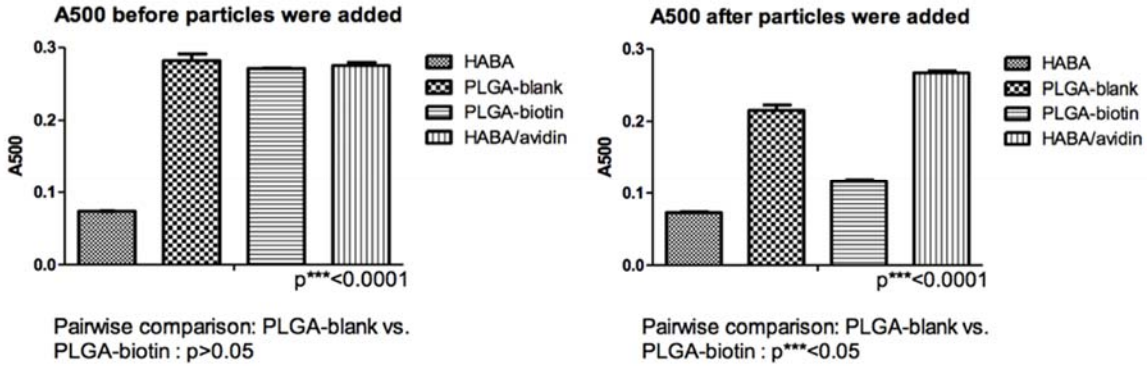

Figure 2-25. The results of the HABA/avidin binding assay before and after adding particles. (a) A500 of HABA/avidin solutions before particles were added (one-way ANOVA proved the four groups were significantly different with a p value <0.0001. Next,

Turkey's multiple comparison test was used to compare PLGA-blank with PLGA-biotin, the p value>0.005 indicates these two groups were similar prior to the incubation with particles), (b) A500 of HABA/avidin solutions before after the incubation with particles (one-way ANOVA proved the four groups were significantly different with a p value <0.0001. Next, Turkey's multiple comparison test was used to compare PLGA-blank with PLGA-biotin, the p value<0.005 indicates these two groups are significantly different).

The absorbance (A500) was reduced after adding the particulate samples to the HABA/avidin solution. Adding PLGA-biotin resulted in a decrease of 78%(±1%), while PLGA-blank reduced it by 31%(±5%). According to statistical analysis using one-way ANOVA and Turkey's multiple comparison, wells added with PLGA-biotin particles showed a more significant decrease in the absorption, indicating that the biotin molecules on PLGA-biotin were able to interact with HABA/avidin and displace HABA molecules. The slight change in PLGA-blank group, on the other hand, was likely caused by nonspecific adsorption of HABA/avidin complex on PLGA-blank particles through hydrogen bonding with the alcohol groups of the surfactant PVA.

Based on the measurements and results above, the amount of biotin on PLGA-biotin particles was calculated. After the incubation with PLGA-biotin particles, the average A500 was decreased by 0.116. According to the standard curve $y = -2.4314x + 0.2832$ ($R^2 = 0.9592$), the concentration of biotin in the PLGA-biotin suspension is 0.069 μg/μl. Thus, 1.38 μg (0.0057 μmol) of biotin was attached on the surface of 10 mg PLGA-biotin particles. This was extrapolated that at least 17.20 μg of DSPE-PEG-biotin (molecular

weight: 3016.81 Da) were incorporated into PLGA-biotin particles. As described in the PLGA-biotin particle preparation method, 9 mg of DSPE-PEG-biotin was added and 84 mg of PLGA-biotin particles were collected. Therefore, the maximum amount of DSPE-PEG-biotin in 10 mg of PLGA-biotin particles was determined to be 107.1 μg. Based on this calculation, 16.1% of the DSPE-PEG-biotin initially added were attached to the surface of PLGA-biotin particles.

In a repeated experiment, similar results were observed. The average A500 was significantly reduced to 0.125 when the HABA/avidin solution was incubated with PLGA-biotin particles, while the PLGA-blank particle suspension did not result in a considerable reduction in the A500 of HABA/avidin complex (Figure 2-26). PLGA-biotin reduced A500 by 83%(±3%), while PLGA-blank reduced it by 22%(±7%). Again, this result suggests that PLGA-biotin and PLGA-blank are significantly different and PLGA-biotin showed a stronger ability of displacing HABA and reducing the absorption of the HABA/avidin complex.

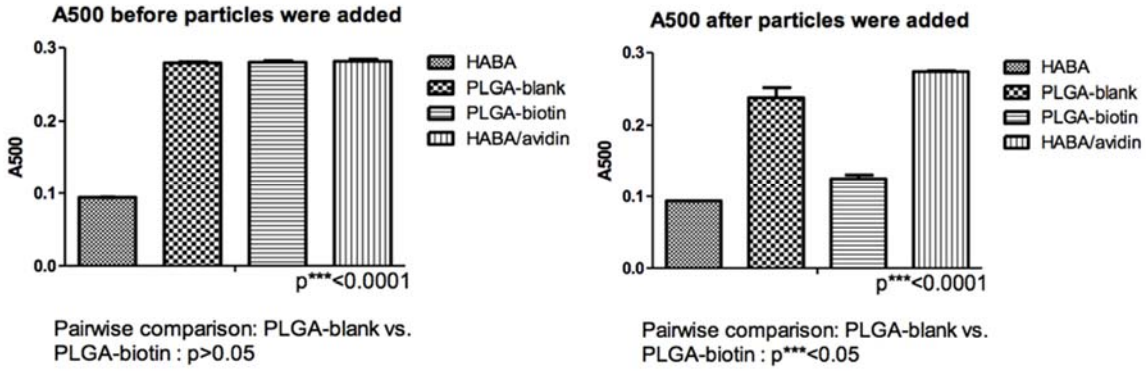

Figure 2-26. The results of the repeated HABA/avidin binding assay before and after adding particles. (a) A500 of HABA/avidin solutions before particles were added(one-way

ANOVA proved the four groups were significantly different with a p value <0.0001. Next, Turkey's multiple comparison test was used to compare PLGA-blank with PLGA-biotin, the p value>0.005 indicates these two groups were similar prior to the incubation with particles), (b) A500 of HABA/avidin solutions before after the incubation with particles (one-way ANOVA proved the four groups were significantly different with a p value <0.0001. Next, Turkey's multiple comparison test was used to compare PLGA-blank with PLGA-biotin, the p value<0.005 indicates these two groups are significantly different).

Based on the standard curve mentioned above, the concentration of biotin in the PLGA-biotin suspension is calculated as 0.063 μg/μl this time. Following the calculation method described in the first experiment, 14.6% of the DSPE-PEG-biotin initially added was attached to the surface of PLGA-biotin particle.

By performing HABA/avidin binding assays, the biotin molecules on PLGA-biotin particles were quantified and the loading efficiency of the biotinylipid DSPE-PEG (2000) biotin on the surface of PLGA-biotin particles was calculated. For the PLGA-biotin particles prepared in this project, the percentage of attached biotin in the total amount added is around 15.4%. This loading efficiency calculated only relates to the amount of the biotinylated lipid that was finally attached onto the surface, but maybe a lot biotin molecules were also incorporated into PLGA-biotin particles, just not exposed on the surface. Thus, a possible way for improving the loading efficiency is to optimize the hydrophobic chain of the biotinylated lipid to achieve a more specific and more effective interaction with the polymer matrix during the particle preparation process. Specifically,

the possible approaches for the optimization of the hydrophobic chain may include modifications such as increasing the chain length and adding hydroxyl groups onto the chain. The former can enhance the hydrophobicity of the chain, making it more likely to be intertwined with the polymer matrix. The latter will enable more non-specific hydrogen binding between the chain and PLGA, but too many hydroxyl groups can also decrease the hydrophobicity. Thus, it is necessary to design and conduct experiments in the future to figure out the optimal length of the chain and most suitable modifications on functional groups including the number of hydroxyl groups added to the chain.

2.3.4. Loading of Antisense Oligonucleotides on PLGA-biotin Particles

2.3.4.1. Standard Curve for the Fluorescence Intensity of Cy3-ASO-DB

The ASO drug Cy3-ASO-DB was loaded on PLGA-biotin as an application example of biological drugs that can be delivered by PLGA-biotin particles. In order to quantify the loading efficiency of Cy3-ASO-DB, the fluorescence intensity of the conjugated dye Cy3 on Cy3-ASO-DB was measured. Thus, based on the standard curve reflecting the relationship between the fluorescence intensity and the concentration of Cy3, the concentration of Cy3-ASO-DB can be determined.

First, from the results of fluorescence intensity measurements, a standard curve was depicted as showed in Figure 2-27. The corresponding linear equation is $y = 3562.5x + 691.85$ ($R^2 = 0.9938$). According to this standard curve, the concentration of Cy3-ASO-DB

in the sample of PLGA-biotin suspension can be calculated. Afterwards, the loading efficiency of the destiobiotinylated ASO drug on PLGA-biotin can also be quantified.

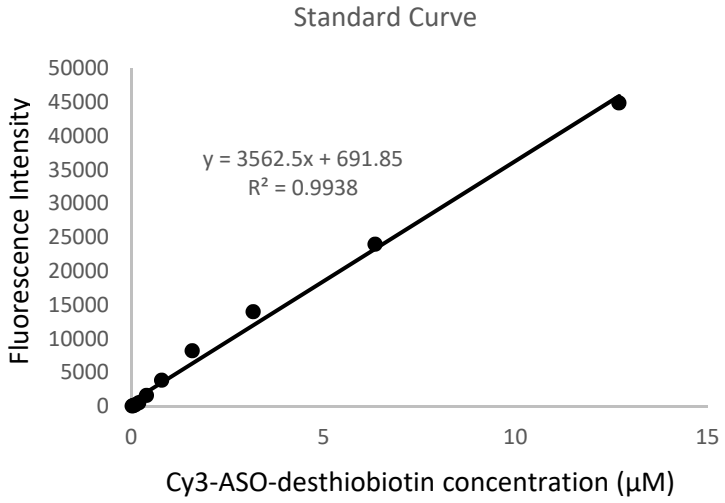

Figure 2-27. Standard curve for the fluorescence intensity of Cy3-ASO-desthiobiotin with PLGA particles added.

2.3.4.2. Loading Efficiency of Cy3-ASO-DB on PLGA-biotin Particles

Three replicates were included. On average, the samples showed a fluorescence intensity of 33473. According to the standard curve y = 3562.5x + 691.85 (R^2=0.9938), the average concentration of Cy3-ASO-desthiobiotin in the samples is 9.2 μM. Based on this result, the amount of Cy3-ASO-desthiobiotin in each sample was calculated to be 0.00092 μmol on average. Since the total amount of Cy3-ASO-desthiobiotin initially added was 0.001397 μmol, the loading efficiency of Cy3-ASO-desthiobiotin turns out to be 65.87% based on this test.

2.3.4.3. Sustained Release of Cy3-ASO-DB on PLGA-biotin Particles

From the fluorescence intensity scans, the concentration of Cy3-ASO-DB in each release sample was calculated and subsequently the cumulative amount of Cy3-ASO-DB released into the release medium was also determined. Finally, the cumulative release of Cy3-ASO-DB was depicted in Figure 2-28. It is demonstrated in this release profile that when adsorbed on PLGA-biotin, Cy3-ASO-DB showed a burst release, followed by a slow release. In addition, 38.7% of the ASO drug was released into the supernatant after the first two weeks.

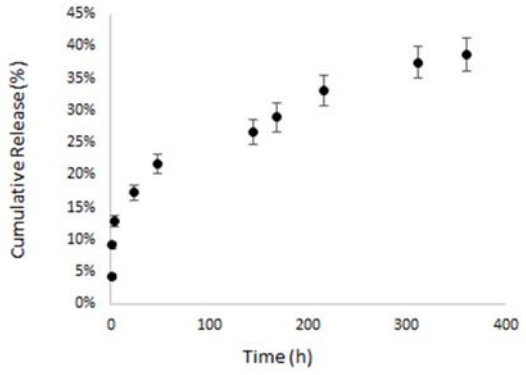

Figure 2-28. The cumulative release of Cy3-ASO-DB from Day 1-Day 16 in PBS at 37 °C (n=3, the excitation/emission wavelength of Cy3 is 550 nm/570 nm).

The initial phase of the release (< 5 h) was likely due to dissociation of Cy3-ASO-DB non-specifically adsorbed on PLGA-biotin particles; the phosphate backbone and bases form hydrogen bonding with the hydroxyl groups in PVA on the surface. There could be two driving forces for the avidin-bound Cy3-ASO-DB drug to be released. First, the

concentration gradient in the release medium drives Cy3-ASO-DB to be dissociated from its interaction with avidin on PLGA-biotin. Second, the degradation of the PLGA matrix resulted in the release of Cy3-ASO-DB in a delayed fashion after ~20 days. Since the dissociation constant of desthiobiotin-avidin interaction is small ($K_d = 10^{-11}$ M), a high percentage of Cy3-ASO-DB was not released until the PLGA matrix in PLGA-biotin particle was degraded. But according to the study on the degradation of PLGA polymers (Figure 1-1), the $PLGA_{50:50}$ polymer matrix would not be degraded in the first two weeks. Thus, the slow release phase in Figure 2-28 should be mainly from the Cy3-ASO-DB released after the dissociation of desthiobiotin from avidin, which is also demonstrated as Phase 2 in the release scheme (Figure 2-29). If the release study was prolonged, a third phase (Phase 3 in Figure 2-29) driven mainly by the degradation of $PLGA_{50:50}$ polymer matrix would appear, where the remaining Cy3-ASO-DB would be released from PLGA-biotin.

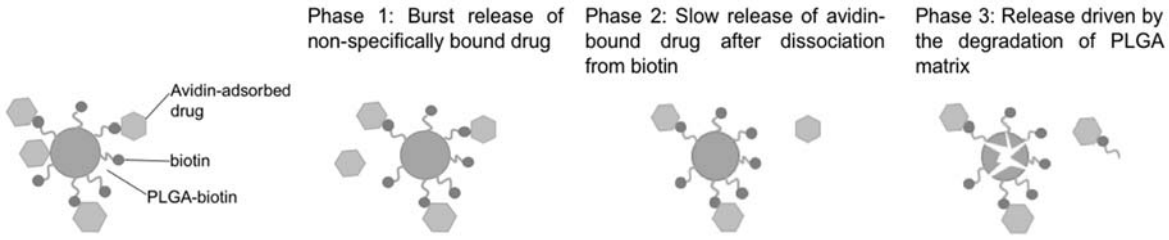

Figure 2-29. Scheme for the proposed release mechanisms of desthiobiotinylated drug from PLGA-biotin particles (for each release phase, there is one dominant release mechanism).

Under physiological conditions, the endogenous biotin molecules will displace desthiobiotin from avidin and facilitate the release of Cy3-ASO-DB from PLGA-biotin. The normal concentration of biotin in plasma ranges from 400-1200 ng/L (Trueb, R. M.

2016), with approximately 81% of biotin in the free form. Thus, it is possible that the adsorbed ASO drug will be displaced by biotin *in vivo,* preceding the dissociation of desthiobiotin from avidin.

2.3.5. Targeting Effect of Anti-DEC205 Ab Adsorbed and Delivered by PLGA-biotin Particles

Anti-DEC205 antibody is believed to be capable of targeting DEC205 molecules expressed on bone marrow cells. Therefore, when anti-DEC205 antibody is adsorbed on PLGA-biotin particles, the biological drug delivered by PLGA-biotin has the potential to achieve a higher uptake by bone marrow cells. To evaluate the targeting effect of anti-DEC205 antibody and its impact on the accumulation of the ASO drug in bone marrow cells, the fluorescence intensity from Cy3 in bone marrow cells was measured by flow cytometry analysis, with and without anti-DEC205 antibody loaded onto PLGA-biotin particles.

For bone marrow cells in Control 1 that were not stained and not treated by Cy3-ASO-DB-avidin-PB, more than 96% of the cells were showed as double negative in Figure 2-30. No significant fluorescence signal was observed from the fluorescent dye APC or Cy3.

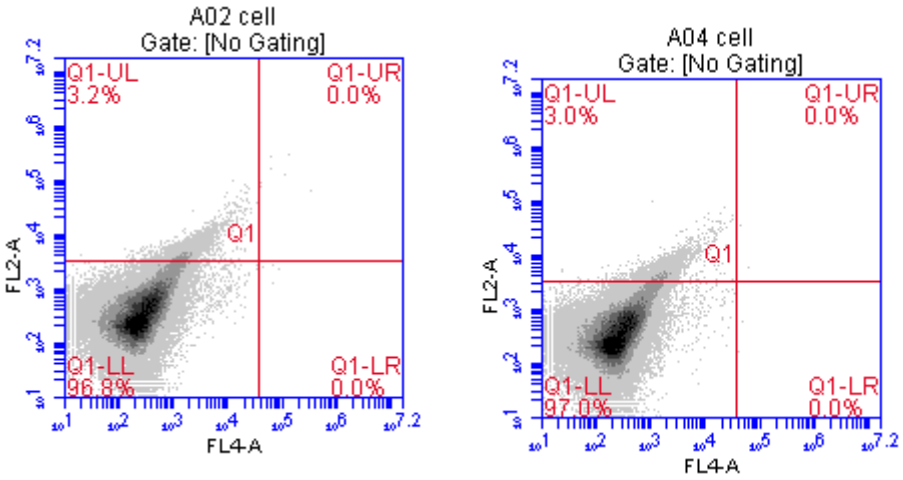

Figure 2-30. The percentage of cells from Control 1 that showed fluorescence in FL2-A and FL4-A.

In Control 2, cells were only incubated with PLGA particles that were not loaded with Cy3-ASO-desthiobiotin. No staining was conducted using APC labeled antibody. However, about 7.7% of the cells showed fluorescence in FL4-A, suggesting that this signal could come from the background (Figure 2-31). No significant fluorescence signal was detected from Cy3 in channel FL2-A.

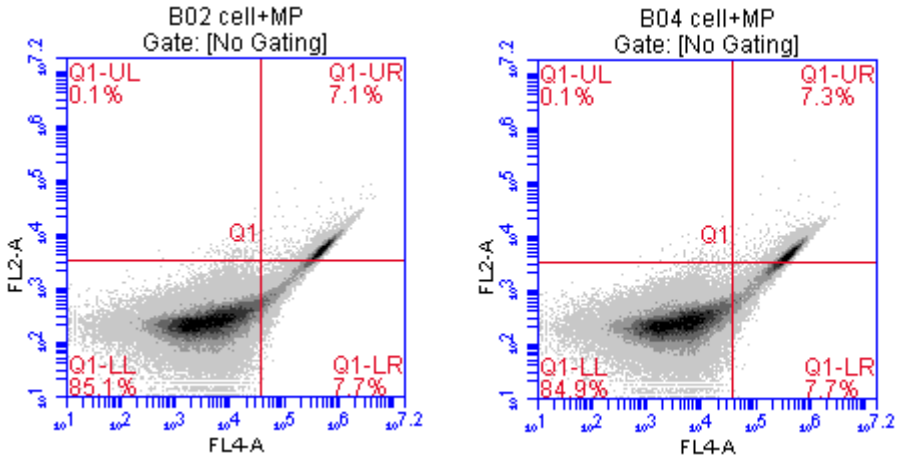

Figure 2-31. The percentage of cells from Control 2 that showed fluorescence in FL2-A and FL4-A.

Bone marrow cells were stained and incubated with PLGA particles in Control 3, but the particles were not treated with Cy3-ASO-dethiobiotin. Around 7.5% of the cells showed fluorescence in FL4-A (Figure 2-32), which is close to the background measured in Control 2. The reasons for this result might be that the bone marrow cells were not completely stained or the cells did not express many CD86 molecules in the first place. In channel FL2-A, still no significant fluorescence signal was observed from Cy3.

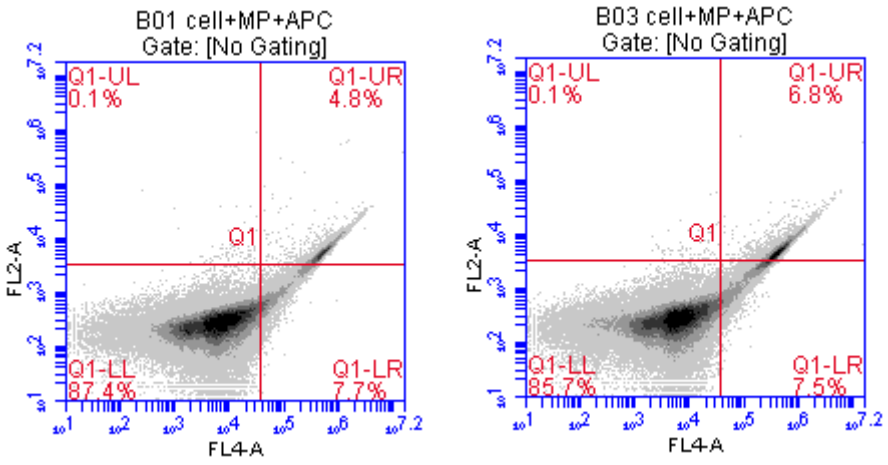

Figure 2-32. The percentage of cells from Control 3 that showed fluorescence in FL2-A and FL4-A.

As showed in Figure 2-33, when the cells were only stained with APC anti-mouse CD86 Ab, only 1% of the cells showed fluorescence from APC and no significant fluorescence signal was detected from Cy3 in FL2-A. Again, this weak fluorescence signal suggests that marrow cells were not completely stained or the cells did not express a significant amount of CD86.

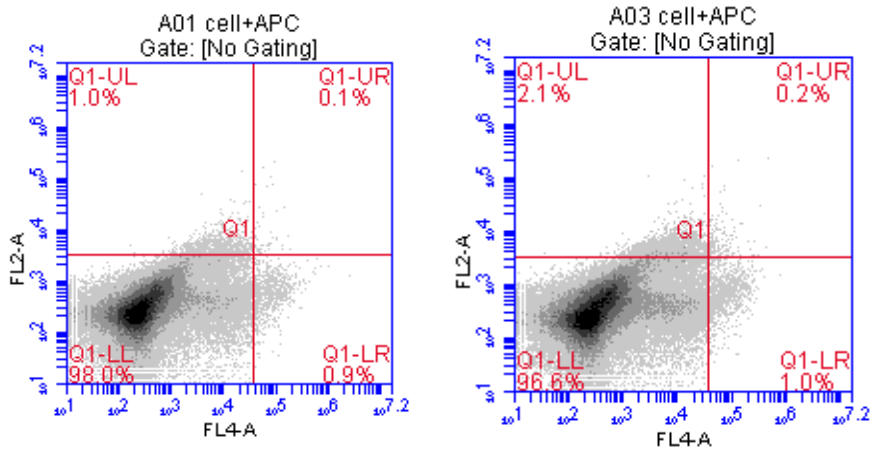

Figure 2-33. The percentage of cells from Control 4 that showed fluorescence in FL2-A and FL4-A.

In Control 5, bone marrow cells were only incubated with ASO-loaded particles, without APC staining or the treatment of anti-DEC205 Ab. In the result (Figure 2-34), about 25% of the cells showed fluorescence signal from Cy3, indicating that these cells were able to uptake ASO. But around 19% of the cells were showed as positive in FL4-A channel even though they were not stained with APC. It is possible that the signal from Cy3 influenced channel FL4-A. However, there were still roughly 9% cells that are negative in FL4-A showed significant fluorescence from Cy3 in FL2-A. This result is used later to assess the effect of anti-DEC205 antibody on the uptake of ASO.

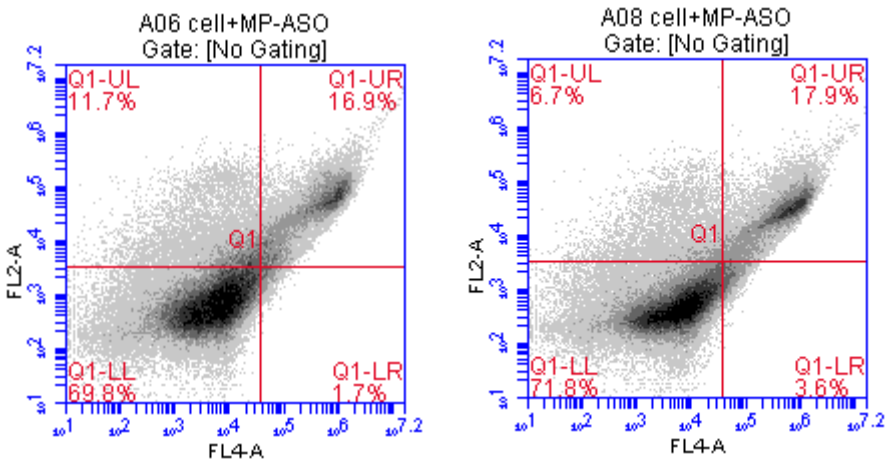

Figure 2-34. The percentage of cells from Control 5 that showed fluorescence in FL2-A and FL4-A.

Cells from Control 6 were included in measurements A05 and A07 (Figure 2-35). These bone marrow cells were stained with APC and incubated with ASO-loaded particles, but anti-DEC205 Ab was not added. About 14% of these cells were detected as double positive, suggesting their ability of taking up Cy3-conjugated ASO. Whether ASO can reduce the expression of CD 86 is later determined by comparing this result with the percentage of double-positive cells in Exp. 2.

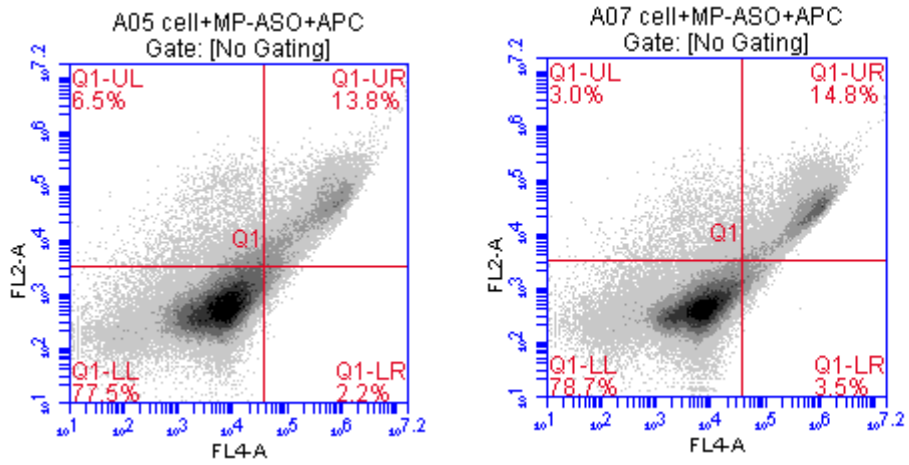

Figure 2-35. The percentage of cells from Control 6 that showed fluorescence in FL2-A and FL4-A.

In Exp. 1, cells were incubated with anti-DEC205 Ab and particles adsorbed with ASO-Cy3, but APC anti-mouse CD86 Ab was not used for staining. As showed in Figure 2-36, about 60% of the cells had fluorescence in FL2-A, indicating that they took up ASO and were labeled by Cy3. But around 20% of the cells were detected as positive in FL4-A channel even though they were not stained. This percentage can be used as a background of APC in analyzing Exp. 2.

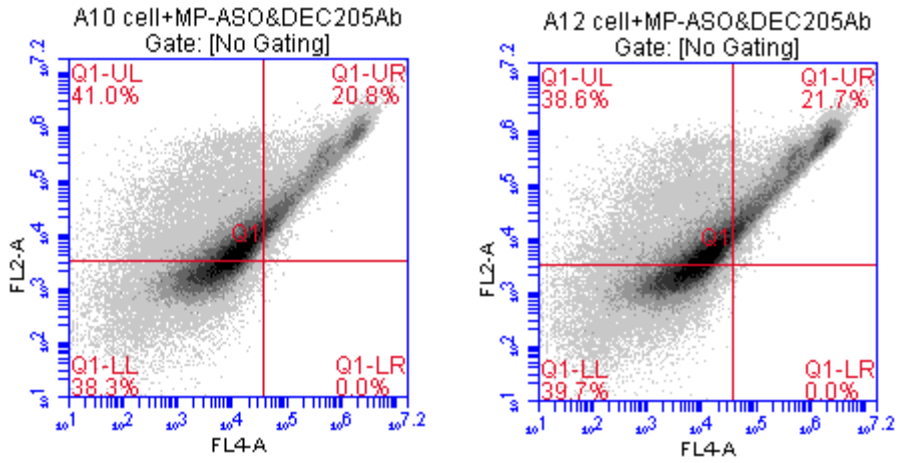

Figure 2-36. The percentage of cells from Exp. 1 that showed fluorescence in FL2-A and FL4-A.

Bone marrow cells were stained by APC and incubated with both anti-DEC205 Ab and ASO-Cy3 adsorbed PLGA-biotin particles in Exp. 2. In Figure 2-37, near 55% cells had fluorescence from Cy3, but only around 16% of the cells were double positive. Comparing with the percentage of double-positive cells in Control 6, i.e. 14%, there is no significant decrease proving the expected effect of ASO on the expression CD86 in bone marrow cells. However, it is noticeable that the cells showed fluorescence signal from Cy3 increased significantly from 25% in Control 5 and 19% in Control 6 to 55% in Exp. 2. Thus, anti-DEC205 still showed an impact on the uptake of ASO in bone marrow cells.

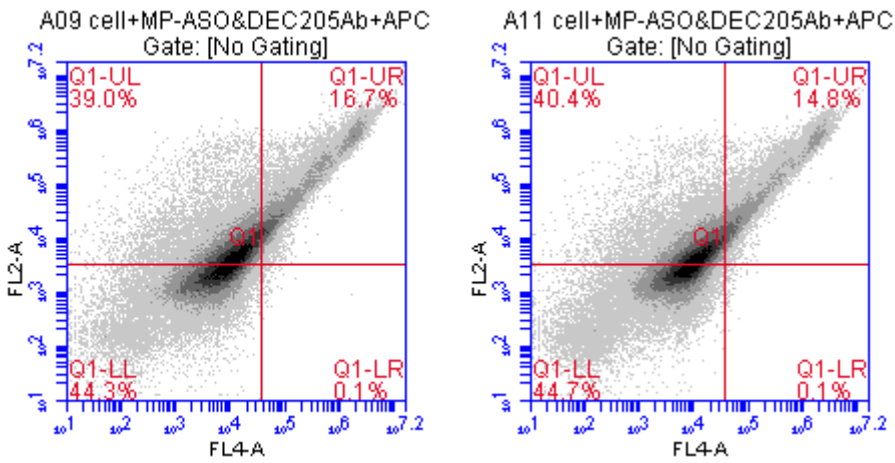

Figure 2-37. The percentage of cells from Exp. 2 that showed fluorescence in FL2-A and FL4-A.

To assess the effect of anti-DEC205 Ab on the uptake of Cy3-conjugated ASO, the fluorescence from Cy3 in FL2-A was corrected by removing the influence of FL-4 in Figure 2-38, Figure 2-39 and Figure 2-40. When there were only cells (Figure 2-38), no fluorescence signal was detected in FL2-A. But after incubating with ASO-loaded particles, more than 55% of the cells were positive in FL2-A channel without the treatment of anti-DEC205 antibody (Figure 2-39). However, after loading anti-DEC205 antibody on PLGA-biotin, over 90% cells incubated with Cy3-ASO-DB adsorbed particles showed positive fluorescence signals from Cy3 in FL2-A (Figure 2-40). This significant increase in the percentage of cells positive in fluorescence channel of Cy3 suggests that anti-DEC205 antibody facilitates the uptake of the ASO drug in bone marrow cells.

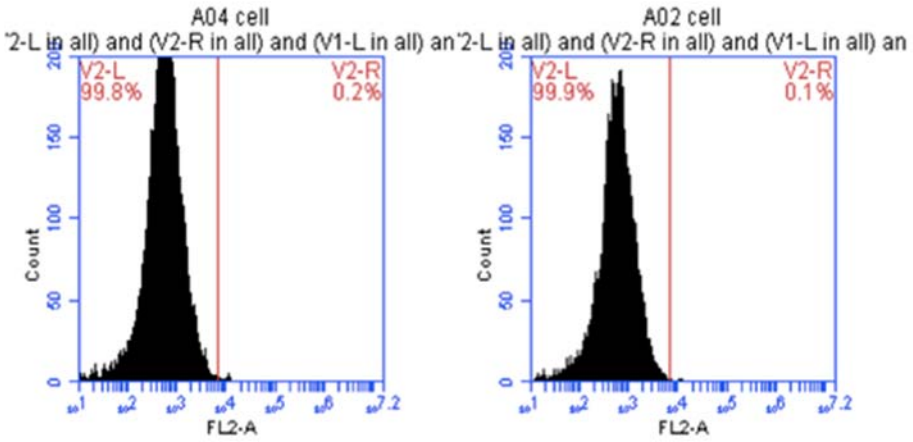

Figure 2-38. The percentage of cells from Control 1 that showed fluorescence in FL2-A with color correction.

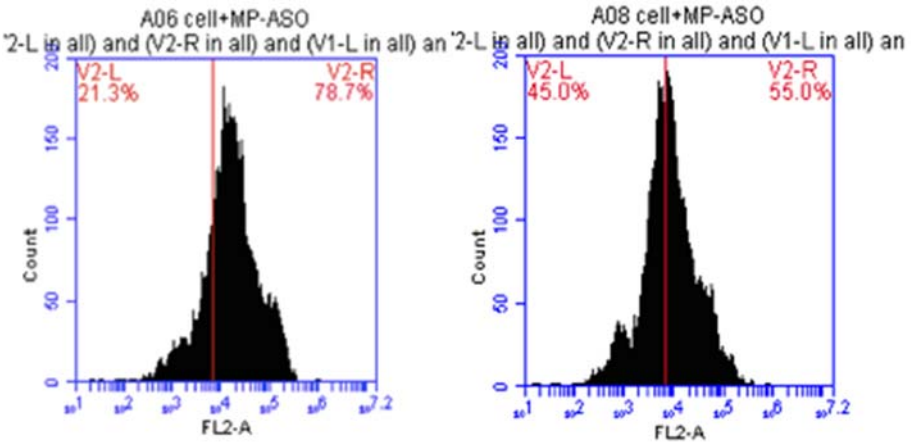

Figure 2-39. The percentage of cells from Control 5 that showed fluorescence in FL2-A with color correction.

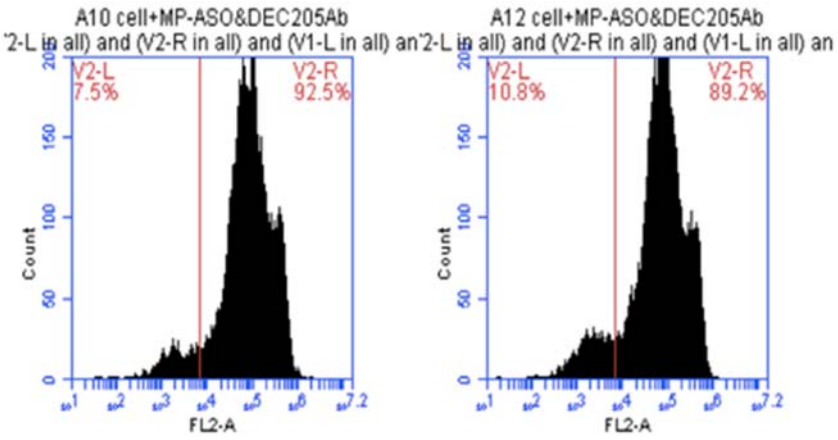

Figure 2-40. The percentage of cells from Exp. 1 that showed fluorescence in FL2-A with color correction.

Chapter 3: Conclusion, Discussion and Future Work on PLGA Particles

3.1. Conclusion and Discussion

From what has been discussed above, we can draw a conclusion that by co-emulsifying the biotinylated lipid DSPE-PEG (2000) biotin with the polymer matrix $PLGA_{50:50}$ during the preparation of PLGA particles, a novel particle, PLGA-biotin, was prepared. Using the method of double-emulsion solvent evaporation, PLGA particles were finally functionalized with biotin molecules on the surface. In this project, PLGA-biotin particles have demonstrated significantly different particle properties against PLGA-blank particles, which could be taken advantage of in delivering biological drugs.

PLGA-biotin particles have particle sizes in the range of microparticles, with Zeta potential in the range of the stability threshold for colloidal suspensions. The endotoxin levels in PLGA-biotin is in the acceptable range for *in vivo* studies. The result from SDS-PAGE electrophoresis proves the identity of proteins adsorbed on PLGA-biotin particles, indicating that PLGA-biotin particles only have binding affinity for avidin and its analogues. By performing the HABA/avidin binding assay, the amount of solvent-accessible biotin on the surface of PLGA-biotin was calculated to be 15.4% of the initially added biotinylated lipid. FTIR analysis also proved the existence of biotin molecules on the surface of PLGA-biotin particles.

PLGA-biotin particle is specific to the proteins that can be adsorbed directly onto its surface. Since the binding is based on the interaction between biotin and avidin, avidin plays a bridging role in loading biological macromolecules onto PLGA-biotin particles. The loading of all the macromolecules on PLGA-biotin in this project is through chemisorption based on the chemical interaction between biotin and avidin. For example, desthiobiotinylated biological drugs need to bind to avidin first, and then the resulting complex interacts with PLGA-biotin if not all the binding sites in avidin are occupied. Therefore, the molar ratio used for the reaction must be properly designed. For instance, with the molar ratio of Cy3-ASO-dethiobiotin: avidin: biotin on PLGA-biotin equals 1: 2: 10, the loading efficiency of Cy3-ASO-desthiobiotin on PLGA-biotin particles was measured to be 65.87%. In the bone marrow experiment, PLGA-biotin particles showed a significantly higher uptake of Cy3-conjugated ASO when loaded with anti-DEC205

antibody. However, the mechanism of introducing the oligonucleotides into cells by PLGA-biotin particles remains as an unresolved issue.

For research in the future, it is also necessary to continue improving the efficiency of loading desthiobiotinylated biologics onto PLGA-biotin particles. By optimizing the structure of the hydrophobic chain in the biotinylated lipid, it is possible to achieve a more effective interaction with PLGA matrix and increase the percentage of solvent-accessible biotin on PLGA-biotin.

3.2. Adsorption of His-tagged Proteins on PLGA-Ni Particles for Biotherapeutics Delivery

The previous study in our lab has prepared a PLGA particle functionalized with nickel atoms on the surface, i.e., PLGA-Ni (Reger, N., et al. 2017). In order to compare the properties of PLGA-Ni and PLGA-biotin in the delivery of biological drugs, the adsorption of His-tagged proteins on PLGA-Ni particles was also studied in this project.

The interaction between nickel-nitrilotriacetic acid (Ni^{2+}–NTA) matrix and polyhistidine tag was employed in this project to enable the adsorption of proteins on PLGA-Ni particles, which is adopted as the approach to deliver biologic drugs circumventing the potential protein degradations during encapsulation. As demonstrated in Figure 3-1, the nickel atoms in the Ni^{2+}–NTA matrix can interact with the lone pairs on the imidazole rings in polyhistidine tags (Bornhorst, J. A. and J. J. Falke, 2000). Most proteins with one His tag

dissociate rapidly from the Ni^{2+}–NTA surface, and the K_d for the interaction between His tag and Ni^{2+}–NTA was estimated to be about 10^{-6} M at neutral pH (Nieba, L., et al. 1997). Based on this mechanism, recombinant proteins with polyhistidine tags can be loaded onto PLGA particles if the particle surface is functionalized with Ni^{2+}–NTA.

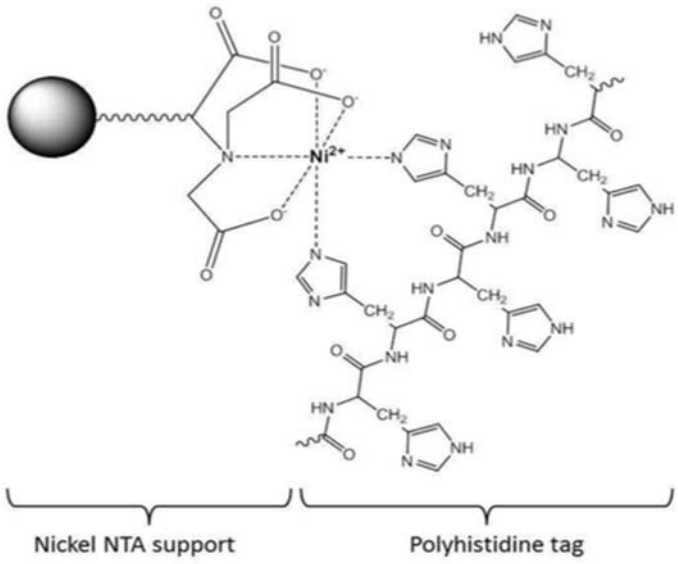

Figure 3-1. Interaction between Ni^{2+}–NTA and polyhistidine tag.

Previous studies done by our group have shown that Ni^{2+}–NTA can be localized on PLGA particles by incorporating the metal chelating lipid in the organic phase using the solvent evaporation method (Kovacs, J. R., et al. 2009). In this project, the metal chelating lipid DOGS-NTA-Ni was used in the organic phase when preparing PLGA-Ni particles. Through interweaving with the PLGA matrix, DOGS-NTA-Ni can be incorporated into PLGA particles and consequently generate particles with nickel atoms on the surface. The recombinant His-tagged protein G (HpG), a 21.6 kDa globular originated from

Staphylococcal bacteria, will be utilized as the model protein drug. Other his-tagged proteins, such as His-tagged green fluorescent protein (His-GFP) and His-tagged transforming growth factor beta (His-TGFb), are also used to illustrate the interaction between His-tag and nickel. In future studies, the ultimate goal is to utilize PLGA-Ni particles (Figure 3-2) to deliver transforming growth factor beta-1 (TGFβ-1) in animal models to suppress inflammation.

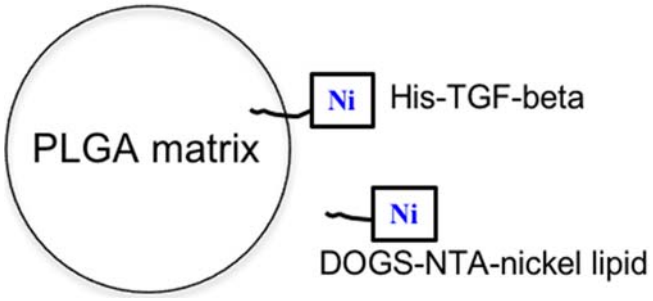

Figure 3-2. Deliver His-TGF-beta through PLGA-Ni particles.

3.2.1. Introduction

3.2.1.1. Nickel

Nickel is a silvery-white metal and also a chemical element with symbol Ni and atomic number 28. People can be exposed to nickel by inhalation, ingestion, and contact with skin or eye. However, nickel is immediately dangerous to life and health at 10 mg/m^3 and the lowest-observed-adverse-effects level (LOAEL) of Ni is 50 mg/kg/day determined in human, according to Center for Disease Control (CDC)-NIOSH pocket guide to chemical hazards for nickel metal and other compounds (CDC, ATSDR/U. S. 1988).

The nickel atoms can be used to bind the hexahistidine motif, which is commonly referred as "His tag", through chelation. This reversible interaction is estimated to have binding affinities (K_d) between 10^{-5} to 10^{-7} M at neutral pH, an intermediate range that allows loading and release of His-tagged proteins (Nieba, L., et al. 1997). This coordination interaction has been used in affinity purification of genetically modified proteins, detecting protein-protein interaction in binding assays and developing fluorescent tags for protein migration (Kim, S. H., et al. 2007, Zhao, C., et al. 2010).

3.2.1.2. His-tagged Protein

One of the most commonly used fusion tags for recombinant protein expression and purification is the His tag, which contains six or more consecutive histidine residues. His-tagged proteins are recombinant proteins commonly expressed with a His-tag at the N or C terminus of the polypeptide (Waugh, D.S., 2005). In contrast to other affinity tags, due to its small size (0.84 kDa in the case of a hexahistidine tag) and the fact that it is uncharged at physiological pH, the His tag typically does not affect folding in most cases does not alter the activity of the fusion protein (Carson, M., et al. 2007). It has a low immunogenicity and is compatible with most downstream applications.

Since the affinity of the His tag toward the Ni-NTA depends only on its primary structure, His-tagged proteins can be purified under native or denaturing conditions (Hochuli, E., et al. 1987). For instance, His-tagged proteins can be purified by a single-step affinity

chromatography, namely immobilized metal ion affinity chromatography (IMAC), which is commercially available in different kinds of formats, Ni-NTA matrices being the most widely used (Spriestersbach, A., 2015). Purification of His-tagged proteins by IMAC is based on the affinity of histidine residues for immobilized metal ions (e.g., Ni^{2+} or Cu^{2+}). The metal ions are immobilized on chromatographic matrices by a chelating ligand, most commonly nitrilotriacetic acid (NTA) or iminodiacetic acid (IDA). While IDA has only three metal-chelating sites, NTA contains four and hence binds the metal ions more stably resulting in reduced ion leaching (Hochuli, E., et al. 1987, Block, H., et al. 2009). In this project, the nickel-hexahistidine coordination is utilized for adsorbing candidate therapeutic proteins onto PLGA particles that are functionalized with nickel atoms attached on the surface.

3.2.2. Materials and Methods

3.2.2.1. Materials

18:1 DOGS-NTA-Ni (Nickel salt,1057 Da) was purchased from Avanti Polar Lipids, Inc. Poly (D, L-lactide-co-glycolide) (PLGA, 50:50, IV 1.0 dl/g, 150000 g/mol, overall PDI 1.5-2.0) was purchased from Polysciences, Inc. Polyvinyl alcohol (PVA, 86-89% hydrolyzed, low molecular weight), Invitrogen NativePAGE 4-16% Bis-Tris gel (1.0 mm x 10 well), Novex sharp protein standard, dichloromethane (DCM, 99.9%), bovine serum albumin (BSA), Tris base, D-(+)-trehalose dihydrate, Pierce LAL chromogenic endotoxin quantitation kit, Pierce BCA protein assay kit, endotoxin-free ultrapure water, and EMD

Millipor Millex sterile syringe filters were purchased from Thermo Fisher Scientific. Transforming growth factor-beta 1 human recombinant, His tag (His-TGFβ1) and Protein G human recombinant, His tag (His-pG) were purchased from ProSpec. Imidazole was purchased from Sigma-Aldrich. Green fluorescent protein with a polyhistide tag at the N-terminus, Aequorea victoria, recombinant (His-tagged GFP, 5 μg/tube) was purchased from Sino Biological Inc. Papain, Carica papaya (activity>30,000 USP units/mg) was purchased from MilliporeSigma.

3.2.2.2. PLGA-Ni Particle Preparation

PLGA-Ni particles were prepared by incorporating metal chelating lipid 18:1 DOGS-NTA-Ni (Figure 3-3) into the PLGA matrix using the method of double-emulsion solvent evaporation. Then, His-tagged proteins can be adsorbed onto the surface of PLGA-Ni microparticles based on the chelation reaction between nickel and polyhistidine tag (Figure 2-1). Specifically, DCM was used as the organic phase and 1% PVA aqueous solution was selected as the water phase. The aqueous solution of 1% PVA was prepared by stirring with heating at 90 °C overnight. Prior to emulsification, 90 mg $PLGA_{50:50}$ were dissolved in 2.4 ml DCM and combined with 0.6 ml 10 mg/ml DOGS-NTA-Ni in DCM, followed by the addition of 20 ml 1% PVA aqueous solution to the organic phase. Homogenization was performed at 25000 rpm for 5 min on ice. By magnetic stirring in hood for 4 h to evaporate DCM, the residual of the organic solvent was removed.

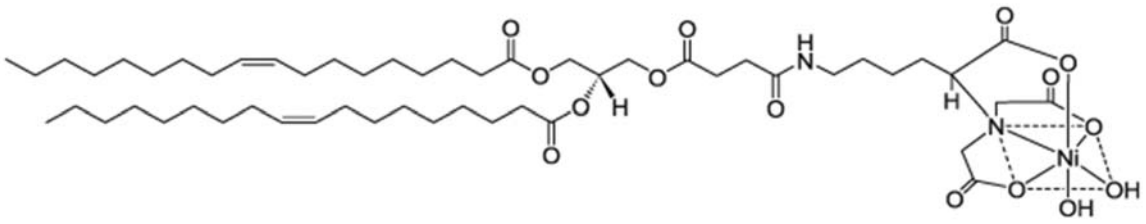

Figure 3-3. The chemical structure of 18:1 DOGS-NTA-Ni.

Particles were collected through centrifugation and then washed twice with 10 ml of ultrapure water by centrifuging at 15k rcf, 4 °C for 20 min. To protect the freeze-dried material, lyoprotectants such as trehalose and sucrose are often added before lyophilization (Fonte, P., et al. 2016). In this experiment, particles were re-suspended in 12 ml 2% trehalose aqueous solution. Then, pre-freezing was performed by rotating the glassware containing particle suspension in dry ice-acetone bath, where the temperature was as low as around -77 °C (Percy, J., Moody, C., Harwood, L, 1998). Pre-freezing is one of the most essential steps of the freeze dry process because creating more surface during the pre-freezing process can speed up lyophilization, provide a thinner crust on the top layer of the sample, prevent breaking of the glassware, and allow greater heat transfer during lyophilization (Tang, X. and M. J. Pikal, 2004). After lyophilization for 3 days, particles were collected and stored in a glass vial wrapped with parafilm and foil, and then saved inside a desiccator at 4 °C. After complete lyophilization, the yield of PLGA-Ni particle preparation experiment is 275 mg of white powder.

3.2.2.3. PLGA-Ni Particle Characterization

3.2.2.3.1. Characterize Particle Size and Zeta Potential of PLGA-Ni Particle

The size and Zeta potential of PLGA-Ni particles were measured by the Malvern Zetasizer Nano-S (Malvern Instruments, UK) using the method of dynamic light scattering (DLS) (Stetefeld, J., et al. 2016). To begin with, a series of PLGA-Ni particle suspensions were prepared to find the most suitable concentration for DLS measurements. First, 5 mg of PLGA-Ni particles were washed with 1ml of ultrapure water to get rid of trehalose, followed by re-suspending in 1 ml of ultrapure water. Next, this suspension was diluted 2X, 10X, 20X, 50X, and 100X to make particle suspensions with different concentrations. Then, particle size was measured on different dilutions using DLS. The concentration at which both the attenuation and number of runs were ideal was selected for the following tests. Accordingly, both particle size and Zeta potential of PLGA-Ni particles were then measured at this concentration.

3.2.2.3.2. Characterize the Morphology of PLGA-Ni Particle

Scanning electron microscope (SEM) was used to characterize the morphology of PLGA-Ni particles. To compare the difference between plain PLGA-Ni particles and PLGA-Ni particles with proteins loaded, 5 mg of PLGA-Ni particles were washed and incubated with His-TGFb for 1 h while another 5 mg of PLGA-Ni particles were not incubated with His-TGFb. Pellets were then centrifuged down at 13600 rcf, 4 °C for 20 min and transferred to eppendorf tubes on a rack, covering with aluminum film. A needle was used to punch small holes on the film to ensure the particles inside can be dried effectively. The rack was placed in a desiccator overnight. On the second day, the dried pellets were transferred to PELCO

tabs (12 mm OD) and loaded onto SEM instrument for imaging. The mode selected is variable pressure (VP) SEM with following setups: 5 kV of electron beam; probe current: 60; fast imaging mode for VP mode.

3.2.2.3.3. Characterize the Viscosity of PLGA-Ni Particle Suspension

The viscosity of PLGA-Ni particle suspension was measured for different particle concentrations, i.e., 5 mg/ml, 10 mg/ml and 20 mg/ml. To make 500 µl of each particle suspensions for the microVISC multi shear rates measurement, 5 mg, 10 mg, 20 mg of PLGA-Ni particles are weighed out, washed with 1 ml of ultrapure water by centrifuging at 4 °C, 16000 rcf for 10 min, followed by re-suspending in 500 µl of PBS, respectively.

Viscometer measurements were performed using the advanced settings: measurements volume: Auto; priming volume: Auto; pausing time: 5 seconds; Temperature: 25 ºC; shear rates: 8000 s^{-1}, 6000 s^{-1}, 4000 s^{-1}, 3000 s^{-1}, 2000 s^{-1}, 1000 s^{-1}. Measurements were conducted from high shear rates to low shear rates. Water was included as the control.

3.2.2.3.4. Determine the Endotoxin Level in PLGA-Ni Particles

By testing the endotoxin standard solutions, an endotoxin standard curve was established. Then, PLGA-Ni suspensions were measured on a microplate absorbance reader at 405 nm within about 30 minutes. Finally, the endotoxin concentrations of the samples, in this case

PLGA-Ni suspensions, were calculated based on the linear regression equation from the standard curve.

3.2.2.4. Loading of His-tagged Proteins on PLGA-Ni Particles

3.2.2.4.1. Determine the Optimal Imidazole Concentration for Eluting Proteins

By taking advantage of the interaction between polyhistidine tag and the imidazole ring, imidazole solution was used to elute the His-tagged proteins adsorbed on PLGA-Ni particles. To optimize the concentration of imidazole for measuring the loading efficiency of His-TGFb on PLGA-Ni particles, the effect of variation in imidazole concentration on its ability to compete with polyhistidine tags in binding PLGA-Ni particles was tested. Different imidazole aqueous solutions with concentrations including 0 mM, 10 mM, 25 mM, 50 mM, 75 mM, 100 mM, 150 mM, and 200 mM were prepared. For each imidazole concentration, 5 mg of PLGA-Ni particles were washed and incubated with 250 µl of 0.02 µg/µl His-GFP and 250 µl imidazole solution of the specific concentration for 1 h at room temperature. Tris buffer and His-GFP stock solution were included as the blank and the control. After centrifuging and washing each pellet with cold Tris pH 8 buffer. Each supernatant and pellet were saved and measured by plate reader. The excitation wavelength and emission wavelength of His-tagged GFP are 487 nm and 508 nm, respectively. Therefore, plate reader was used in the final step to detect the fluorescence intensity from GFP by scanning the wells at 508 nm.

3.2.2.4.2. Determine the Optimal pH Value for Tris Buffer to Eluting Proteins

Previous studies showed that the reaction between nickel atom and polyhistidine tag is dependent on the pH of the environment (Bornhorst, J. A. and J. J. Falke, 2000, Nieba, L., et al. 1997). To achieve desired efficiency of eluting proteins adsorbed, different pH values were test and the optimal pH was determined.

Tris buffers with different pH values were made by dissolving tris base in ultrapure water, followed by adjusting pH with HCl and NaOH. Because pH lower than 6 or higher than 9 is likely to denature protein, pH 6, pH 7 and pH 8 were selected for the test. For each concentration, 5 mg of PLGA-Ni particles were washed and re-suspended in 250 µl Tris buffer of the concentration being tested. Next, His-GFP was loaded on PLGA-Ni particles. First, 5 µg of His-GFP was reconstituted in 250 µl Tris buffer of the concentration being tested, and then added to the particle suspension immediately. All samples were incubated for 1 h at room temperature. Pellets were centrifuged down and washed with cold Tris buffer. Both the supernatants and pellets were analyzed by testing the fluorescence intensity from GFP using plate reader.

3.2.2.4.3. Loading Efficiency of His-tagged Proteins on PLGA-Ni Particles

Loading efficiency of His-TGFb on the surface of PLGA-Ni particles was measured by the bicinchoninic acid assay (BCA assay), which is a biochemical assay for determining the concentration of protein in a solution. The total protein concentration is exhibited by a color

change of the sample solution from green to purple, which is in proportion to protein concentration and can be measured using colorimetric techniques. The BCA assay primarily relies on two reactions. First, the peptide bonds in protein reduce Cu^{2+} ions to Cu^{+}. The amount of Cu^{2+} reduced is proportional to the amount of protein in the sample solution. Second, two molecules of bicinchoninic acid chelate with each Cu^{+} ion, forming a purple-colored complex that strongly absorbs light at a specific wavelength around 540-590 nm (Smith, P.K., et al. 1985).

According to the previous experiments, pH 8 Tris buffer and imidazole aqueous solution with concentration of 200 mM were chosen for loading and eluting His-tagged proteins on PLGA-Ni particles, respectively. In order to remove trehalose, 5 mg PLGA-Ni particles were first washed with PBS solution 3 times before being added to 0.5 ml pH 8 Tris buffer. Then, PLGA-Ni particle suspension was combined with 50 µl 0.07 µg/µl His-TGFb aqueous solution. Samples were incubated for 1 h at room temperature to allow His-TGFb to interact with PLGA-Ni particles. However, not all His-TGFb molecules adsorbed on the surface of PLGA-Ni particles were caused by the specific binding between nickel and His-tag. Thus, pellets were centrifuged and washed 3 times with cold pH 8 Tris buffer to get rid of unspecific binding. Imidazole solution was then used to elute the remaining His-TGFb on PLGA-Ni particles; i.e., the pellets were re-suspended in the mixture of 0.5 ml pH 8 Tris buffer and 0.5 ml 200 mM of imidazole aqueous solution and incubated for 0.5 h at room temperature. The supernatant from elution contains His-TGFb that was successfully loaded onto the surface of PLGA-Ni particles through Ni-polyhistidine tag interaction.

Next, BCA assay was performed using diluted BSA standard (2.5-40 μg/ml) as standards, PBS solution as blank, and the supernatants saved from elution as samples. The BCA working reagent (Pierce BCA Reagent A (MA): Pierce BCA Reagent B (MB): Pierce BCA Reagent C (MC) = 25: 24: 1) was prepared by mixing 2.5 ml MA, 2.4 ml MB and 0.1 ml MC. To mix samples with the working reagent, 150 μl sample including BSA standard was added to 96 well plate, and then 150 μl working reagent was added to each sample. The microplate was well mixed and incubated for 2 h at 37 °C after sealing. After cooling the plate to room temperature, the absorbance at 595 nm of each well in the microplate was measured on a plate reader.

A standard curve was then established by plotting the average blank-corrected 595 nm measurement for each BSA standard vs. its concentration. The standard solutions used have following concentrations: 1.25 μg/ml, 2.5 μg/ml, 5 μg/ml, 10 μg/ml, 20 μg/ml, 40 μg/ml, and 80 μg/ml. Finally, the protein concentration of each unknown sample was determined based on the standard curve and the linear equation.

3.2.2.4.4. Identify the Protein Adsorbed on PLGA-Ni Particles

Although the BCA assay result suggests that proteins were detected in the supernatants collected from eluting the PLGA-Ni particles incubated with His-TGFb, there is no direct evidence proving the identity of these proteins. Thus, sodium dodecyl sulfate

polyacrylamide gel (SDS-PAGE) electrophoresis was used to examine the molecular weight of the proteins adsorbed on PLGA-Ni particles after the loading experiment.

SDS-PAGE electrophoresis is an electrophoretic technique widely used in biotechnology, biochemistry, and other life science laboratories. In SDS-PAGE, proteins are separated in a palyacrylamide gel based on their molecular weight. Proteins have both positive and negative charges. To make proteins move in a single direction, a uniform negative charge is created on them. Sodium dodecyl sulfate (SDS) is a detergent having a negative charge, therefore it denatures the native proteins by disturbing the non-covalent forces (Saraswathy, N. and Ramalingam, P., 2011). SDS also gives a uniform net negative charge to the protein molecules. The denatured linear protein molecules are loaded onto the polyacrylamide gel (PAGE) which is made by polymerizing the acrylamide monomers. PAGE has two phases: a stacking gel and a separating gel. Under an applied electric field, the stacking gel concentrates the SDS-loaded linear protein molecules while the separating gel separates the proteins on the basis of molecular weight (Delves, P., 1998). After the run, PAGE gel is stained to visualize the separated protein molecules as bands.

To prepare molecular weight marker, Novex Sharp protein standard was diluted by mixing 5 µl protein standard with 10 µl sample buffer and 25 µl PBS solution. Duplicates of PLGA-Ni particles suspension saved after the incubation with His-TGFb in the loading experiment were tested. Samples were prepared by mixing 5 µl sample buffer and 10 µl PBS solution with 5 µl PLGA-Ni suspension, followed by heating at 70 °C for 10 min before loading. The solution of molecular weight marker was kept at room temperature.

Prior to running the electrophoresis under 200 V for 35 min, 20 µl of each sample and molecular weight marker were loaded onto the wells in SDS-PAGE gel. The SDS-PAGE gel was then stained through silver staining.

3.2.2.5. *In Vitro* Release of His-tagged Protein from PLGA-Ni Particles

3.2.2.5.1. *In Vitro* Release of His-GFP from PLGA-Ni Particles

The study of protein drug release in PLGA-Ni microparticles was performed with His-GFP first. Specifically, 5 mg of PLGA-Ni particles were washed and resuspend in 100 µl of pH 8 Tris buffer. Particle suspension was then added to 200 µl of 0.025 µg/µl His-GFP to 0.2 ml pH 8 Tris buffer (0.5 ml Tris buffer in total), followed by incubation at room temperature for 1 h. Then, pellets were centrifuged down by spinning at 13600 rcf, 4 °C for 20 min. To remove unspecific binding, each pellets was washed for another 3 times with 0.5 ml of cold pH 8 Tris buffer prior to re-suspending in 1 ml of release medium, which was then transferred into a 1 ml syringe. Syringes were then incubated at 37 ºC to mimic the release condition *in vivo*. The release medium in this experiment is 0.1% bovine serum albumin (BSA) in PBS solution, considering the fact that BSA can reduce the adsorption of proteins on the walls of containers (Goebel-Stengel, M, et al. 2011). Syringes were used with 0.22 µm syringe filters attached to trap the PLGA-Ni particles during dispensing.

In order to monitor the release of His-GFP from PLGA-Ni particles in the release medium, samples were drawn everyday from Day 1 to Day 14. On Day 1, i.e. the first day of release, 100 µl of solution was dispensed through the 0.2 µm filter on the syringe after 1 h, 2 h, 3 h, 4 h and 5 h of incubation at 37 ºC. Each dispensing was followed by replenishing the syringe with another 100 µl release medium. From Day 2 to Day 14, 100 µl of solution was dispensed through the syringe filter at the same time as the last time point on Day 1. Every time a sample was collected, the syringe was replenished with 100 µl of release medium. The fluorescence intensity of every sample was measured by plate reader at 508 nm, which reflects the amount of His-GFP contained in each release sample.

A standard curve was established for subsequent quantification of the release samples. The concentrations of His-GFP standards include 0.0098 µg/ml, 0.0195 µg/ml, 0.0391 µg/ml, 0.0781 µg/ml, 0.1563 µg/ml, 0.3125 µg/ml, 0.625 µg/ml, 1.25 µg/ml, and 2.5 µg/ml. The fluorescence intensity from GFP in each His-GFP standard is measured by plate reader at 508 nm with gain value of 255, which is in consistent with the gain used for the release study. The release of His-GFP was then quantified by calculating the cumulative released percentage based on the standard curve.

3.2.2.5.2. *In Vitro* Release of His-TGFb from PLGA-Ni Particles

Not only His-GFP, His-TGFb was also used for the release study. Specifically, 5 mg of PLGA-Ni particles were washed and resuspend in 100 µl of pH 8 Tris buffer. Particle suspension was then added to 61 µl of 0.164 µg/µl His-TGFb to 339 µl Tris pH 8 buffer

(0.5 ml Tris buffer in total), followed by incubation at room temperature for 1 h. Then, pellets were centrifuged down by spinning at 13600 rcf, 4 °C for 20 min. To remove unspecific binding, each pellets was washed for another 3 times with 0.5 ml of cold pH 8 Tris buffer prior to re-suspending in 1 ml of release medium, which was then transferred into a 1 ml syringe. Then, syringes were incubated at 37 ºC to mimic the release condition *in vivo*. The release medium in this experiment is also 0.1% BSA in PBS solution. Syringes were attached with 0.22 μm syringe filters to trap the PLGA-Ni particles during dispensing.

Release samples were collected using the same method described above and studied by conducting SDS-PAGE electrophoresis.

3.2.2.6. Enzymatic Degradation of Protein Absorbed on PLGA-Ni Particles

PLGA-Ni particles are expected to not only be able to bind His-tagged proteins on the surface, but also have a protective effect for protein drugs. To test whether adsorbed proteins are protected from enzymatic degradation by PLGA-Ni particles, papain was selected to evaluate the enzyme effect on proteins adsorbed or not adsorbed onto PLGA-Ni particles.

To achieve this purpose, PLGA-Ni particle were first loaded with His-tagged protein G (His-pG) as following: 10 mg of PLGA-Ni particles were washed and re-suspended in 470 μl pH8 Tris buffer with 30 μl of 10 μg/μl His-pG stock solution added, followed by

incubation for 1 h at room temperature. In order to reveal the impact of enzyme concentration on the rate of protein degradation, two papain concentrations were used in this experiment: high enzyme concentration with a ratio of 10 U of papain activity per microgram of His-pG for the first experiment group (Exp. 1), and low enzyme concentration with a ratio of 2 U of papain activity per microgram of His-pG for the second experiment group (Exp. 2). Specifically, 3000 U of papain was added to the particle suspension after loading in Exp. 1 while 600 U of papain was added in Exp. 2. The controls did not include PLGA-Ni particles, in order to show the effect of papain on proteins not adsorbed on particles. There are four groups of control, i.e., the first control group (Control 1) tested the influence of high enzyme concentration on His-pG, the second control group (Control 2) tested the influence of low enzyme concentration on His-pG, the third control group (Control 3) tested the change in His-pG when no enzyme was added, and the fourth control group (Control 3) only included papain and Tris bufer. More details were provided in Table 3-1.

Table 3-1. Sample order of papain degradation experiment.

	PLGA-Ni (mg)	Tris buffer (µl)	His-pG (µl)	papain (U/ml)
Exp 1	10	470	30	30000
Exp 2	10	470	30	6000
Control 1	0	470	30	30000
Control 2	0	470	30	6000
Control 3	0	470	30	0
Control 4	0	470	0	30000

All samples were incubated at 37 ºC with sampling at 30 min, 4h, 18h (overnight) by centrifuging and collecting the supernatants. Then, the supernatants saved were used for SDS-PAGE electrophoresis via silver staining (Figure 2-23). The protein G His Tag recombinant used is produced in E. coli with 201 amino acids and a C-terminal 6-His tag, having a molecular mass of 21.6 kDa. But it should be pointed out that His-pG migrates with an apparent molecular mass of 32 kDa in SDS-PAGE.

3.2.3. Results

3.2.3.1. PLGA-Ni Particle Characterization

3.2.3.1.1. Characterize Particle Size and Zeta Potential of PLGA-Ni Particle

As showed in Figure 3-4, when PLGA-Ni microparticles were not loaded with His-TGFb, particle size was 867.5 nm (PDI 0.183). But when His-TGFb was loaded, particle size increased to 1088.6 nm (PDI 0.168). These measurements showed that the size of the PLGA-Ni particles prepared using the method described above is in the range of microparticles. Additionally, the low PDI values indicate that PLGA-Ni particles have a good uniformity, no matter His-TGFb was adsorbed or not.

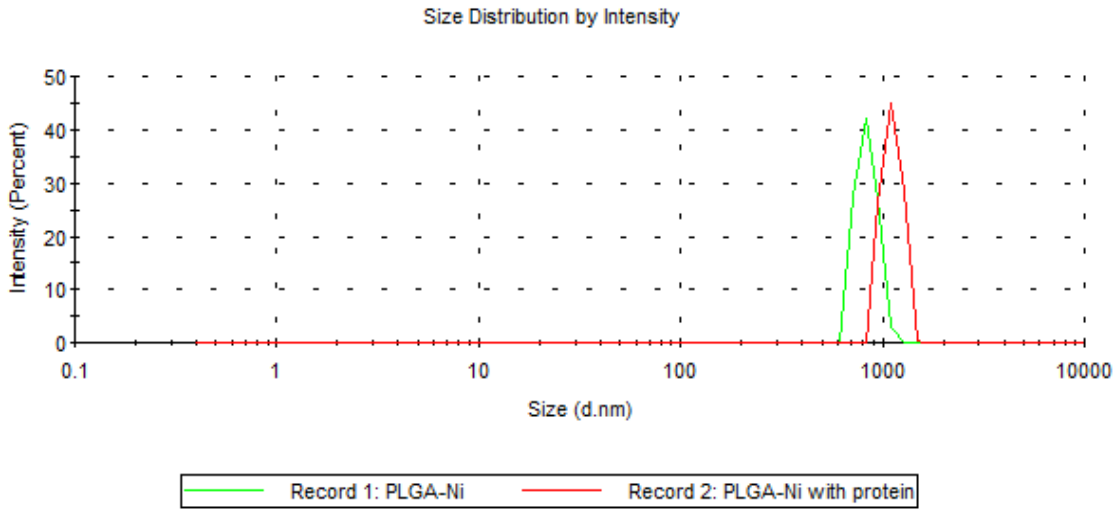

Figure 3-4. Particle size distribution of PLGA-Ni particles with and without His-TGFb loaded (the concentration of PLGA-Ni is 2.5 mg/ml in pH 7 PBS solution with ionic strength of 162.7 mM).

On the other hand, Zeta potential of plane PLGA-Ni particle was around -29.37±0.153 mV without His-TGFb (Figure 3-5). But PLGA-Ni particle with His-TGFb loaded has a Zeta potential of 0.44 mV. This result suggested that loading His-TGFb onto PLGA-Ni particles disturbs the colloidal stability of the particles. The reason for this change in Zeta potential is that the negative charges on PLGA-Ni particles was neutralized after the loading of His-TGFb. Therefore, the decrease in Zeta Potential indicates the adsorption of His-TGFb on the surface of PLGA-Ni particles.

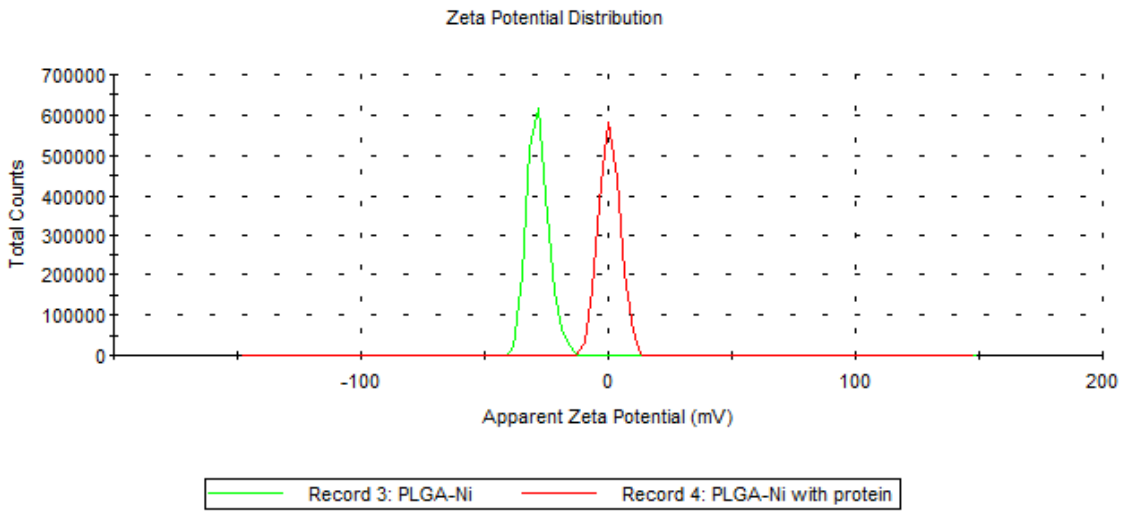

Figure 3-5. Zeta potential of PLGA-Ni particles with and without His-TGFb loaded (the concentration of PLGA-Ni is 2.5 mg/ml in de-ionized water).

3.2.3.1.2. Characterize the Morphology of PLGA-Ni Particle

The SEM images demonstrated that PLGA-Ni particles have spherical shape as expected (Figure 3-6). The plain PLGA-Ni particles tend to be individual spheres under SEM scanning, but the His-TGFb adsorbed PLGA-Ni particles formed clumps because of aggregation.

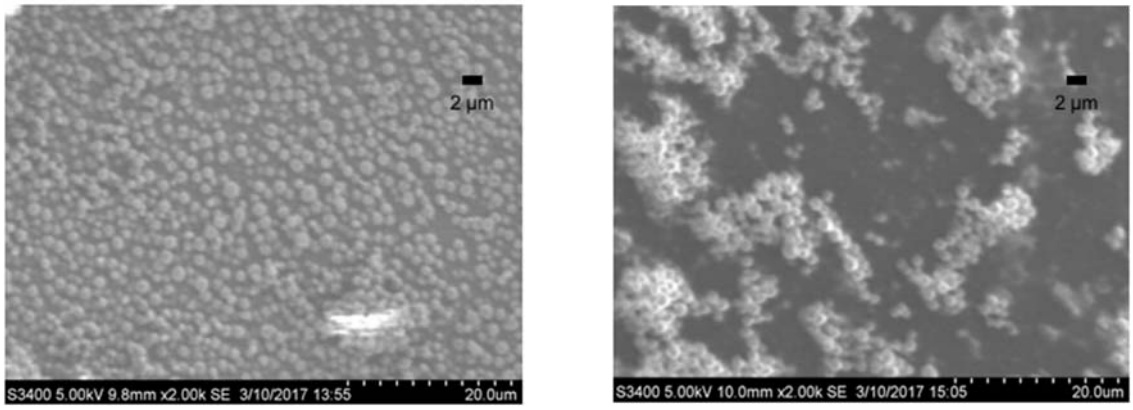

(a) (b)

Figure 3-6. Particle morphology of PLGA-Ni particles: (a) without His-TGFb loaded, (b) with His-TGFb adsorbed.

There are two main reasons for the aggregation in protein adsorbed PLGA-Ni particles. First, the electrostatic repulsive forces between particles were reduced due to the adsorption of protein on particle surface, which is confirmed by the decrease noticed in electronegative zeta potential values when comparing plain PLGA-Ni particles with PLGA-Ni particles loaded with His-TGFb. In addition, it is possible that the amount of protein added was high enough that protein molecules on particle surface were likely to aggregate with the proteins adsorbed on another particle, resulting in large clusters in the SEM image (Figure 3-6, b). Thus, incubating less His-tagged proteins with PLGA-Ni particles should reduce this aggregation in the loading process.

3.2.3.1.3. Characterize the Viscosity of PLGA-Ni Particle Suspension

It is showed in Figure 3-7 that the viscosity of PLGA-Ni particle suspension increases as particle concentration increases. When the concentration is lower than 5 mg/ml, the viscosity of PLGA-Ni particle suspension is close to water. Moreover, the viscosity of particle suspension did not increase significantly when the concentration changes from 5 mg/ml to 10 mg/ml. This result suggests that in experiments where the concentration of PLGA-Ni suspension is in the range of 0-10 mg/ml, the influence of viscosity on particle performance is negligible. In the following experiments, the concentration of the PLGA-Ni suspensions used did not exceed 5 mg/ml.

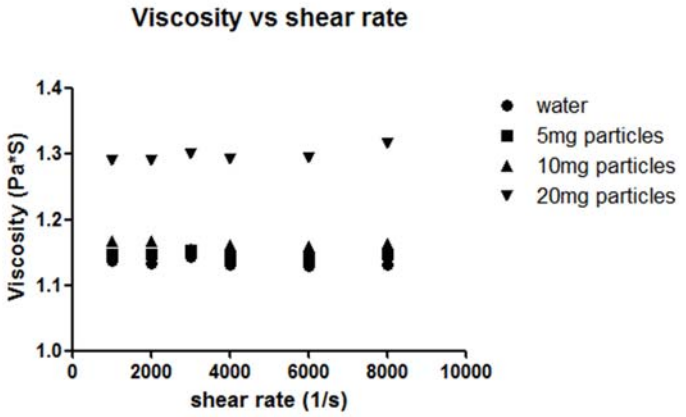

Figure 3-7. Viscosity of PLGA-Ni particle suspension under different shear rate.

3.2.3.1.4. Determine the Endotoxin Level in PLGA-Ni Particles

As showed in Figure 2-12, endotoxin standard curve has been established and the linear regression equation was y = 3.2435x - 0.2669, R^2=0.9724. The measurement of PLGA-Ni suspensions showed that endotoxin concentration of PLGA-Ni particles was 1.01 EU/ml or 0.202 EU/mg, which basically meets the 0.1-1.0 EU/ml range. According to this

endotoxin level, the dose of PLGA-Ni particles for animal study in preclinical evaluation can be calculated using the USP recommended endotoxin limit of 5 EU/kg.

3.2.3.2. Loading of His-tagged Proteins on PLGA-Ni Particles

3.2.3.2.1. Determine the Optimal Imidazole Concentration for Eluting Proteins

In Figure 3-8, preliminary results showed that the concentration of His-GFP in supernatants increases as imidazole concentration increases. In contrast, the percentage of His-GFP retained in PLGA-Ni pellets decreases when imidazole concentration increases (Figure 3-9). Therefore, among the imidazole concentrations tested, 200 mM of imidazole aqueous solution is selected for eluting the adsorbed His-tagged protein effectively and determining the loading efficiency of protein drugs on PLGA-Ni particles.

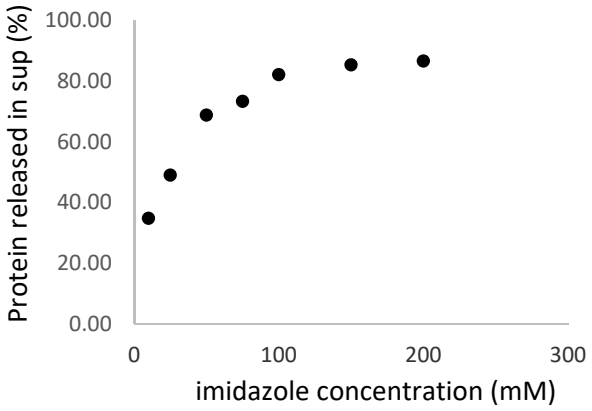

Figure 3-8. Preliminary results on the change in the percentage of His-GFP released in supernatant with varying imidazole concentrations (error bars are not included since this is a titration experiment that is not repeated yet).

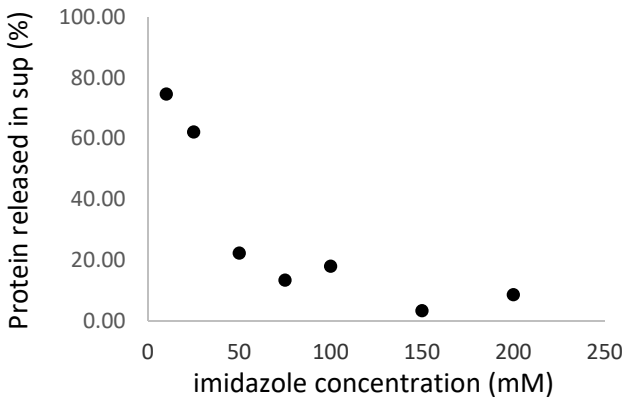

Figure 3-9. Preliminary results on the change in the percentage of His-GFP retained in pellet with varying imidazole concentrations (error bars are not included since this is a titration experiment that is not repeated yet).

3.2.3.2.2. Determine the Optimal pH Value for Tris Buffer to Eluting Proteins

From the preliminary results on the percentage of His-GFP released in the supernatants and retained in the pellets (Figure 3-10 and Figure 3-11), pH 8 Tris buffer demonstrated the strongest ability in eluting proteins adsorbed on PLGA-Ni particles. This result is due to the fact that the imidazole rings in polyhistidine tag are less likely to be protonated under weakly alkaline condition. Based on these comparisons, pH 8 Tris buffer is considered as the optimal pH environment for the adsorbed proteins to be released from PLGA-Ni particles.

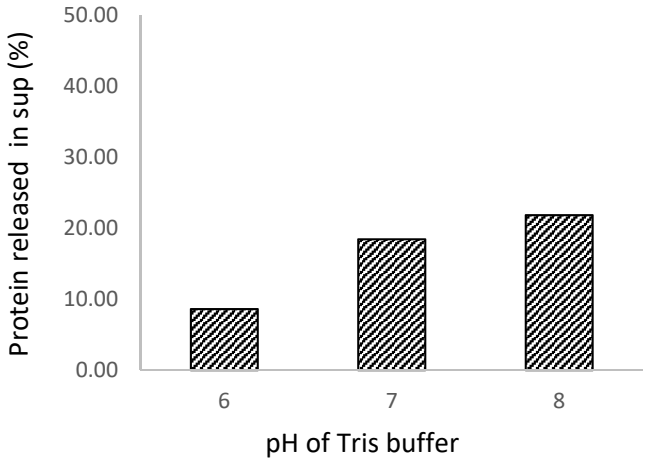

Figure 3-10. Preliminary results on the percentage of His-GFP released in supernatants at different pH (error bars are not included since this is a titration experiment that is not repeated yet).

Figure 3-11. Preliminary results on the percentage of His-GFP retained in pellets at different pH (error bars are not included since this is a titration experiment that is not repeated yet).

3.2.3.2.3. Loading Efficiency of His-tagged Proteins on PLGA-Ni Particles

Based on the standard curve y = 0.0066x + 0.0003 (R^2=0.9981), the protein concentration of each unknown sample was determined (Figure 3-12). According to the readout of plate scanning, the average concentration of protein in samples is 1.567 µg/µl. Therefore, on average 1.567 µg of His-TGFb was eluted by imidazole after incubating PLGA-Ni particles with 3.445 µg of His-TGFb in pH 8 Tris buffer. Accordingly, around 45.52% of the initial loading amount of His-TGFb was adsorbed onto PLGA-Ni particles through Ni-polyhistidine tag interaction.

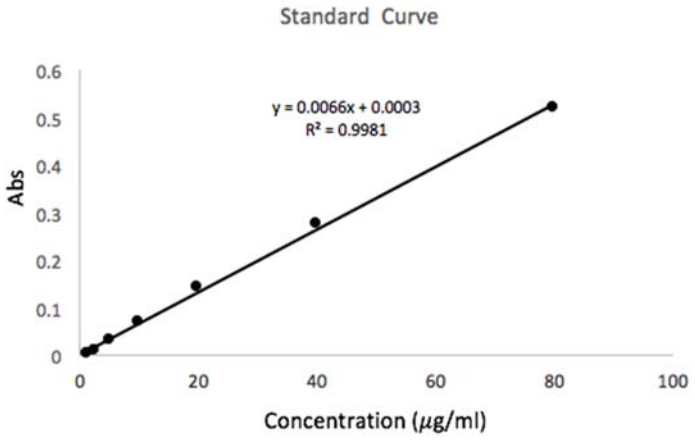

Figure 3-12. Standard curve for BCA assay.

3.2.3.2.4. Identify the Protein Adsorbed on PLGA-Ni Particles

The result from SDS-PAGE electrophoresis is showed in Fig 3-13. The first lane on the right is loaded with molecular weight marker. The two lanes on the left are both PLGA-Ni particles saved after incubating with His-TGFb and imidazole in the previous experiment,

which showed a band at 20 kDa. This result indicates that a protein with molecular weight of 20 kDa was adsorbed on PLGA-Ni particles. According to the molecular weight of His-TGFb (21.8 kDa), this band should be denatured His-TGFb, suggesting that His-TGFb was successfully adsorbed onto PLGA-Ni particles via specific binding.

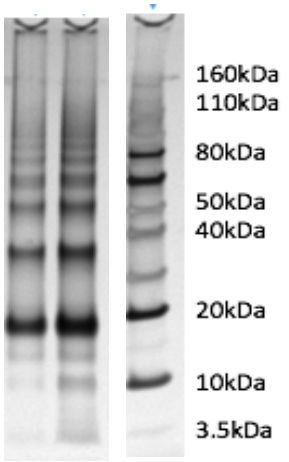

Figure 3-13. SDS-PAGE electrophoresis result after loading His-TGFb onto PLGA-Ni particles (The first two lanes on the left: duplicates of PLGA-Ni particles incubated with His-TGFb; The first lane on the right: molecular weight marker).

3.2.3.3. *In Vitro* Release of His-tagged Protein from PLGA-Ni Particles

3.2.3.3.1. *In Vitro* Release of His-GFP from PLGA-Ni Particles

The standard curve (Figure 3-14) showing the relationship between the concentration of His-GFP and the fluorescence intensity from GFP was depicted as the following with a linear equation of $y = 11803x + 4528.9$ ($R^2 = 0.9965$).

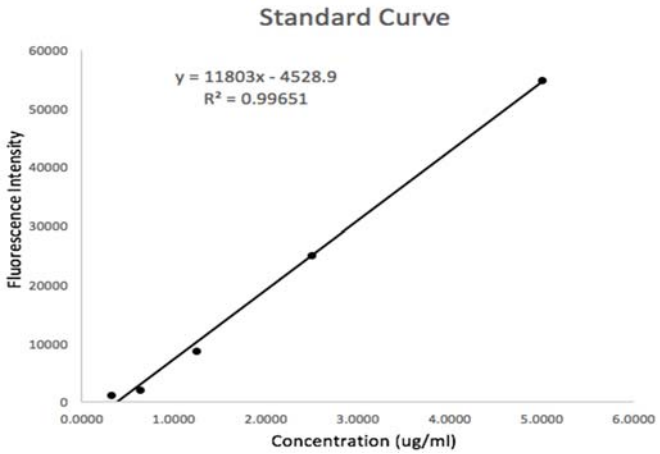

Figure 3-14. Standard curve for the fluorescence intensity of His-GFP.

The result showed in Figure 3-15 illustrated that the release of His-GFP was sustained for 8 days. More than 80% of His-GFP loaded was released from PLGA-Ni particles during the first week of release. Compared to the solution of His-GFP, the release of His-GFP was prolonged when PLGA-Ni particle was used to deliver the protein. This result suggests that PLGA-Ni particle is a viable carrier for delivering His-tagged proteins and sustaining the release rate.

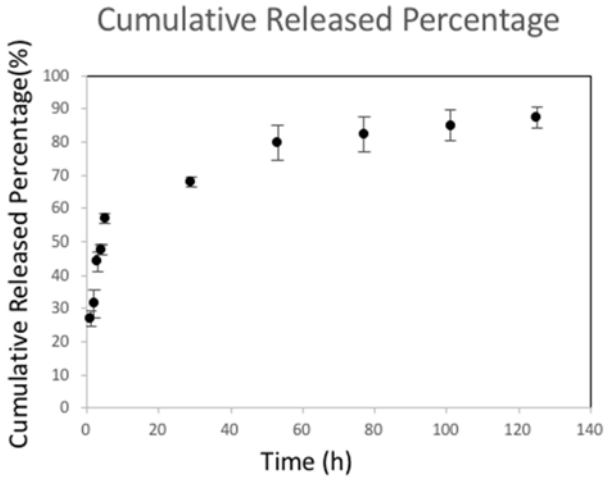

Figure 3-15. Release of His-GFP from PLGA-Ni particles from Day 1 to Day 8 in PBS at 37 °C (n=3, the excitation/emission wavelength of GFP is 487 nm/508 nm).

Compared to the release profile of desthiobiotinylated drug adsorbed on PLGA-biotin particles, His-tagged proteins showed a faster release from PLGA-Ni particles. The main reason for this difference is that the dissociation constant (K_d) for the interaction between avidin and biotin is 10^{-15}, which indicates that the binding between avidin and biotin is much stronger than the interaction between Ni and polyhistidine tag where K_d is 10^{-6} in the pH 7 release medium (Bornhorst, J. A. and J. J. Falke 2000). Therefore, avidin-bound drug takes a longer time to be dissociated and released from PLGA-biotin than His-tagged proteins adsorbed on PLGA-Ni if biotin is not presented in the release medium.

3.2.3.4. Enzymatic Degradation of Protein Absorbed on PLGA-Ni Particles

Papain was used to probe the extent to which proteins adsorbed on PLGA-Ni could be digested. In the electrophoresis result (Figure 3-16), lane 9 indicates the band of pure His-pG is around 30 kDa. When the concentration of papain was high (30000 U/ml), both PLGA-adsorbed His-pG and plain His-pG were degraded to a large extent and no specific band showed up around 30 kDa. But when the papain concentration was relatively low (6000 U/ml), PLGA-adsorbed His-pG (lane 2) showed a much stronger band around 30 kDa than His-pG alone (lane 4). This result suggests that PLGA-Ni particle has the ability to protect surface-adsorbed protein against low concentration of enzyme. But high concentration of enzyme could still damage the proteins absorbed.

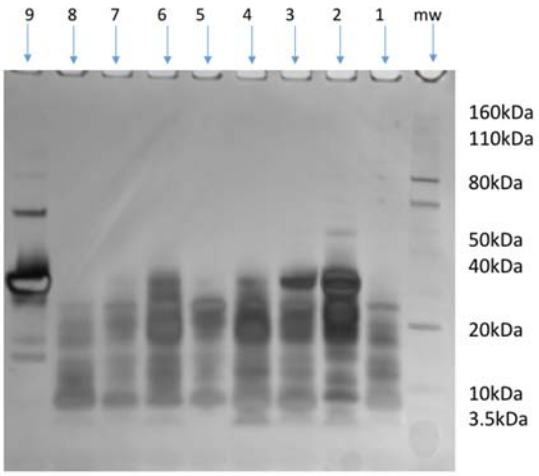

Figure 3-16. SDS-PAGE electrophoresis result of His-pG degradation with and without being absorbed on PLGA-Ni particles. Sample order: lane 1-30 min after incubating PLGA-absorbed His-pG with 30000 U/ml papain, lane 2-30 min after incubating PLGA-absorbed His-pG with 6000 U/ml papain, lane 3-30 min after incubating His-pG with 30000 U/ml papain, lane 4-30 min after incubating His-pG with 6000 U/ml papain, lane 5-4 h after incubating PLGA-absorbed His-pG with 30000 U/ml papain, lane 6-4 h after incubating PLGA-absorbed His-pG with 6000 U/ml papain, lane 7-4 h after incubating His-pG with 30000 U/ml papain, lane 8-4 h after incubating His-pG with 6000 U/ml papain, lane 9-His-pG.

3.3. Incorporation of PLGA-Ni Particles into EAK Hydrogel

3.3.1. EAK16-II: self-assembling peptide

Considering the fact that the biological drugs adsorbed on the surface of PLGA-Ni have the potential to be denatured by proteases and other factors in the environment or under

physiological conditions in vivo, EAK16-II hydrogel will be used to incorporate the drug loaded PLGA-biotin particles in future studies since the network of EAK16-II gel is resistant to acids and proteases and can work as the barrier against protein denaturation.

EAK16-II is a self-assembling amphiphilic peptide, consisting of alternating hydrophobic (A) and hydrophilic (E and K) amino acids (amino acid sequence: AEAEAKAK) (Zhang, S., et al. 1993). Through ionic complementary interactions between the residues with periodic negative and positive charges, EAK16-II spontaneously undergoes β-fibrillizition when exposed to high ionic strength (>20 mM) (Wen, Y., et al. 2014). Subsequent cross-linking of these self-assembled nanofibers leads to insoluble quaternary β-structures, which are resistant to acids and proteases (Zhang, S., et al. 1994). Dissociated biological drugs may bind to these fibrils, further delaying their release into the environment. The density of EAK16-II concentration can alter the stability of the released protein. However, dense network may also impede the diffusion of particles to the extent that they are virtually immobilized.

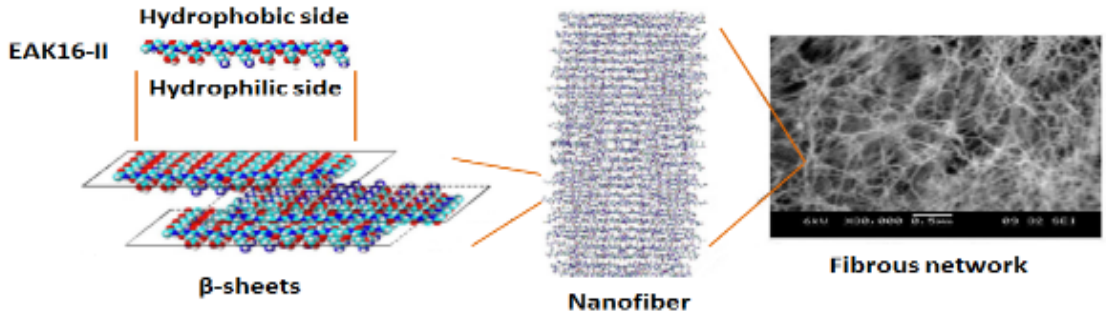

Figure 3-17. The formation of EAK16-II fibrous network through self-assembling and β-fibrillizition.

Loading protein on the surface of microparticles, however, can destabilize the colloidal stability. This can be addressed by embedding the particles in the EAK16-II gel, in which the fibriller matrix serves as a barrier against particle aggregation and protein denaturation. Therefore, EAK16-II gel is believed to be able to work as a second barrier against chemical and physical reagents in environment or serum that may cause protein degradation. An ideal particle-EAK16-II system should have reasonably high loading efficiency, reduced burst release effect, sustained release profile and retained bioactivity. Thus, it is necessary to find out the optimal EAK16-II density for incorporating particles. The following experiments were the preliminary studies on the incorporation of PLGA-Ni particles in EAK16-II hydrogel, in order to provide a basis for the further research on the optimal formulation of EAK16-II hydrogel and PLGA-Ni particles in the future.

3.3.2. Materials

EAK16-II was custom synthesized by American Peptide Company (Sunnyvale, CA) at greater than 95% purity with the N-terminus acetylated and C-terminus amidated. Green fluorescent protein with a polyhistide tag at the N-terminus, Aequorea victoria, recombinant (His-tagged GFP, 5 μg/tube) was purchased from Sino Biological Inc. Slowfade Diamond anti-fade mounting solution (2 ml in total) was purchased from Thermo Fisher Scientific.

3.3.3. Method and Result

In the preliminary studies, a high concentration of EAK16-II, 5 mg/ml was used for gel formation. However, in contrast to individual spheres when not incorporated (Figure 3-18), the particles became aggregates and attached to gel matrix after incorporated into EAK16-II gel as showed in the microscopic images in Figure 3-19. This might be due to the high viscosity of EAK16-II gel formed, which results in uneven distribution of the particles. It is important to adjust the concentration of EAK16-II and consequently the viscosity of EAK16-II gel to reduce this aggregation and ensure the protein drug is not denatured after being incorporated into the hydrogel.

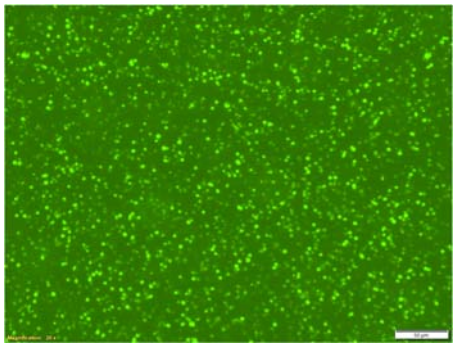

Figure 3-18. Microscopic image of PLGA-Ni particle loaded with His-GFP.

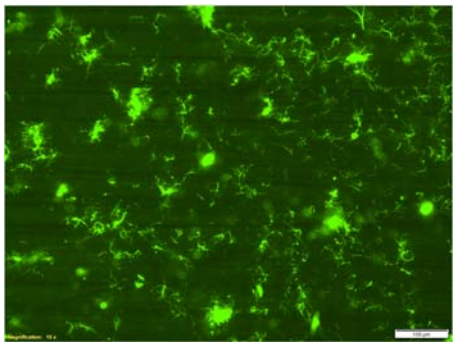

Figure 3-19. Microscopic image of PLGA-Ni particle loaded with His-GFP in EAK16-II gel.

3.4. Dual Delivery of ATRA and TGF-beta 1 through PLGA-Ni Particles

3.4.1. All-trans Retinoic Acid (ATRA)

Not only biological drugs such as His-tagged proteins can be loaded onto PLGA-Ni particles through surface adsorption, but small molecules can also be delivered by PLGA-Ni particles. In this project, all-trans retinoic acid, or ATRA, was encapsulated into the polymer matrix of PLGA-Ni particles to enhance the drug efficiency of the macromolecule drug, which in this case is TGF-beta 1, that was adsorbed on the surface of PLGA-Ni.

All-trans retinoic acid (ATRA), also known as tretinoin, has been reported to be able to improve the drug effect of TGF-beta 1 by synergizing in suppressing inflammation. The chemical structure of ATRA is demonstrated in Figure 3-20.

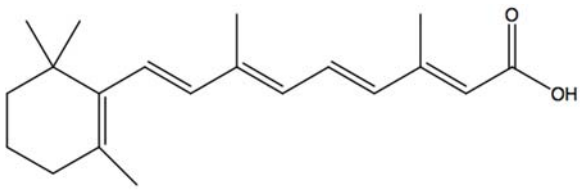

Figure 3-20. The chemical structure of ATRA.

According to the literature, ATRA and TGF-beta 1 induce CD4 cells (Schiavinato, J., et al. 2017), a type of islet antigen-specific T cells, to develop into regulatory T cells (Figure 3-21). Subsequently, the amount of CD4 cells differentiated into T helper 17 cells will be

reduced. T helper 17 (Th17) cells are a subset of pro-inflammatory T helper cells and have been implicated in autoimmune and inflammatory disorders. Therefore, ATRA is believed to be promising in assisting TGF-beta 1 to reduce inflammation. In order to achieve a better drug efficiency, dual loading of TGF-beta 1 and ATRA on PLGA-Ni particles is considered as one of the future research directions of studying PLGA-Ni particles.

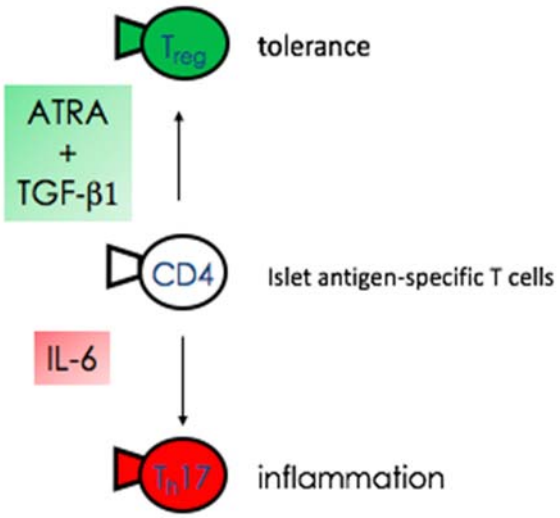

Figure 3-21. ATRA synergizes with TGF-beta 1 in suppressing inflammation.

3.4.2. Materials

All-trans retinoic acid (ATRA), powder, ⩾98% (HPLC) was purchased from Sigma-Aldrich. 18:1 DOGS-NTA-Ni (Nickel salt,1057 Da) was purchased from Avanti Polar Lipids, Inc. Poly (D, L-lactide-co-glycolide) (PLGA, 50:50, IV 1.0 dl/g) was purchased from Polysciences, Inc. Polyvinyl alcohol (PVA, 86-89% hydrolyzed, low molecular weight), dichloromethane (DCM, 99.9%) and D-(+)-trehalose dihydrate were purchased from Thermo Fisher Scientific.

3.4.3. Method and Results

First, PLGA (ATRA)-Ni particles was prepared using the method of double-emulsion solvent evaporation as following. DCM was used as the organic phase and 1% PVA aqueous solution was selected as the water phase. The aqueous solution of 1% PVA was prepared by stirring with heating at 90 °C overnight. Prior to emulsification, 90 mg $PLGA_{50:50}$ and 5 mg ATRA were dissolved in 2.4 ml DCM and combined with 0.6 ml 10 mg/ml of the metal chelating lipid DOGS-NTA-Ni in DCM, followed by the addition of 20 ml 1% PVA aqueous solution to the organic phase. Theoretically, 0.57 μmol nickel should be incorporated in the particles. Homogenization was performed at 25000 rpm for 5 min on ice. By magnetic stirring in hood for 4 h to evaporate DCM, the residual of the organic solvent was removed. Particles were collected through centrifugation and then washed twice with 10 ml of ultrapure water by centrifuging at 15k rcf, 4 °C for 20 min. To protect the freeze-dried material, particles were re-suspended in 12 ml 2% trehalose aqueous solution. Then, pre-freezing was performed by rotating the glassware containing particle suspension in dry ice-acetone bath. After lyophilization for 3 days, particles were collected and stored in a glass vial wrapped with parafilm and foil, and then saved inside a desiccator at 4 °C. Finally, the yield of this PLGA (ATRA)-Ni particle preparation is 300 mg of yellow particles.

To determine the drug content of ATRA in PLGA (ATRA)-Ni particles, UV absorbance of PLGA (ATRA)-Ni particle sample dissolved in DCM was measured at 366 nm.

According to the UV absorbance of standard ATRA solution, drug content of ATRA in prepared particles was calculated to be 4.42 μg/mg and the loading efficiency of ATRA was calculated as 26.51%.

Moreover, to verify the purity of ATRA we load in particles and to establish a method for quantifying the release of ATRA, the method of HPLC was utilized. Figure 3-22 showed the standard curve of ATRA using HPLC, according to which the amount of ATRA in the release samples can be determined.

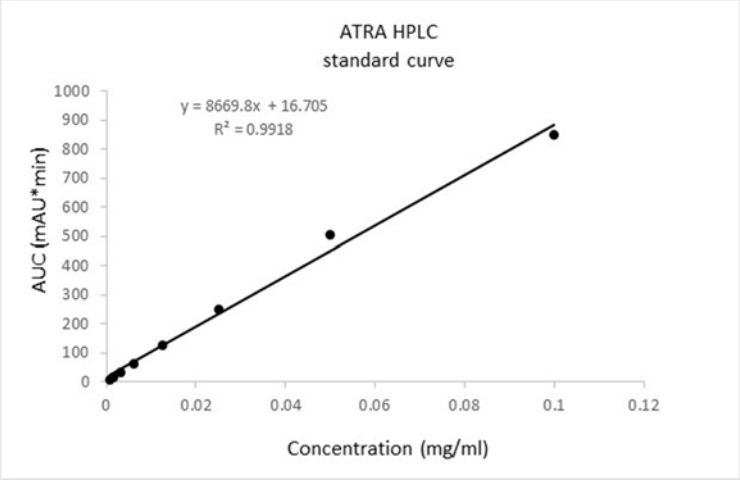

Figure 3-22. HPLC standard curve for ATRA.

Figure 3-23 shows the HPLC analysis result of the ATRA solution used for preparing PLGA (ATRA)-Ni particles, which is in consistency with the expected HPLC result for pure ATRA in literatures (Agadir, A., et al. 1995). This result suggests that the ATRA solution used for PLGA (ATRA)-Ni particles has a high level of purity.

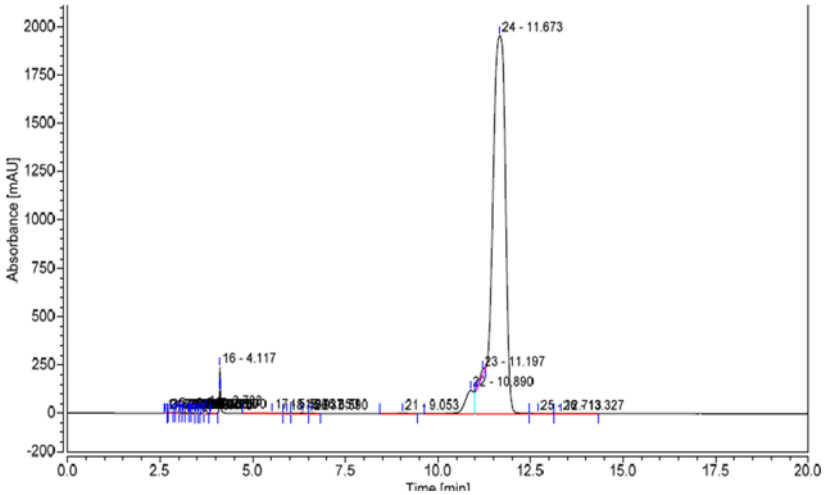

Figure 3-23. HPLC analysis result for ATRA standard solution.

3.5. Future Work on PLGA-biotin Particles

The polydispersity index and average Zeta potential of PLGA-biotin particles indicate that the formulation variables and production process of PLGA-biotin needs to be optimized to improve the homogeneity and stability of PLGA-biotin. In addition, in order to stabilize the colloidal suspension of PLGA-biotin, two main mechanisms for stabilization against aggregation should be taken into consideration, i.e., electrostatic stabilization and steric stabilization.

Electrostatic stabilization is based on the mutual repulsion between electrical charges. In a stable colloid suspension, mass of a dispersed phase is so low that its kinetic energy can hardly overcome the electrostatic repulsion between the charged layers in the dispersing phase (Jacob, I. 1991). Steric stabilization consists in covering the particles in polymers,

which prevents the particles to get close in the range of attractive forces (Elimelech, M., et al. 1998).

The role of ionic strength in promoting flocculation or stabilization of colloidal dispersions is mainly determined by the predominant electrostatic interaction between particles (Zhang, H., et al. 2007). The addition of salt also has the potential to weaken the particle–particle and particle–interface repulsive electrostatic forces, which leads to destabilization of the suspension (Bizmark, N. and M. A. Ioannidis, 2015). Therefore, the gel network stabilization represents a better way to produce colloid suspension of PLGA-biotin particles that is stable to both aggregation and sedimentation. In future studies, EAK16-II self-assembling peptide could be used to form a hydrogel network that can stabilize PLGA-biotin particles in dispersions, because the long fibers in EAK16-II gel can provide a steric stabilization to dispersed particles. Accordingly, the concentration of EAK16-II added in PLGA-biotin suspension also needs to be optimized in future studies to ensure both a decent stability and a desired release profile.

References

Agadir, A., et al. (1995). "All-trans retinoic acid pharmacokinetics and bioavailability in acute promyelocytic leukemia: intracellular concentrations and biologic response relationship." J Clin Oncol **13**(10): 2517-2523.

Auman, J. T. (2010). "Gene therapy: Have the risks associated with viral vectors been solved?" Curr Opin Mol Ther **12**(6): 637-638.

Bayer, E. A., et al. (1986). "An improved method for the single-step purification of streptavidin." J Biochem Biophys Methods **13**(2): 103-112.

Berthomieu, C. and R. Hienerwadel (2009). "Fourier transform infrared (FTIR) spectroscopy." Photosynth Res **101**(2-3): 157-170.

Birkholz, K., et al. (2010). "Targeting of DEC-205 on human dendritic cells results in efficient MHC class II-restricted antigen presentation." Blood **116**(13): 2277-2285.

Bissoyi, A., et al. (2016). "Recent Advances and Future Direction in Lyophilisation and Desiccation of Mesenchymal Stem Cells." Stem Cells Int **2016**: 3604203.

Bizmark, N. and M. A. Ioannidis (2015). "Effects of Ionic Strength on the Colloidal Stability and Interfacial Assembly of Hydrophobic Ethyl Cellulose Nanoparticles." Langmuir **31**(34): 9282-9289.

Block, H., et al. (2009). "Immobilized-metal affinity chromatography (IMAC): a review." Methods Enzymol **463**: 439-473.

Bonjour, J.P. (1984). "Biotinin: Handbook of Vitamins II. Series: Food Science. " Marcel Dekker, Inc., ISBN 0-8247-7051-X.

Bornhorst, J. A. and J. J. Falke (2000). "Purification of proteins using polyhistidine affinity tags." Methods Enzymol **326**: 245-254.

Brault, J. W. (1996). "New approach to high-precision Fourier transform spectrometer design." Appl Opt **35**(16): 2891-2896.

Carson, M., et al. (2007). "His-tag impact on structure." Acta Crystallogr D Biol Crystallogr **63**(Pt 3): 295-301.

Chapman-Smith, A. and J. E. Cronan, Jr. (1999). "The enzymatic biotinylation of proteins: a post-translational modification of exceptional specificity." Trends Biochem Sci **24**(9): 359-363.

Chivers, C. E., et al. (2010). "A streptavidin variant with slower biotin dissociation and increased mechanostability." Nat Methods **7**(5): 391-393.

Chivers, C. E., et al. (2011). "How the biotin-streptavidin interaction was made even stronger: investigation via crystallography and a chimaeric tetramer." Biochem J **435**(1): 55-63.

Crosby, J. R., et al. (2007). "Inhaled CD86 antisense oligonucleotide suppresses pulmonary inflammation and airway hyper-responsiveness in allergic mice." J Pharmacol Exp Ther **321**(3): 938-946.

Danhier, F., et al. (2012). "PLGA-based nanoparticles: an overview of biomedical applications." J Control Release **161**(2): 505-522.

Delves, P. (1998) "Encyclopedia of Immunology, 2nd edition" Elsevier Ltd. ISBN: 978-0-12-226765-9.

Elimelech, M., et al. (1998). Particle deposition and aggregation: measurement, modelling and simulation. Butterworth-Heinemann. ISBN 0-7506-7024-X.

Evers, M. M., et al. (2015). "Antisense oligonucleotides in therapy for neurodegenerative disorders." Adv Drug Deliv Rev **87**: 90-103.

Felcone, L. H. (2004). "The Long and Winding Road to Biologic Follow-ons." Biotechnol Healthc **1**(2): 20-29.

Fonte, P., et al. (2016). "Facts and evidences on the lyophilization of polymeric nanoparticles for drug delivery." J Control Release **225**: 75-86.

Fu, K., et al. (2000). "Visual evidence of acidic environment within degrading poly(lactic-co-glycolic acid) (PLGA) microspheres." Pharm Res **17**(1): 100-106.

Furth, R. (1998) Encyclopedia of Immunology (2nd Edition), 1755–1758.

Galanos, C. and M. A. Freudenberg (1993). "Mechanisms of endotoxin shock and endotoxin hypersensitivity." Immunobiology **187**(3-5):346-56.

Gentile, P., et al. (2014). "An overview of poly(lactic-co-glycolic) acid (PLGA)-based biomaterials for bone tissue engineering." Int J Mol Sci **15**(3): 3640-3659.

George Socrates "Infrared and Raman characteristic group frequencies: tables and charts, 3rd edition" John Wiley and Sons ISBN: 978-0-470-09307-8.

Gitlin, G., et al. (1987). "Studies on the biotin-binding site of avidin. Lysine residues involved in the active site." Biochem J **242**(3): 923-926

Green, N. M. (1975). "Avidin." Adv Protein Chem **29**: 85-133.

Green, N. M. (1965). "A Spectrophotometric Assay for Avidin and Biotin Based on Binding of Dyes by Avidin." Biochem J **94**: 23C-24C.

Green, N. M. and E. J. Toms (1973). "The properties of subunits of avidin coupled to sepharose." Biochem J **133**(4): 687-700.

Goyal, N. and P. Narayanaswami (2018). "Making sense of antisense oligonucleotides: A narrative review." Muscle Nerve **57**(3): 356-370.

Gregoriadis, G., et al. (2005). "Improving the therapeutic efficacy of peptides and proteins: a role for polysialic acids." Int J Pharm **300**(1-2): 125-130.

Hirsch, J. D., et al. (2002). "Easily reversible desthiobiotin binding to streptavidin, avidin, and other biotin-binding proteins: uses for protein labeling, detection, and isolation." Anal Biochem **308**(2): 343-357.

Hochuli, E., et al. (1987). "New metal chelate adsorbent selective for proteins and peptides containing neighbouring histidine residues." J Chromatogr **411**: 177-184.

Hofstetter, H., et al. (2000). "A labeling, detection, and purification system based on 4-hydroxyazobenzene-2-carboxylic acid: an extension of the avidin-biotin system." Anal Biochem **284**(2): 354-366.

Jacob, I. (1991). Intermolecular and Surface Forces. Academic Press. ISBN 978-0-12-391927-4.

Jacob, S., et al. (2006). " Stability of proteins in aqueous solution and solid state." Indian J Pharm Sci **68**(2): 154-163.

Jiskoot, W., et al. (2012). "Protein instability and immunogenicity: roadblocks to clinical application of injectable protein delivery systems for sustained release." J Pharm Sci **101**(3): 946-954.

Katakowski, J. A., et al. (2016). "Delivery of siRNAs to Dendritic Cells Using DEC205-Targeted Lipid Nanoparticles to Inhibit Immune Responses." Mol Ther **24**(1): 146-155.

Kim, S. H., et al. (2007). "Dual-mode fluorophore-doped nickel nitrilotriacetic acid-modified silica nanoparticles combine histidine-tagged protein purification with site-specific fluorophore labeling." J Am Chem Soc **129**(43): 13254-13264.

Kimple, M. E., et al. (2013). "Overview of affinity tags for protein purification." Curr Protoc Protein Sci **73**: Unit 9 9.

Kocak, A., et al. (2009). "Some advances in Fourier transform infrared transflection analysis and potential applications in forensic chemistry." Appl Spectrosc **63**(5): 507-511.

Korpela, J. (1984). "Avidin, a high affinity biotin-binding protein, as a tool and subject of biological research." Med Biol **62**(1): 5-26.

Kovacs, J. R., et al. (2009). "Characterization of nickel-decorated PLGA particles anchored with a his-tagged polycation." J Biomater Sci Polym Ed **20**(9): 1307-1320.

Laitinen, O. H., et al. (2006). "Genetically engineered avidins and streptavidins." Cell Mol Life Sci **63**(24): 2992-3017.

Larche, M., et al. (1998). "Costimulation through CD86 is involved in airway antigen-presenting cell and T cell responses to allergen in atopic asthmatics." J Immunol **161**(11): 6375-6382.

Levy, M. and A. D. Ellington (2008). "Directed evolution of streptavidin variants using in vitro compartmentalization." Chem Biol **15**(9): 979-989.

Liao, W., et al. (2017). "Oligonucleotide Therapy for Obstructive and Restrictive Respiratory Diseases." Molecules **22**(1).

Lin, S. (2015) "Salmon calcitonin: conformational changes and stabilizer effects. " AIMS Biophysics **2**(4): 695-723.

Lindsay, G. K., et al. (1989). "Single-step, chromogenic Limulus amebocyte lysate assay for endotoxin." J Clin Microbiol **27**(5): 947-951.

Livnah, O., et al. (1993). "The structure of the complex between avidin and the dye, 2-(4'-hydroxyazobenzene) benzoic acid (HABA)." FEBS Lett **328**(1-2): 165-168.

Magnotti, R., et al. (1999). "Methods to determine biotin-binding capacity of streptavidin-coated magnetic particles." J Magnetism and Magnetic Materials **194**(1-3): 69-75.

Makadia, H. K. and S. J. Siegel (2011). "Poly Lactic-co-Glycolic Acid (PLGA) as Biodegradable Controlled Drug Delivery Carrier." Polymers (Basel) **3**(3): 1377-1397.

Meir, A., et al. (2012). "Structural adaptation of a thermostable biotin-binding protein in a psychrophilic environment." J Biol Chem **287**(22): 17951-17962.

Mock, D. M. and M. I. Malik (1992). "Distribution of biotin in human plasma: most of the biotin is not bound to protein." Am J Clin Nutr **56**(2): 427-432.

Moor, N., et al. (2007). "Synthesis of a Reversible Streptavidin Binder for Biomimetic Assemblies." Australian J Chem **60**(5) 363-368.

Morrow, T. and L. H. Felcone (2004). "Defining the difference: What Makes Biologics Unique." Biotechnol Healthc **1**(4): 24-29.

Mujumdar, R. B., et al. (1993). "Cyanine dye labeling reagents: sulfoindocyanine succinimidyl esters." Bioconjug Chem **4**(2): 105-111.

Nieba, L., et al. (1997). "BIACORE analysis of histidine-tagged proteins using a chelating NTA sensor chip." Anal Biochem **252**(2): 217-228.

Paulo, C. S., et al. (2011). "Nanoparticles for intracellular-targeted drug delivery." Nanotechnology **22**(49): 494002.

Percy, J., Moody, C., Harwood, L. (1998). "Experimental organic chemistry: standard and microscale, 2nd edition". Blackwell Publishing. ISBN 978-0-632-04819-9.

Pisal, D. S., et al. (2010). "Delivery of therapeutic proteins." J Pharm Sci **99**(6): 2557-2575.

Reger, N., et al. (2017). "Surface modification of PLGA nanoparticles to deliver nitric oxide to inhibit Escherichia coli growth." Applied Surface Science 401: 162–171.

Resende, R. R., et al. (2007). "Delivery systems for in vivo use of nucleic acid drugs." Drug Target Insights **2**: 183-196.

Roslansky, P. F. and T. J. Novitsky (1991). "Sensitivity of Limulus amebocyte lysate (LAL) to LAL-reactive glucans." J Clin Microbiol **29**(11): 2477-2483.

Ross, C., et al. (2014) Modern Nutrition in Health and Disease. 11th ed. Lippincott Williams & Wilkins; 390-398.

Saraswathy, N. and Ramalingam, P. (2011). "Concepts and techniques in genomics and proteomics." ISBN 978-1-907568-10-7.

Schiavinato, J., et al. (2017). "TGF-beta/atRA-induced Tregs express a selected set of microRNAs involved in the repression of transcripts related to Th17 differentiation." Sci Rep **7**(1): 3627.

Smith, P.K., et al. (1985). "Measurement of protein using bicinchoninic acid". Anal. Biochem **150** (1): 76–85.

Spriestersbach, A. (2015). "Methods in Enzymology," **559**: 1-15. ISBN: 978-0-12-800279-7.

Stetefeld, J., et al. (2016). "Dynamic light scattering: a practical guide and applications in biomedical sciences." Biophys Rev **8**(4): 409-427.

Stierand, K. and M. Rarey (2010). "Drawing the PDB: Protein-Ligand Complexes in Two Dimensions." ACS Med Chem Lett **1**(9): 540-545.

St. Thomas "Spectroscopic Tools" (URL: http://www.science-and-fun.de/tools/).

Szlachcic, A., et al. (2011). "Longer action means better drug: tuning up protein therapeutics." Biotechnol Adv **29**(4): 436-441.

Tahara, K., et al. (2008). "Establishing chitosan coated PLGA nanosphere platform loaded with wide variety of nucleic acid by complexation with cationic compound for gene delivery." Int J Pharm **354**(1-2): 210-216.

Tan, M. L., et al. (2010). "Recent developments in liposomes, microparticles and nanoparticles for protein and peptide drug delivery." Peptides **31**(1): 184-193.

Tang, X. and M. J. Pikal (2004). "Design of freeze-drying processes for pharmaceuticals: practical advice." Pharm Res **21**(2): 191-200.

Thomas, M. and A. M. Klibanov (2003). "Non-viral gene therapy: polycation-mediated DNA delivery." Appl Microbiol Biotechnol **62**(1): 27-34.

Trueb, R. M. (2016). "Serum Biotin Levels in Women Complaining of Hair Loss." Int J Trichology **8**(2): 73-77.).

van de Weert, M., et al. (2000). "Protein instability in poly(lactic-co-glycolic acid) microparticles." Pharm Res **17**(10): 1159-1167.

Verdoliva, A., et al. (2010). "Biochemical and biological characterization of a new oxidized avidin with enhanced tissue binding properties." J Biol Chem **285**(12): 9090-9099.

von Burkersroda, F., et al. (2002). "Why degradable polymers undergo surface erosion or bulk erosion." Biomaterials **23**(21): 4221-4231.

Waugh, D.S., (2005). " Making the most of affinity tags." Trends in Biotechnology **23**(6): 316-320.

Wen, Y., et al. (2014). "Antibody-functionalized peptidic membranes for neutralization of allogeneic skin antigen-presenting cells." Acta Biomater **10**(11): 4759-4767.

Xiong Y.L. (1997) Protein Denaturation and Functionality Losses. Springer, Boston, MA.

Ye, M., et al. (2010). "Issues in long-term protein delivery using biodegradable microparticles." J Control Release **146**(2): 241-260.

Xue, X. Y., et al. (2018). "Advances in the delivery of antisense oligonucleotides for combating bacterial infectious diseases." Nanomedicine **14**(3): 745-758.

Zempleni, J., et al. (2007) Handbook of vitamins. 4th ed. Boca Raton, FL: CRC Press; 361-383.

Zhang, H., et al. (2007). "Effect of Ionic Strength on the Stability of Binary Ceramic Suspensions." J American Ceramic Society **90**(11): 3435-3440.

Zhang, S., et al. (1993). "Spontaneous assembly of a self-complementary oligopeptide to form a stable macroscopic membrane." Proc Natl Acad Sci **90**(8): 3334-3338.

Zhang, S., et al. (1994). "Unusually stable beta-sheet formation in an ionic self-complementary oligopeptide." Biopolymers **34**(5): 663-672.

Zhao, C., et al. (2010). "Hexahistidine-tag-specific optical probes for analyses of proteins and their interactions." Anal Biochem **399**(2): 237-245.